Stratigraphic and Structural Evolution of the Early Diligencia Basin, Orocopia Mountains, Southeastern California

by

Cole M. Davisson

Thesis submitted to the faculty of the Virginia Polytechnic Institute and State University in partial fulfillment of the requirements for the degree of

MASTERS OF SCIENCE

in

GEOLOGY

APPROVED:

Richard D. Law, Co-Chairman

Kenneth A. Eriksson, Co-Chairman

Richard K. Bambach

October, 1993

Blacksburg, Virginia

Stratigraphic and Structural Evolution of the Early Diligencia Basin, Orocopia Mountains, Southeastern California

by

Cole M. Davisson
K. A. Eriksson and R. D. Law (Co-Chairmen)
Department of Geological Sciences

(Abstract)

The Diligencia Formation comprises approximately 1600 meters of Oligo-Miocene continental siliciclastic sedimentary rocks and intercalated basaltic lavas, located in the eastern Orocopia Mountains of southeastern California. These deposits exhibit characteristics which may link them to tectonic processes diagnostic of both the Basin and Range physiographic province of North America, and the Transverse Ranges province of California. These different processes were active, however, during different periods in the history of the formation.

The early Diligencia Basin had an asymmetric half-graben geometry, and formed in response to presently north-south directed extension along a listric detachment located along the northern basin margin. Facies associations determined from five measured sections through the lower Diligencia Formation reveal a distinctly asymmetric distribution of facies across the basin. The deposits along the northern margin of the basin are characterized by cobble and boulder conglomerates and very coarse-grained sandstones unconformably overlying marine sedimentary rocks of the Eocene Maniobra Formation. These sedimentary rocks represent a high-gradient alluvial fan system which developed against the steep escarpment of the listric detachment fault. These deposits contrast with those present along the southern basin margin. The sedimentary rocks on the southern margin are characterized by pebble and cobble breccias, pebble conglomerates, very coarse- to fine-grained sandstones and gypsiferous mudstones. These facies define a system of low-gradient alluvial fans/fluvial braidplain that were deposited on the relatively gently sloping hangingwall block of the detachment, and that interfingered with deposits of a playa lake complex that formed in the basin interior.

The age of these deposits, basin geometry, and the style of sedimentation are very reminiscent of half-graben basins known from the Colorado River Extensional Corridor of the Basin and Range. Paleomagnetic studies indicate that the block containing the

Diligencia Formation may have been rotated more than 90° about a vertical axis since deposition ceased. In addition, regional palinspastic reconstructions indicate that the basin may have been significantly further north and east in the Miocene. These observations suggest that the Diligencia Basin may be genetically related to similar basins in the western Basin and Range, and that Diligencia Formation can be better understood if viewed in this tectonic context.

Sometime after deposition had ceased, the rocks of the Diligencia Formation were deformed under an imposed compressional stress field in association with activity along the Clemens Well Fault, a major, dextral wrench fault in the region. The action of the Clemens Well Fault also juxtaposed the Diligencia Basin with distinctive crystalline terranes of the central and western Orocopia Mountains, including the Mesozoic Orocopia Schist. The association of these rock types with structures characteristic of dextral strike-slip deformation have led most workers to tie the Orocopia Mountains to similar complexes in the Transverse Ranges province of southern California. In fact, the post-depositional history of the Diligencia Formation can best be understood only in the context of Transverse Ranges-style tectonic processes.

The complicated history of the sedimentary and volcanic rocks of the Diligencia Formation has made it difficult for previous workers to sort out an appropriate tectonic context in which to describe them. Recent advances in our understanding of the sedimentary responses to Tertiary rifting in the western Basin and Range, provide a new opportunity to evaluate the history of these deposits and this work has determined that the Diligencia Formation has had close ties to both the Basin and Range and the Transverse Ranges at different times during its complex history.

Acknowledgments

First and foremost, I want to thank my parents, Tom and Marilyn Davisson, and the rest of my family. Their support, at all levels, both moral and physical, has made this project as much an accomplishment of theirs as of mine.

I would like to thank my co-advisors, Ken Eriksson and Rick Law, for all of their helpful discussion, and advice, particularly during the last year, as I tried to write up this paper. Their help, and seemingly infinite patience, has been most keenly appreciated. Richard Bambach has been a pleasure to work with. His unbridled enthusiasm and willingness to discuss fairly wild interpretations really boosted my own enthusiasm when it was falling dangerously low.

Mary McMurray, Belinda Pauley, Linda Bland and Dean Hefner have made themselves available, and have always been eager to help, even when it meant going far out of their own way. I always knew that I could stumble into Carolyn Williams' office on a lousy day, and that she would be able to cheer me up, or at least listen to my woes. I may have gone nuts had it not been for her calming influence. Karen Hunt. Everyone knows the role she plays in running the department, but few have had the guts to admit it. I can't possibly list all of the ways she has made my grad student career run most smoothly. It is clear to me, though, that I might not have made it if she had not been there to help.

Lastly, my fellow students have been the aspect of life at Virginia Tech that was most enjoyable. Chris Fedo, in his role and friend and mentor, must be singled out. He was instrumental in the definition of this project, and his advice has proven invaluable. Rich Whitmarsh, Sven Morgan, Eric Gardner and Jane Parks, Bret Bennington, Scott and Leann Rutherford, Mike and Pauline Pope, Ron Wirgard and Barb Munn; all of these people have been eager to help, in any way they could, whenever the need arose. It has been very good to feel that one has family nearby, even when family is really thousands of miles away. Unfortunately, the list is really much longer, but I am short on room, and there are so many people who deserve acknowledgment. I hope that no one will feel slighted at my failure to mention their contribution, I have tried to thank each personally, although, undoubtedly, I have missed some.

This project was partially funded by student research grants from the Geological Society of America.

Table of Contents

List of Figures

CHAPTER 1. Introduction

The Orocopia Mountains are located in eastern Riverside County, in southern California. The mountain range is located in the northeastern corner of the Salton Trough, northeast of the town of North Shore, and south of Interstate 10 (fig. 1). The interior of the range is accessible by the Eagle Mountain Railroad support road, as well as by numerous maintained and unmaintained Bureau of Land Management roads.

The western half of the Orocopia Mountains is composed entirely of Mesozoic metasediments and metavolcanics, the Orocopia Schist. The schist is separated from the Mecca Hills to the west, by the Hidden Spring fault (fig. 2). The central Orocopia Mountains are characterized by a distinctive anorthosite/gneiss complex which is separated from the Orocopia Schist to the west, by the Orocopia Thrust fault (fig. 2).

The eastern portion of the Orocopia Mountains comprises the Diligencia Basin complex. This includes the Miocene sediments of the Diligencia Formation, the underlying Eocene Maniobra Formation, and the associated crystalline basement terranes. These rocks are separated from the anorthosite/gneiss complex of the central Orocopias by the Clemens Well fault (fig. 2). The Clemens Well fault is generally considered to be an oblique-slip fault, with a dominant component of right-lateral offset, and a poorly constrained amount of displacement.

This thesis represents a sedimentological, stratigraphic and structural study of the Diligencia Basin. Work has focused primarily upon the sediments of the Diligencia Formation, although, it would be impossible to characterize the basin without also discussing adjacent and related rocks.

1.1 Previous Work

Crowell first reported the occurrence in the Orocopia Mountains, of non-marine clastic rocks of unknown correlative affinities in 1957, and later named these rocks the

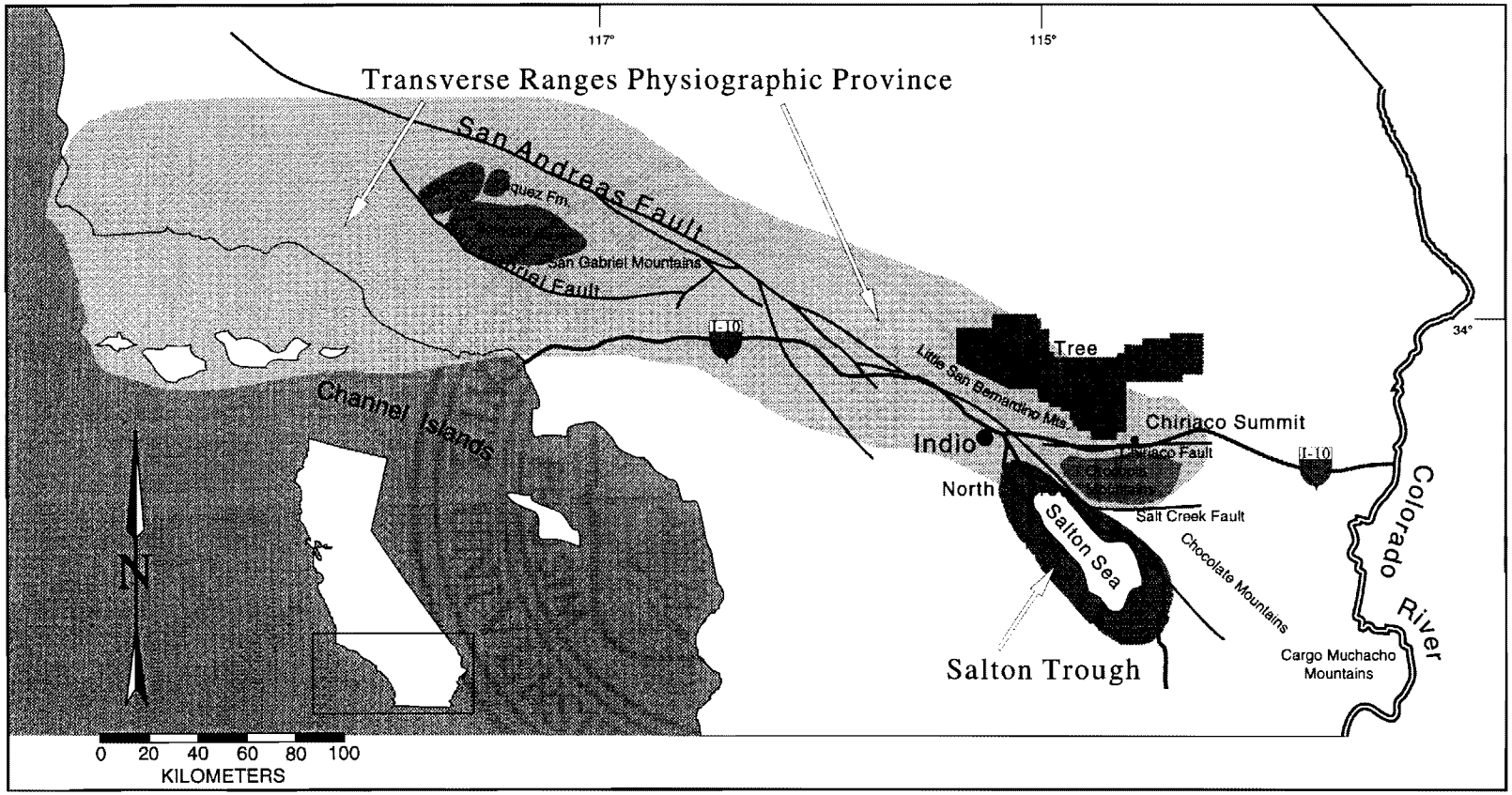

Figure 1. Index map of the Transverse Ranges Physiographic Province and San Andreas Fault system in Southern California.

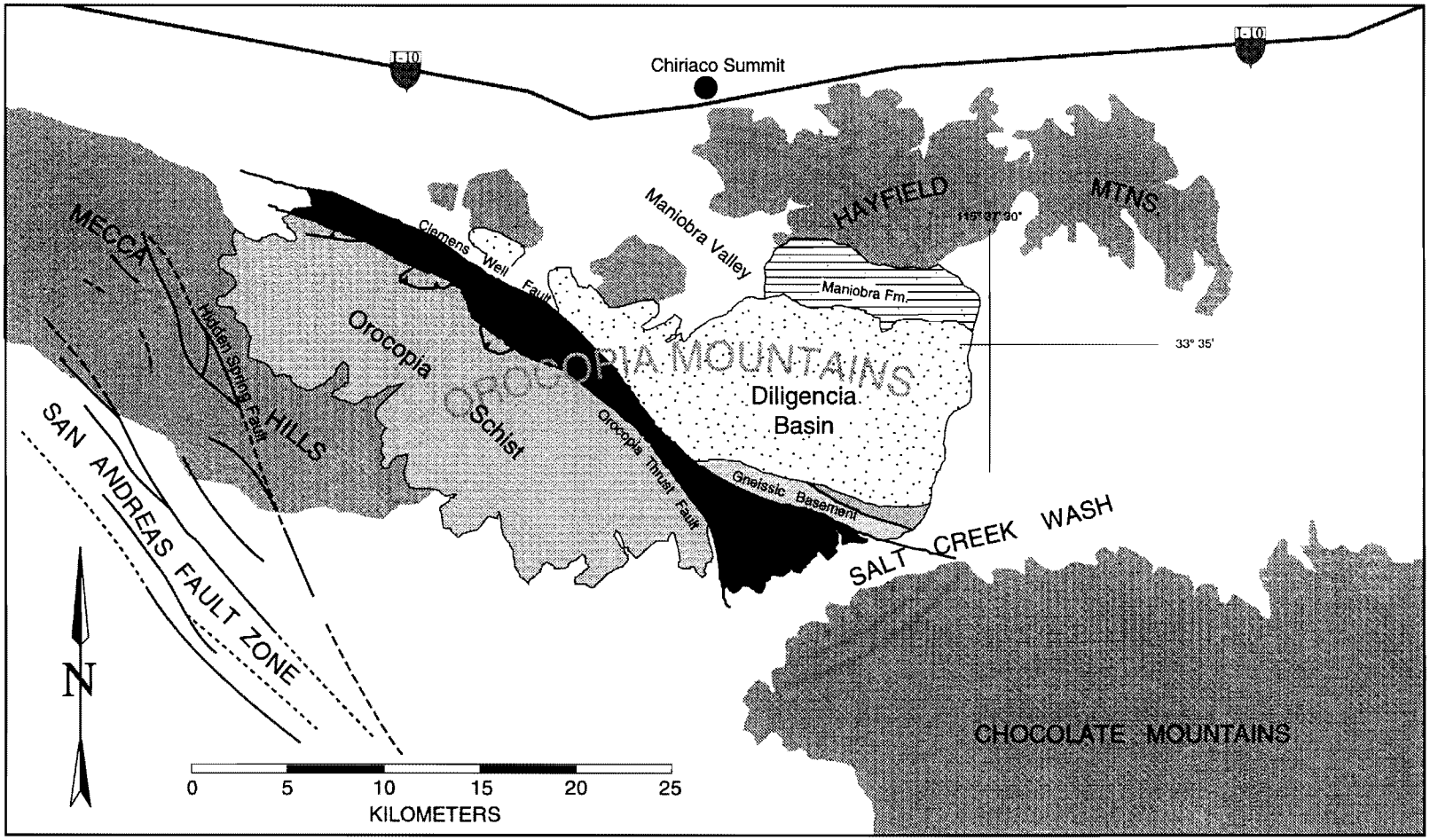

Figure 2. Index map of the Orocopia Mountains and surrounding area (modified from Spittler and Arthur, 1982).

Diligencia Formation (Crowell, 1975a). His observation that the crystalline units outcropping in the Orocopia Mountains, including the Orocopia Schist and the distinctive anorthosite complex suprajacent to the schist above the Orocopia Thrust, bore a striking resemblance to rocks in the San Gabriel Mountains across the San Andreas Fault Zone, set the stage for later studies of the rocks exposed in the Orocopia Mountains (fig. 1) (Crowell, 1957; Crowell and Walker, 1962). The majority of the work done in the Orocopias in the 1960s and 1970s was carried out by groups trying to constrain the amount of offset across the San Andreas Fault by correlating rocks on either side. Crowell and others at the University of California at Santa Barbara, as well as Ehlig and others at California State University at Los Angles, carried out descriptive structural and geochemical projects of the crystalline rocks which are exposed in the Orocopias and in the San Gabriel mountains (Crowell, 1957; Crowell and Walker, 1962; Crowell, 1974; Crowell, 1975b; Ehlig et al., 1975).

M. Woodburne, at the University of California at Riverside, coordinated projects which tested the hypothesis that the Tertiary non-marine sediments and volcanic rocks of the eastern Orocopias may be correlative with the Vasquez, Mint Canyon, or Plush Ranch Formations of the Transverse Ranges (fig. 1) (Crowell and Walker, 1962; Ehlig and Ehlert, 1972; Woodburne and Whistler, 1973; Woodburne, 1974a; Woodburne, 1974b). Two students of Woodburne's, T. Spittler and M. Arthur made the first detailed analysis of the Diligencia sediments and intercalated basaltic volcanic rocks which were summarized in their Masters theses in the early 1970s (Arthur, 1974; Spittler, 1974). Arthur concentrated on the clastic sediments, which he suggested were deposited in an intermontane valley surrounded by highlands of crystalline basement. Spittler characterized the chemistry of the lavas and produced K-Ar dates for the Diligencia Formation of 23.0±2.9, 20.6±8.9, and 19.1±1.9 million years (Arthur, 1974; Spittler, 1974; Spittler and Arthur, 1982). The two authors concluded that the Diligencia

Formation was remarkably similar, both physically and temporally, to the Tertiary basins of the Transverse Ranges, but could find no conclusive evidence that they formed an offset marker across the San Andreas. These conclusions were reiterated a short time later by Bohannon (Bohannon, 1976). In a later, published format, Spittler and Arthur stated that the sediments and volcanic rocks of the Diligencia Formation were deposited in an asymmetrical half-graben, with a steep northern margin and a less-steeply dipping southern margin (Spittler and Arthur, 1982). No significant attempt was made to place the extensional basin into a tectonic setting. The rocks which comprise the Diligencia Formation were described, and the depositional history was developed, but the cause of the extension responsible for basin formation were not considered.

During the 1980s and 1990s, E. Frost and others attempted to place the Diligencia Basin in a plate tectonic context and suggested that the extension which resulted in Diligencia rifting was genetically related to Miocene extension in the Colorado River region of California, Arizona and Nevada (Frost et al., 1982; Morris and Okaya, 1986; Robinson and Frost, 1989; Robinson and Frost, 1991). Frost and his associates have carried out a considerable number of field-based and geophysical projects in southeastern California and western Arizona, and have developed a series of models which describe the reactivation and overprinting of Mesozoic thrusts by late Cenozoic extension (Frost and Otton, 1981; Frost et al., 1981; Frost et al., 1982; Frost and Martin, 1983; Morris et al., 1986; Morris and Okaya, 1986; Okaya and Frost, 1987).

Frost and his students and associates have modeled the Orocopia Mountains as an example of a metamorphic core complex (see reviews of core complexes by Wernicke and Burchfiel, 1982; Coney and Harms, 1984; Lister and Davis, 1989). The Orocopia Schist, which forms a domal structure in the western Orocopias was interpreted to represent the metamorphic core of the complex. The eastern flank of the core is characterized by tilted basement blocks forming a half-graben sedimentary basin in the

hanging wall of a poorly defined detachment fault system (Robinson and Frost, 1989; Robinson and Frost, 1991). The detachment fault, along which the core of schist was progressively unroofed, and which was responsible for basin formation, was alternatively described as a reactivation of the Orocopia Thrust by Miocene normal faulting, or as the Clemens Well Fault, reinterpreted as a normal fault (Frost and Martin, 1983; Morris and Okaya, 1986; Goodmacher et al., 1989; Robinson and Frost, 1989; Robinson and Frost, 1991). Neither Frost nor his associates have yet published a definitive account of the presence of normal faults which separate the Orocopia Schist from the Diligencia Basin to the east.

The scenario presented by Frost and his associates indicates that the extension which acted as the driving force for unroofing of the Orocopia Schist, as well as for formation of the Diligencia Basin was directed approximately east-west. The deformation observed in the Diligencia Formation resulted from drape folding of sediments over tilted basement blocks (Robinson and Frost, 1989). This maximum extension direction is very similar to that observed for the metamorphic core complexes in the Colorado River region, which supports the assertion that the complex of rocks which comprise the Orocopia Mountains is genetically related to the late Cenozoic metamorphic core complexes of the Cordillera. However, this extension direction results in a basin which is oriented at approximately 90° to the east-west elongate basin geometry inferred by Spittler and Arthur. The model proposed by Frost and others also fails to consider any of the paleomagnetic studies carried out by Terres, Luyendyk and others at University of California, Santa Barbara. This work indicates that the Tertiary rocks which are exposed in the eastern Orocopia Mountains have been tectonically rotated by as much as 140° clockwise about a vertical axis (Luyendyk et al., 1985; Hornafius et al., 1986; Carter et al., 1987). Obviously, these data suggest that the

apparent extension direction associated with the Diligencia Basin, as it is oriented today, may be perpendicular to the actual direction of extension in the Miocene.

The past several years have also seen significant work done in the Diligencia Formation by Jerry Brem and Brady Rhodes, and their field camp classes from California State University at Fullerton (C. M. Fedo, Pers. comm., 1991). Although none of this work has been published, their interpretations of the half-graben geometry of the Diligencia Basin have formed the framework around which much of this thesis was built.

1.1.1 Purpose of Study

The present study is intended to shed some new light on the origin of the Diligencia Basin. In the years since Spittler and Arthur worked in the Diligencia Formation, knowledge of the late-Tertiary tectonics of western North America has increased many times. The Diligencia Basin may now be compared with better understood rift basins in the Tertiary of California, Arizona, and Nevada (Miller and John, 1988; Neilson and Beratan, 1990; Fedo and Miller, 1992). In addition, our understanding of rifting processes, in general, has increased significantly. Such new developments in the state of geologic knowledge demand that the Diligencia Formation be evaluated in the light of these recent advances.

Equally instrumental in the direction of this project is the need to evaluate the models of Frost and others, with respect to the sediments which fill the basin they described. Their models are based primarily on correlation of structures observed on seismic lines across the nearby Chocolate Mountains, and Cargo Muchacho Mountains (fig. 1) (Morris and Okaya, 1986; Okaya and Frost, 1987; Wilson et al., 1987; Pridmore and Frost, 1992). Robinson and Frost have carried out petrographic and isotope geochemical studies of fault rocks collected in the Orocopia Mountains, and have used such data to draw conclusions about the basin they assume to have formed in relation to movement on the fault they have associated with these fault rocks. The present study has

attempted to objectively describe the rocks which compose the Diligencia Basin complex, the model of Frost and others, as well as that of Spittler and Arthur, will be assessed in the light of these observations.

CHAPTER 2. Geologic Setting of the Eastern Orocopia Mountains

The Orocopia Mountains are situated the northeast of the Salton Trough in southeastern California. The proximity to the San Andreas Fault, and the generally east-west trend of the range, as well as the presence of several distinctive rock units (fig. 1) have led most workers to include the Orocopia Mountains in the Transverse Ranges physiographic province of California. In contrast, the timing and style of Tertiary rifting, and interpretation of the range as a metamorphic core complex (eg. Frost and Robinson, 1990) suggest an affinity to the Basin and Range Province of North America. In fact, the rocks which occur in the Orocopia Mountains must be considered in the context of both physiographic regions, because tectonic forces associated with each affected the rocks at different times in their history.

2.1 Plate Tectonic Setting

2.1.1 Neogene Extension in Southwestern North America

The Orocopia Mountains (fig. 3) are situated near the western margin of the southern Basin and Range Province of North America (Nelson, 1981) . The portion of the Basin and Range in eastern California, southern Nevada, and western Arizona, centered around the Colorado River, is remarkable for the presence of distinctive rock assemblages known collectively as 'metamorphic core complexes' (Rehrig, 1982; Coney and Harms, 1984; Coney, 1987). Metamorphic core complexes are diagnostic of extreme extension, and estimates of extension in the Basin and Range vary from 15%-300%, or more, in some areas (Gans, 1987). Metamorphic core complexes commonly comprise a central core of high-grade, plastically deformed rock, separated from an overlying plate of brittlely deformed upper crustal rocks by a low-angle normal fault (Gans, 1987; Davis and Lister, 1988;Lister and Davis, 1989). Many of the best studied metamorphic core complexes in California, Arizona, and Nevada, are associated with late Tertiary

extensional sedimentary basins (Miller and John, 1988; Neilson and Beratan, 1990; Fedo and Miller, 1992).

For much of its length, the belt of core complexes is located on the western flank of the Mesozoic Cordilleran fold-and-thrust belt (fig. 3). Their proximity to the Laramide/Sevier orogen, and the unusual character of the low-angle structures associated with the core complexes led early investigators to suggest a genetic relationship between the core complexes and Mesozoic thrusting (Misch, 1960). More recent work suggests that the core complexes are much more closely tied to extensional events in the latter half of the Tertiary Period (Wernicke, 1985; Lister and Davis, 1989).

2.1.2 Late-Tertiary/Quaternary Strike-Slip Faulting, and the Transverse Ranges

The onset of dextral strike-slip faulting in southern California 15-20 million years ago set the stage for the development of the wrench tectonic regime which dominates the neotectonics of the region (Atwater, 1970). The San Andreas Fault system is one of the world's largest, active strike-slip faults, and is the source of much of the complexity of California geology. The San Andreas Fault system, with its large subordinate splays such as the San Gabriel and San Jacinto faults, has accommodated up to 400km of right-lateral displacement in its relatively short history (Norris and Webb, 1976). The San Andreas Fault is hypothesized to have formed in response to the subduction of a spreading center under the western edge of North America (Atwater, 1970; Norris and Webb, 1976). The mechanism and timing of its development are still not completely understood.

The geologic grain of California runs NNW-SSE in general, and the trend of the San Andreas Fault follows suit along most of its length. However, a significant exception to this observation is the Transverse Ranges geomorphic province in southern California. The Transverse Ranges comprise a group of WNW-ESE trending mountain ranges which extends some 500km, from the Channel Islands on the west, to the Little San Bernardino Mountains on the east (fig. 1). Some workers have included the Orocopia Mountains in

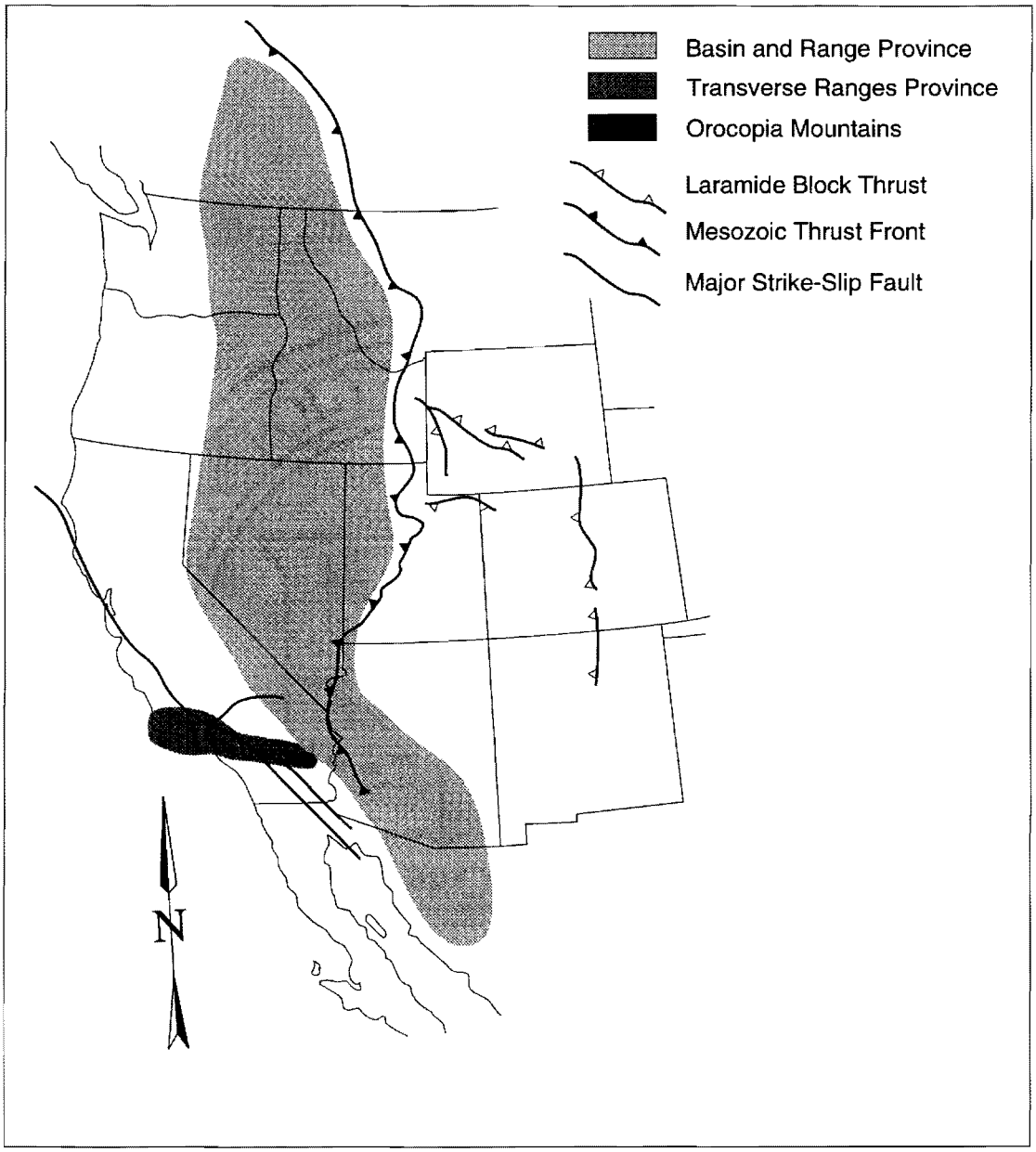

Figure 3. Map of western North America showing the position of the Orocopia Mountains in relation to the Transverse Ranges Physiographic Province of California and the Basin and Range Province of North America.

the Transverse Range, at the southeasternmost extent of the province (Norris and Webb, 1976). Across the Transverse Ranges, even the trend of the San Andreas Fault system curves away from its normal course. While there must be some underlying mechanism influencing the orientation of the structural grain in this area, much of the uplift that we now associate with the Transverse Ranges is undoubtedly related to transpression along the so-called 'big bend' in the San Andreas (Crowell, 1981).

2.2 Basement Rocks

The Orocopia Mountains can be subdivided into three, structurally distinct, packages of rock (fig 2). The western Orocopia Moutains comprise the Mesozoic Orocopia Schist and overlying Quaternary sediments. The Central Orocopia Mountains consist of a distinctive pre-Cambrian anorthosite/syenite/gniess complex which lies structurally above the Orocopia Schist, and is separated from it by the east-dipping Orocopia Thrust Fault. The eastern Orocopia Mountains contain a complex assemblage of rocks, bordered by the Clemens Well Fault on the west, which represent an Eocene marine shoreline, and an Oligo-Miocene continental basin, as well as the pre-Cambrian and Mesozoic crystalline rocks. Brief descriptions of the major rock units which are present in the Orocopia Mountains follow, in order of ascending age.

2.2.1 Precambrian rocks

2.2.1.1 Gneisses

The oldest, well-dated rocks which occur in the study area are augen gneisses of the eastern Orocopia Mountains, which crop out in a triangular belt adjacent to the southern segment of the Clemens Well Fault (fig. 2). These rocks are considered to be part of the Chuckwalla complex of Miller (1944), and have yielded zircon ages of 1670±15 ma (Silver, 1971). The Chuckwalla complex in the Orocopia Mountains is characterized by dark, coarse-grained, biotite gneisses with elliptical, pink microcline

megacrysts up to 10 cm across. Locally, the gneissic fabric is poorly developed, and the rocks exhibit porphyritic igneous textures.

Associated spatially with the augen gneiss of the Chuckwalla complex is a package of quartzofeldspathic gneiss, granitic gneiss, and granite. The quartzofeldspathic gneiss is composed almost entirely of fine-grained quartz and microcline feldspar, and exhibits compositional banding which may represent relict sedimentary bedding. In apparent intrusive contact with the metasedimentary rocks are pods of granite and crudely-banded granitic gneiss. This package is everywhere separated from the augen gneiss to the west, by a brittle fault zone (fig. 2). The fault zone varies in orientation from sub-vertical to approximately 20° SE dip, and is characteristically defined by 1-3 meters of fine-grained, dark green, irregularly foliated fault rock.

The metasediment/granite complex is discussed here in association with the augen gneiss of the Chuckwalla complex because these rocks are always found adjacent to one another. The fault contact by which they are juxtaposed, however, limits our ability to constrain the ages of the metasediments or the granites. Powell (1981) included both the Chuckwalla augen gneiss and the metasediment/granite complex, in addition to related rocks in the region, in his informal San Gabriel basement terrane. If the metasedimentary gneiss of the eastern Orocopia Mountains does, in fact, belong to Powell's San Gabriel terrane, regional observations suggest that these rocks acted as the country rock into which the Chuckwalla porphyritic intrusions were emplaced, thus constraining their age to be greater than about 1600 Ma (Powell, 1982). At present, though, it is certain only that they predate the sediments of the Diligencia Formation, for which the crystalline rocks acted as basement and as a source of clastic material.

Crowell (1975) reported that the Chuckwalla complex in the eastern Orocopia Mountains contains about 20% migmatite, in the form of: 'intermixtures of impure feldspathic and quartz-rich gneiss, gneissic granite, and biotite schist.' Except for the

interpretation as migmatites, this description fits quite well the rocks which are here interpreted as metasedimentary rocks and intrusive granites, in fault contact with the the rocks of the Chuckwalla complex. Migmatitic rocks were not observed during the fieldwork of this project, although the basement terranes were not the primary focus of the project, and failure to observe migmatites may simply be the result of having spent a relatively short time in the crystalline rocks.

2.2.1.2 Anorthosite Complex

The central Orocopia Mountains are composed entirely of a lithologically heterogeneous anorthosite-syenite-gneiss complex (Crowell and Walker, 1962; Powell, 1982). This package of rocks is present in the hangingwall of the Orocopia Thrust Fault, and west of the Clemens Well Fault (fig. 2) and is thus a terrane structurally distinct from others in the Orocopia Mountins. The complex consists of a distinctive gneiss containing blue to violet quartz with dense rutile inclusions, which has been dated at approximately 1475 ma (Silver, 1971). Similar gneiss, containing gray quartz, is exposed in the hills which border the Maniobra Valley, in the eastern Orocopia Mountains, and in the Painted Canyon region of the Mecca Hills to the northwest (Crowell, 1975a). These rocks may be correlative with the blue-quartz gneiss of the central Orocopia Mountains

The gneiss is cut by several generations of igneous intrusions, and the many rock types which intrude the blue-quartz gneiss have been separated into two groups by Crowell (1975): an anorthosite group and a syenite group. The anorthosite group consists of gabbro, diorite, white anorthosite bodies, mafic bodies and basic dikes, while the syenite group includes syenite, quartz-bearing syenite, alkali granite, granophyre, and pegmatitic dikes (Crowell, 1975a). Rocks from the syenite units have yielded ages of 1220 Ma (Silver, 1971).

2.2.2 Mesozoic Plutons

Crowell (1975) reported the presence of young, quartz-monzonitic plutons intruding the anorthosite complex of the central Orocopia Mountains. Similar leucocratic granitoid plutons form the Hayfield Mountains, northeast of the Orocopias, and the hills which make up the northeastern Orocopia Mountains. Armstrong and Suppe (1973) reported K-Ar ages from granitic plutons in the area of 71-88 Ma. However, it is impossible, from their report, to determine precisely where each sample was collected. No detailed study of the Mesozoic plutons in the Orocopia and Hayfield mountains has been conducted, and such fundamental aspects as the number of plutons or their range of ages, are still poorly constrained.

2.2.3 Orocopia Schist

The western part of the Orocopia Mountains, in the footwall of the Orocopia Thrust Fault, is composed almost entirely of the distinctive Orocopia Schist (Miller, 1944). The Orocopia Schist comprises a dome of approximately 2000m of schist, bedded chert and basic volcanic rocks. The bedded schist is generally gray colored, and is composed of muscovite, quartz and plagioclase with minor chlorite, epidote, actinolite and graphite (Crowell, 1975a). The presence of isoclinally folded quartz-rich layers indicates that the schist is locally intensely deformed

Studies of the Orocopia Schist, as well as its correlatives, the Pelona Schist in the San Gabriel Mountains, and Rand Schists in the northwestern Mojave Desert, indicate that these units may represent the metamorphic remnants of greywackes and cherts deposited as part of the Mesozoic subduction complex of western North America (Ehlig et al., 1975; Crowell, 1981; Ehlig, 1981). The ages of these schist units are not well constrained, but the Orocopia Schist is most likely of Mesozoic age, and the age of metamorphism is considered to be latest Cretaceous (Ehlig et al., 1975; Crowell, 1981; Ehlig, 1981). Lithologies found in the Orocopia Schist do not occur as clasts in the

Diligencia Formation sediments, therefore, the role of the Schist in the evolution of the Diligencia Basin is probably very limited importance.

2.3 Cenozoic Sediments

2.3.1 Maniobra Formation

The Eocene-age Maniobra Formation is the oldest, unmetamorphosed sedimentary unit that is developed in the Orocopia Mountains. The Maniobra Formation comprises approximately 1500m of fossiliferous, marine sandstone, shale, conglomerate and breccia, and rare, non-marine facies (Crowell and Susuki, 1959; Advocate, 1983). The sediments of the Maniobra Formation lie unconformably on granitic basement in the northeastern Orocopia Mountains and the Hayfield Mountains (fig. 2). Sedimentological studies of the mildly deformed strata indicate that the Maniobra Formation represents an Eocene shoreline/submarine canyon complex (Crowell and Susuki, 1959; Advocate, 1983). Many fine-grained facies within the Maniobra contain marine invertebrate fossils, which readily distinguish these strata from superficially similar sediments in the overlying Diligencia Formation. The coarse, breccia facies, however, contain no fossils, and scree-covered exposures on low hills make conclusive identification difficult.

The Maniobra Formation is most extensively exposed in the northeastern Orocopia Mountains and in the Maniobra Valley. However, it does crop out in a thin, discontinuous belt along the entire northern margin of the Orocopia Mountains (fig 2). The sediments are deformed into a series of faulted, open folds, and are unconformably overlain by the younger sediments of the Diligencia Formation. The bedding of the Maniobra Formation is commonly discordant with respect to the bedding in the overlying Diligencia Formation. Locally, however, deformation of the Eocene sediments results in parallelism with the units above (fig. 4).

Figure 4- Photograph of the unconformable contact between Maniobra and Diligencia formations. This exposure is an example of the contact where the angle between the Diligencia beds and the underlying maniobra beds is low.

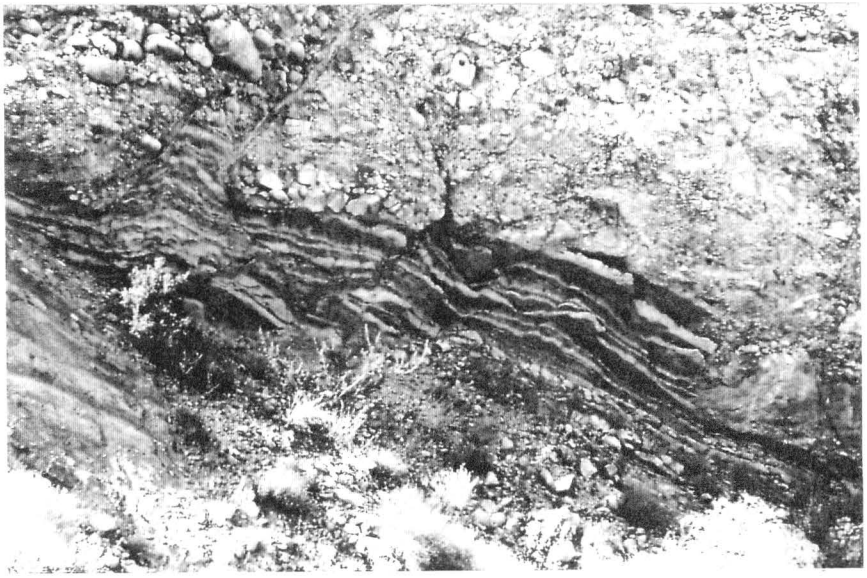

2.3.2 Diligencia Formation

Above the Maniobra Formation, the Diligencia Formation comprises up to 2000m of Oligo-Miocene, non-marine clastic sediments, evaporites and basalt flows (Crowell, 1975a; Spittler and Arthur, 1982). These sediments and volcanic rocks are interpreted to represent the fill of a continental, half-graben rift basin (Spittler and Arthur, 1982). The basin fill rocks were subsequently deformed during transpression along the Clemens Well Fault, which truncates the Diligencia Formation on its western end. The formation and evolution of the Diligencia Basin, including its infilling and closure, is the subject of the present study, and will be discussed in detail in the following sections of this thesis.

2.3.3 Quaternary Sediments

Unconformably overlying the Diligencia Formation, and widespread regionally, are at least three generations of Quaternary alluvial and fluvial deposits. Although the Quaternary sediments are superficially similar to facies within both the Maniobra and Diligencia formations, they are readily distinguished from the Tertiary deposits by the ubiquitous occurrence of Orocopia Schist as a clast lithology in the Quaternary sediments. The Tertiary sediments are devoid of clasts of Orocopia Schist.

The oldest Quaternary deposits in the Orocopia Mountains include relatively rare conglomeratic sands which have been correlated to the Pliocene-age Mecca and Palm Spring formations (Sylvester and Smith, 1975; Spittler and Arthur, 1982). These sediments are very well indurated and form polished pavements in washes, and cliffs perched well above current base level. Locally, the oldest Quaternary deposits are cut by calcite-filled fracture sets which also cut across older Diligencia sediments, but do not affect younger deposits.

A second generation of Quaternary gravels is found throughout the Orocopia Mountains, but is best developed in the eastern end of the range. These sediments have been correlated to the Pleistocene Ocotillo Formation, and are characteristically resistant

conglomerates and sandstones which form cliffs and tors, up to 20m high, in the Red Canyon area (fig. 5); (Crowell, 1975a; Sylvester and Smith, 1975; Spittler and Arthur, 1982).

The youngest sediments in the Orocopia Mountains are recent gravels and sands that occur as canyon bottom beds in the interior of the mountain range, and extend out as modern alluvial fans and fluvial braidplains on the periphery of the range, in the Maniobra Valley and Salton Creek wash (fig. 2).

2.4 Structural Features

2.4.1 Mesozoic Thrust System

The Orocopia Thrust Fault is the oldest structure in the study area that is geometrically well studied. The fault separates greenschist facies, Mesozoic rocks in the footwall, from granulite facies, pre-Cambrian rocks in the hangingwall (fig. 2). The fault is defined by gouge zones which include lenses of mylonite (Crowell, 1974; Crowell, 1975a). This assemblage of fault rocks has been interpreted to indicate early, deep-seated motion on a fault plane which was later reactivated by shallow, brittle deformation (Crowell, 1975a).

The Orocopia Thrust is generally considered to be a segment of a major, Mesozoic thrust system that was subsequently dissected and folded by Neogene strike-slip faulting. The Orocopia Thrust is correlated with the Chocolate Mountains Thrust, to the south, as well as the Vincent Thrust in the San Gabriel Mountains and the Mule Mountain Thrust to the east (Crowell, 1974; Crowell, 1975a; Haxel and Dillon, 1978; Ehlig, 1981). Palinspastic reconstructions indicate the presence of a large reverse fault system associated with Mesozoic subduction along the west coast of North America (Crowell, 1981), perhaps with backthrusts represented by the Mule Mountain Thrust Fault (fig. 6).

Figure 5- Photograph of Quaternary (Pliocene?) gravels in the easternmost Orocopia Mountains.

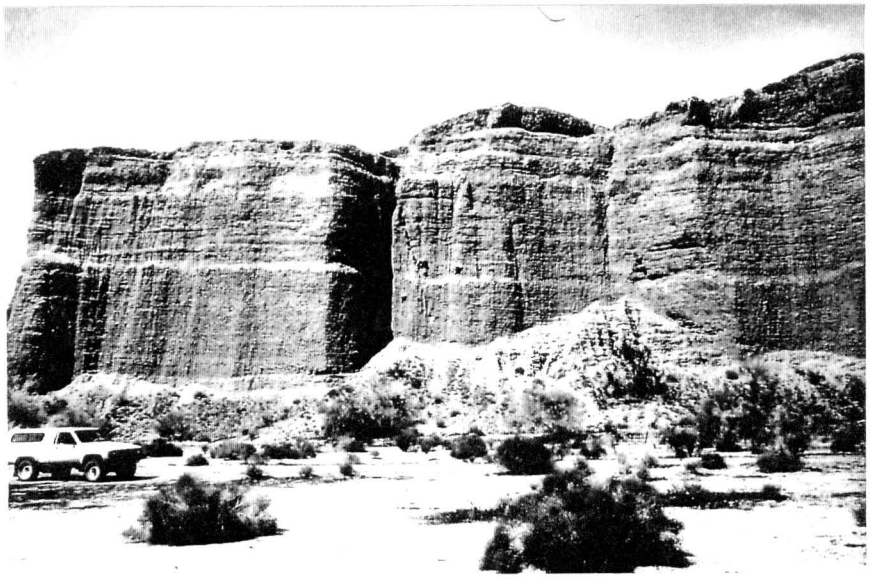

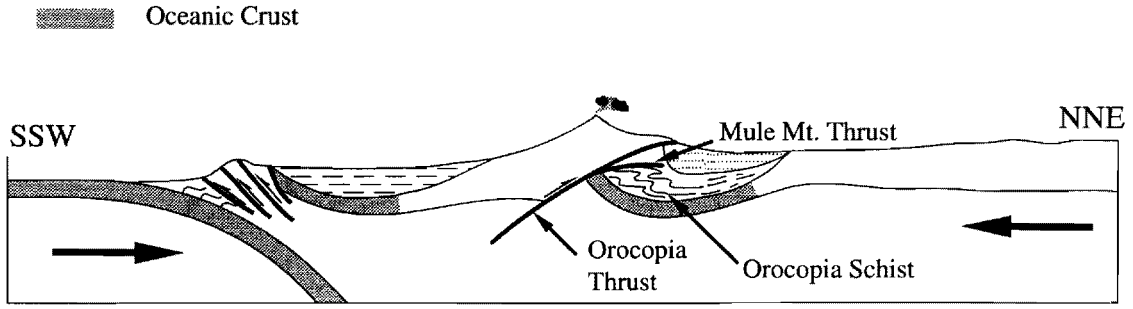

Figure 6. Diagrammatic cross-section across southeastern California during earliest Tertiary time. (from Crowell, 1981)

2.4.2 Interpretive Neogene Extensional Faults

Neogene normal faults in and around the Orocopia Mountains are not apparent in outcrop, but the presence of some two kilometers of rift-basin fill indicates that such faults must exist. The nature of these extensional structures is a matter of some controversy. As discussed in Chapter 1, early workers interpreted the formation of the Diligencia Basin by dip-slip motion along east-west striking normal faults (Arthur, 1974; Spittler and Arthur, 1982). More recently, the basin has been interpreted to have developed in response to motion along north-south striking, east-dipping normal faults (Robinson and Frost, 1989; Robinson and Frost, 1991). Examination of this incompatibility between two proposed models has been a primary objective of the present study, and will be discussed more thoroughly later in this thesis.

2.4.3 San Andreas Fault System

The San Andreas Fault itself is exposed in the Painted Canyon area of the Mecca hills, approximately 10 kilometers west of the Orocopia Mountains (fig. 2). This strand, as well as the Hidden Springs Fault a short distance to the east (fig. 2), are currently active and cut across recent alluvium in the Mecca Hills (Sylvester and Smith, 1975). More important in the evolution of the Diligencia Basin, is one of the abandoned splays of the San Andreas system, the Clemens Well Fault.

The Clemens Well Fault is a major, high-angle structure which forms a stark lineament across the central Orocopia Mountains (fig. 2). The fault has been most often interpreted as a dextral strike-slip fault, and displacement across the structure is poorly known. Rock units older than Quaternary are truncated by the fault (fig. 2). However, no clear, off-set markers occur, and attempts at correlation of basement lithologies across the fault give offset estimates from several kilometers to 175km (Crowell, 1975b; Powell, 1982). Some workers report the occurrence of blue quartz and anorthosite clasts high in the Diligencia section, suggesting that there has not been more than several kilometers of

offset along the Clemens Well Fault since late Diligencia time. However, the degree of post-sedimentary deformation of the Diligencia sediments indicates significant tectonic activity (Crowell, 1975a; Spittler and Arthur, 1982).

2.4.4 East-west Striking Faults

The final set of structures to be discussed are probably very close in age to the faults of the San Andreas system. These faults comprise a series of nearly east-west trending structures including the Chiriaco and Salton Creek faults (fig. 1). These faults are not exposed at the surface, as they are covered with great thicknesses of sediments which fill the valleys between the local mountain ranges, but there is seismic evidence for high-angle discontinuities along these large, linear valleys (Terres, 1984). Sense of motion along these faults is not constrained by direct observation, however, paleomagnetic data suggest that dextral motion along these faults, in conjuction with motion on faults of the San Andreas system may have accommodated large-scale rotation of crustal blocks around vertical axes (fig. 7) (Terres, 1984; Luyendyk et al., 1985; Hornafius et al., 1986; Carter et al., 1987). Paleomagnetic reconstructions offer significant insight into the late stages of the evolution of the Diligencia Basin, and will be discussed in more detail later in this thesis.

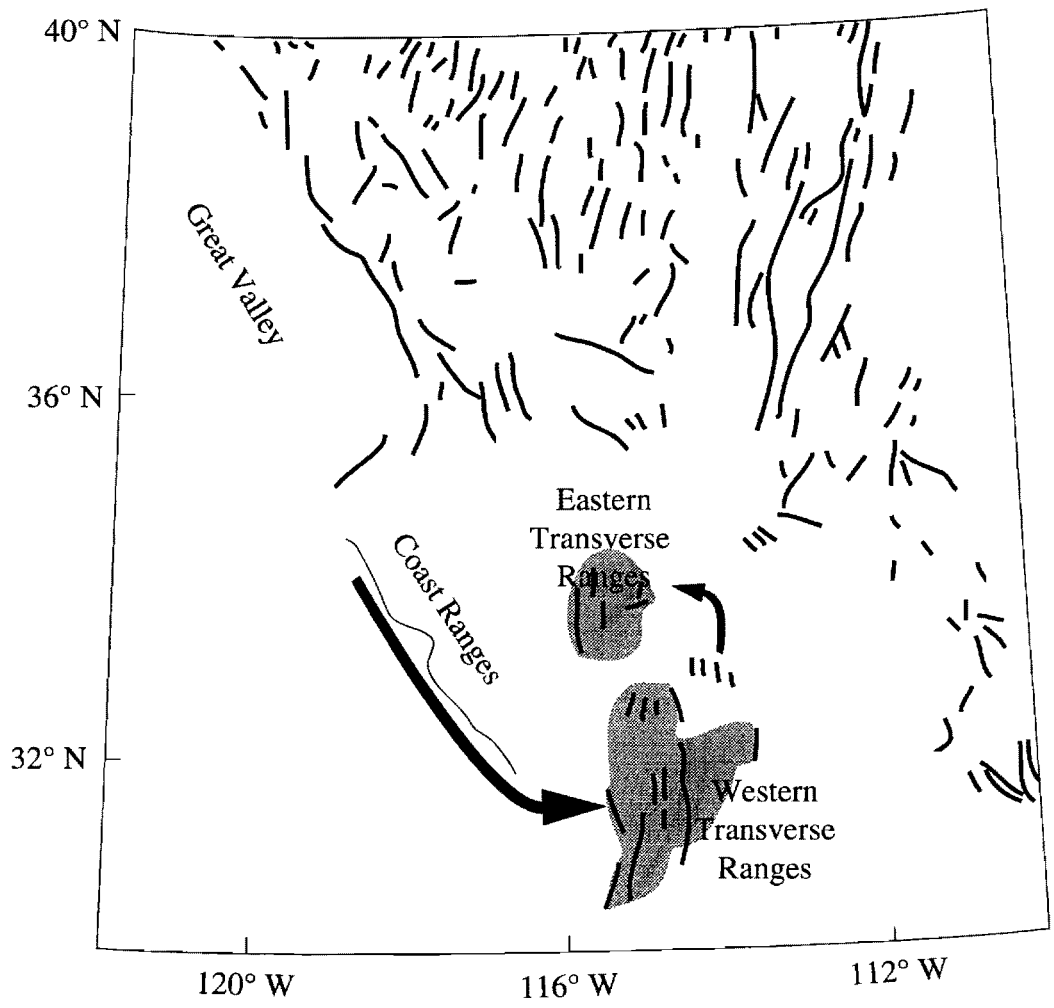

Figure 7. Late Oligocene-early Miocene palinspastic reconstruction of the southwestern United States showing the Transverse Ranges back-rotated and slip on the San Andreas Fault removed (from Luyendyk, et al., 1985).

CHAPTER 3. Structural Analysis of the Diligencia Basin

3.1 Methodology

3.1.1 Geologic Mapping of Basal Diligencia Formation

The basal units of the Diligencia Formation were mapped at a scale of 1:12000. The topographic base was provided by the U.S.G.S. Red Canyon 7.5 minute quadrangle, and parts of the Orocopia Canyon, Hayfield, and Cottonwood Spring 7.5 minute quadrangles. The topographic base from these quads was enlarged by a factor of 2 and used to make multiple ozalid copies. Following completion of fieldwork, the mapping was compiled onto original topographic quadrangle maps, at a scale of 1:24000 (Plate 1). Because only the lowermost units of the Diligencia Formation were mapped during this study, geological information for the remainder of the formation was compiled from the work of Arthur and Spittler (Arthur, 1974; Spittler, 1974). In the event of any conflict between maps during compilation, preference was given to the mapping completed by the author.

3.1.2 Structural Analysis

3.1.2.1 Analysis of Mapped Structures

Orientation data for mapped structures were compiled from field notes, and by direct measurement from geologic maps. Several different classes of structural data were analyzed by methods similar to those of Terres (1984), with the aim of making inferences of paleostress field orientation. The analysis presented incorporates many of the same data used by Terres, and augments this with data and data types collected during the fieldwork for this thesis. The classes of data analyzed include: bedding orientation, trend of minor fault traces, and trend of fold hinge traces. Whenever possible, data were taken from field notes, rather than measured from the map, in the hope of foregoing any error in transcription. Data were collected in areas not specifically covered by the mapping in

this project by direct measurement from the maps of Arthur and Spittler (Arthur, 1974; Spittler, 1974).

3.2 The Structural Geology of the Diligencia Basin

3.2.1 Structures associated with contacts between basement and sediment

The edges of the outcrop area of the Diligencia Formation have all been modified to some degree since deposition ceased. The edges of the outcrop, therefore, do not represent the original basin margins, but the erosional or tectonic remnants of the original basin. The low angle of dip and the extreme coarseness of the Diligencia Formation along the northern margin of the outcrop suggest that the present margin is a close approximation to the original basin margin. The southern margin of the outcrop area is more problematic. Because the contact, and the overlying sediments have been tilted to vertical along this margin, there is a possibility that considerable rock has been eroded away. References to the present basin margins should be understood to represent an approximation of the original basin margins.

The approximate margins of the Diligencia basin are defined by four different types of structural surface. The outcrop belt is presently an elongate trough whose axis trends west-northwest/east-southeast. The western end of the outcrop belt is truncated at an oblique angle by the Clemens Well Fault (Plate 1), while the eastern end of the trough is unconformably overlain by younger continental sediments. Sediments similar to the Diligencia Formation do not crop out anywhere to the east of the main sediment body. The southern margin of the basin is a buttress unconformity, against which sediments of the Diligencia Formation overlie pre-Cambrian basement, while the northern margin of the basin is the inferred position of the normal fault system along which extension was localized. Chapter 4 presents the sedimentological portion of the project and interpretations of fault geometry will be developed based upon this information.

3.2.1.1 Basin formation structures along southern margin

Along most of its length, the contact between basement and sediment is a buttress unconformity that has been tilted to vertical or slightly overturned. Sedimentary beds are commonly observed to lap onto basement at an angle of less than 40°, without disruption, even when observed beds are thin and delicate (fig. 8). In areas with significant local basement paleotopography, however, the angle of unconformity can be greater than 60° (fig. 9). There is no evidence that the southern margin of the Diligencia Formation has never been active as a normal fault.

The southern nonconformity is locally offset by at least one, northeast/southwest striking fault which appears to affect the thickness of the basal sediment package on either side of it (see plate 1, east half of section 24). This fault has a normal sense of offset when rotated back to an inferred original orientation. Growth faults of this type are more common higher in the section, and the presence of this fault, and several others which may have formed sub-basins of smaller scale, indicate that in addition to a major component of extension sub-perpendicular to the basin axis, some minor component of extension at a low angle to the basin axis must have existed.

3.2.1.2 Basin inversion structures along southern margin

Along several segments of its length, the southern basement-sediment contact has been activated, under compression, as a reverse fault. In addition, a system of reverse faults parallel to the southern margin are inferred from bedding orientations which appear to represent thrust culmination cut-off angles. Along segments of the sediment-basement contact which have been activated under compression, the sediments have detached at the contact with basement, and reverse sense displacement has occurred between the rocks on either side of the active contact. Activated segments of the southern contact are generally only several tens of meters long, and are always defined by a layer of fault gouge concordant to the basement surface. One structurally activated segment of the contact,

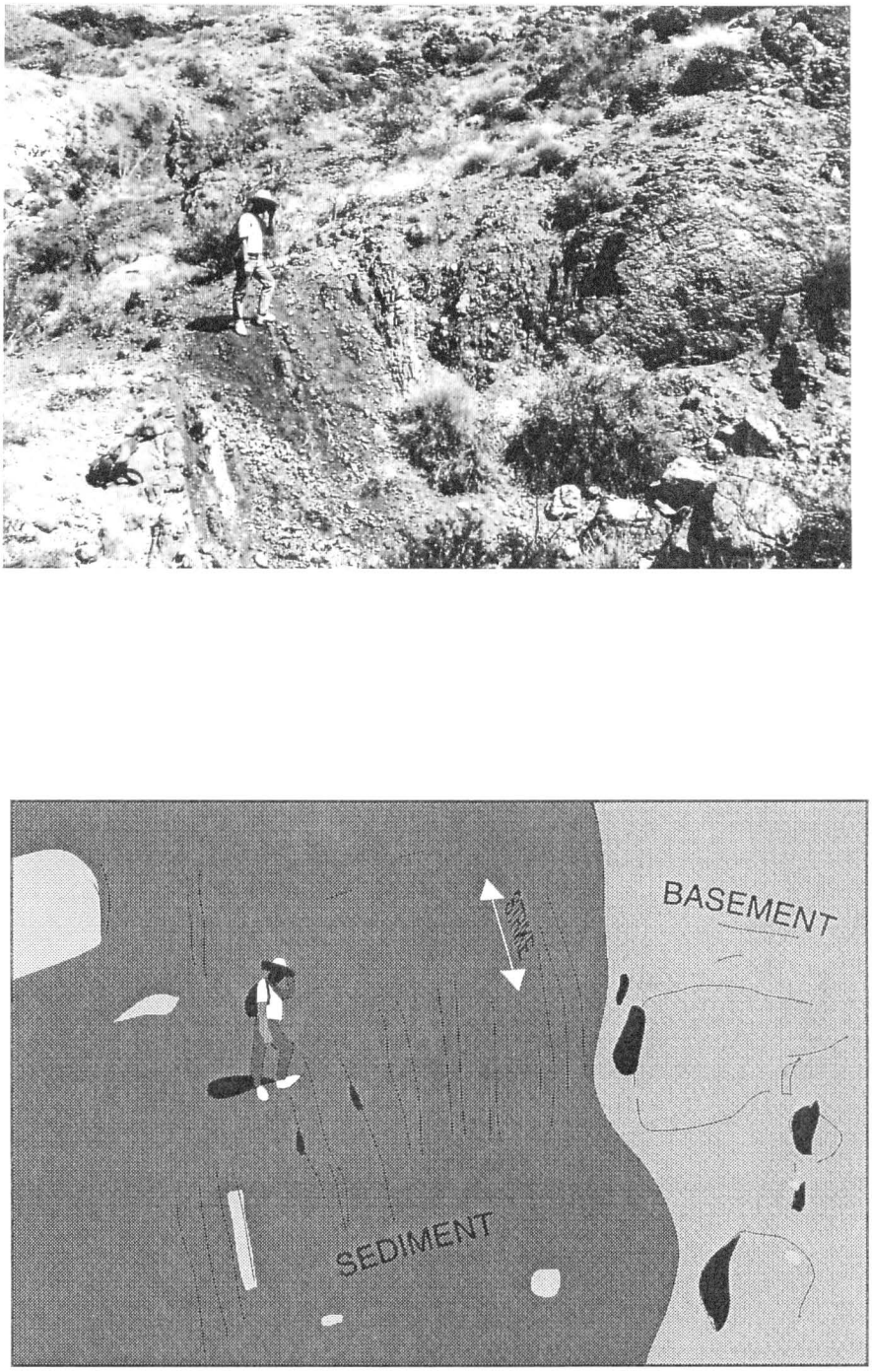

Figure 8. Photograph and interpretive sketch of low-angle nonconformity between Proterozoic basement and overlying Diligencia Formation.

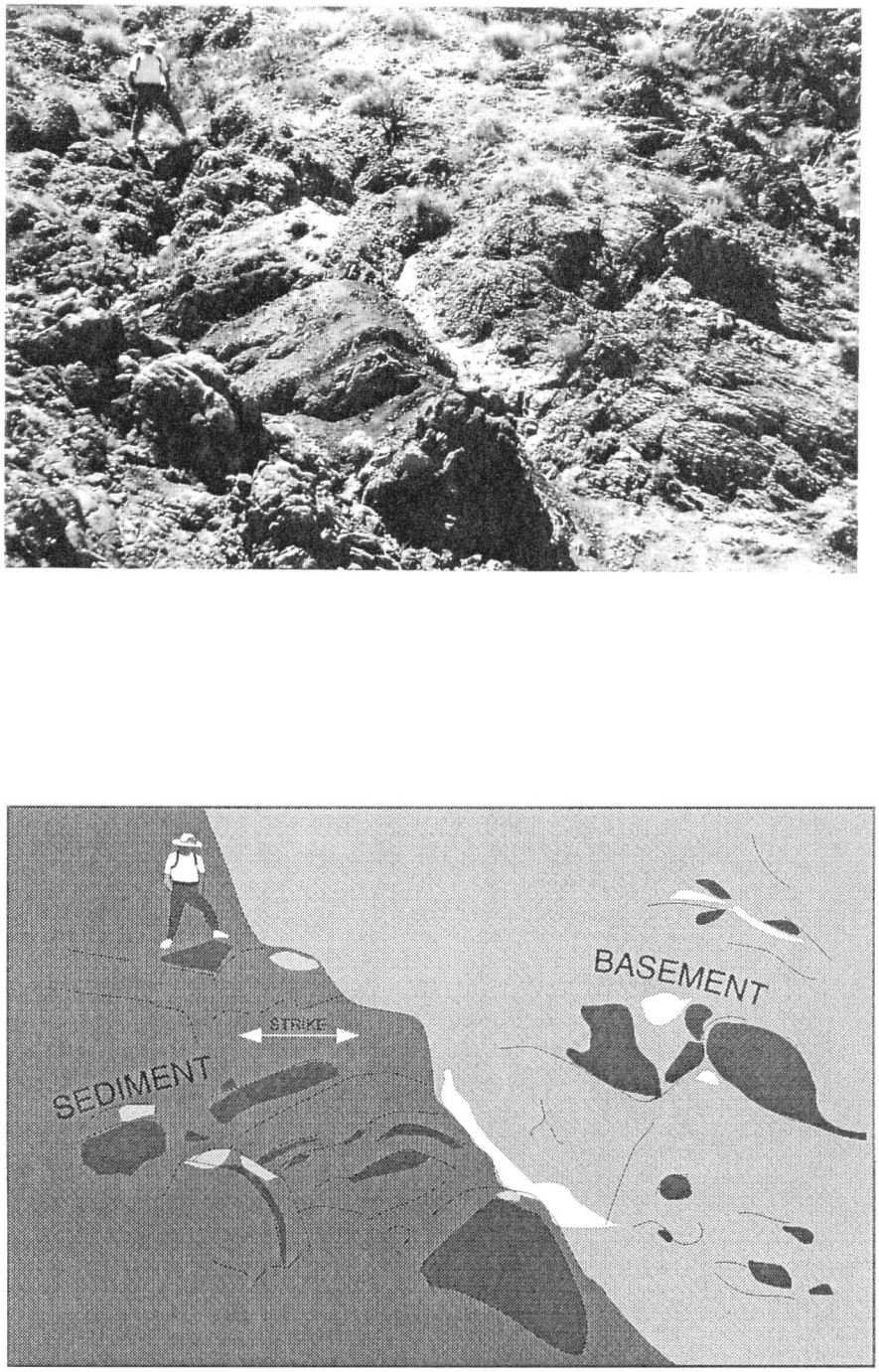

Figure 9. Photograph and interpretive sketch of high-angle nonconformity between Proterozoic basement and overlying Diligencia Formation.

located in the northeast quarter of section 23, is significantly longer than any other, and is defined not only by a thick gouge zone, but also by anticlinal folding of the sediments above the contact (fig. 10).

This structure is the best exposed example of a structure associated with basin inversion. However, structures with similar geometries and orientations are inferred from bedding orientation data taken near the contact between the first two informal map units in the Diligencia section. Local segments along the contact between the basal sandstones and the overlying mudstones of the lower Diligencia Formation are observed to be characterized by significant changes in dip angle over short distances. Figure 11 shows a generalized map of one such segment, and an interpretive cross-section. Bedding along these segments generally strikes in a constant direction. However, dip angle, and locally, dip direction, vary in a manner which suggests thrust fault cut-off geometries (fig. 11). Although the inferred thrust culminations are never observed in cross-section, the dip anomalies are observed in several places along a trend roughly parallel to the basal contact, and the inferred geometry is consistent with better constrained basin inversion structures, which are observed along the southern sediment/basement contact.

3.2.1.3 Basin formation structures along the northern margin

The nature of syndepositional normal faulting associated with the Diligencia Basin is a significant aspect of this study. Although such faults are not extensively exposed in the Orocopia Mountains, their influence is apparent from a detailed study of the sedimentary fill of the Diligencia Basin. The discussion of the basin-bounding normal fault system will be developed in detail in chapters 4 and 5, based upon interpretations from the sedimentological portion of this study. However, the direct evidence for the presence of extensional faults on the margin of the basin does bear discussion and is presented here.

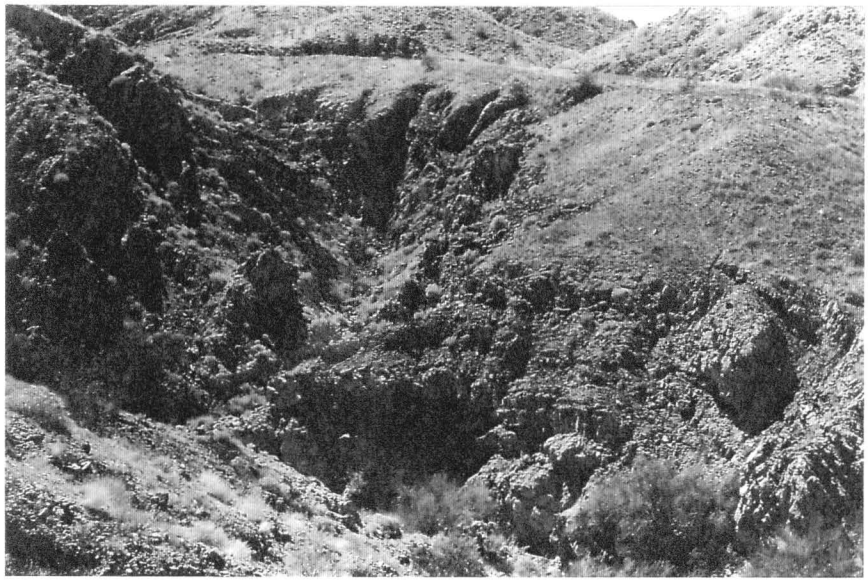

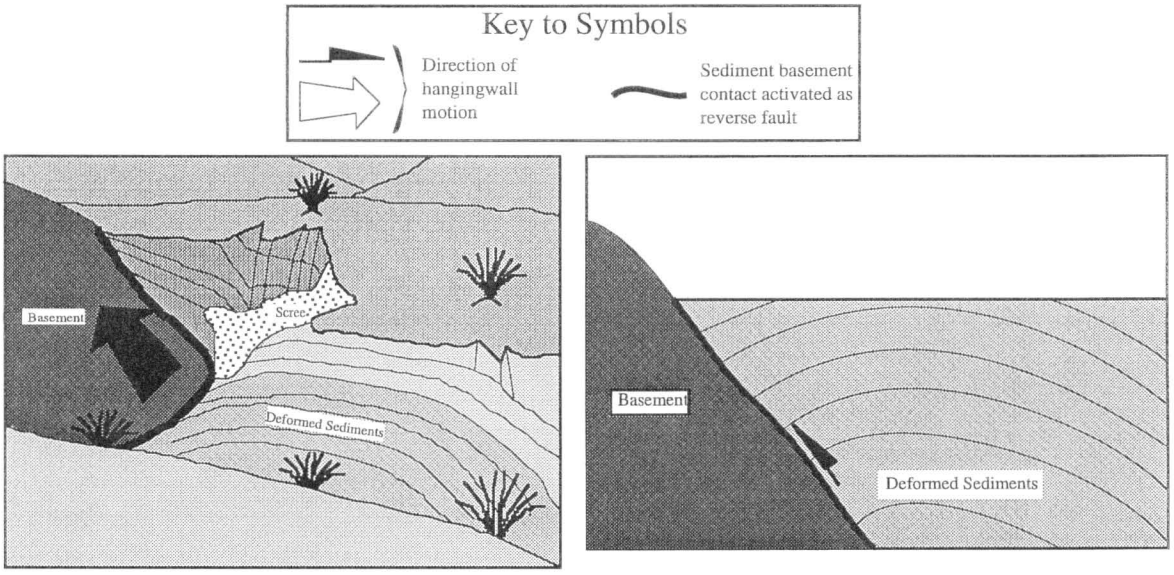

Figure 10. Photograph and diagrammatic sketches of a segment of the southern nonconformity surface that has been subsequently activated as a reverse fault.

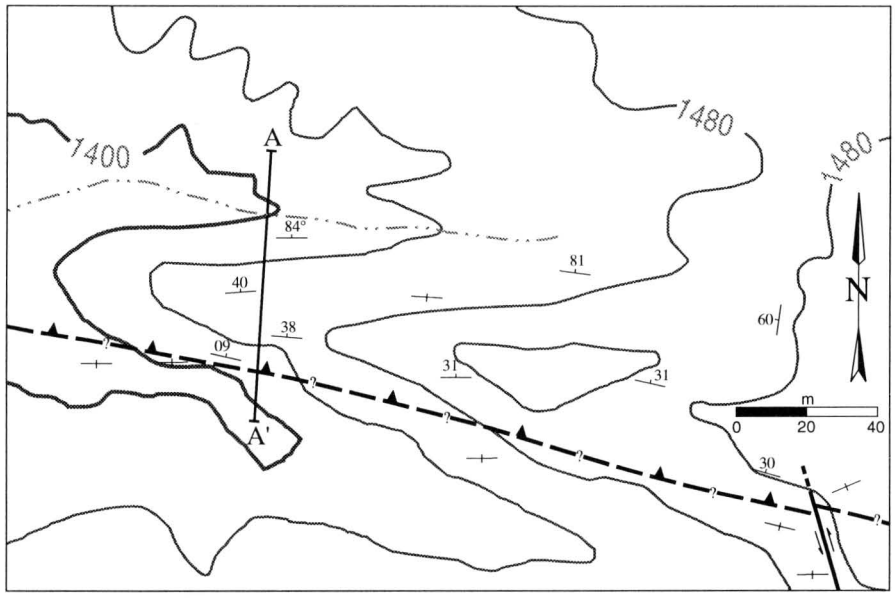

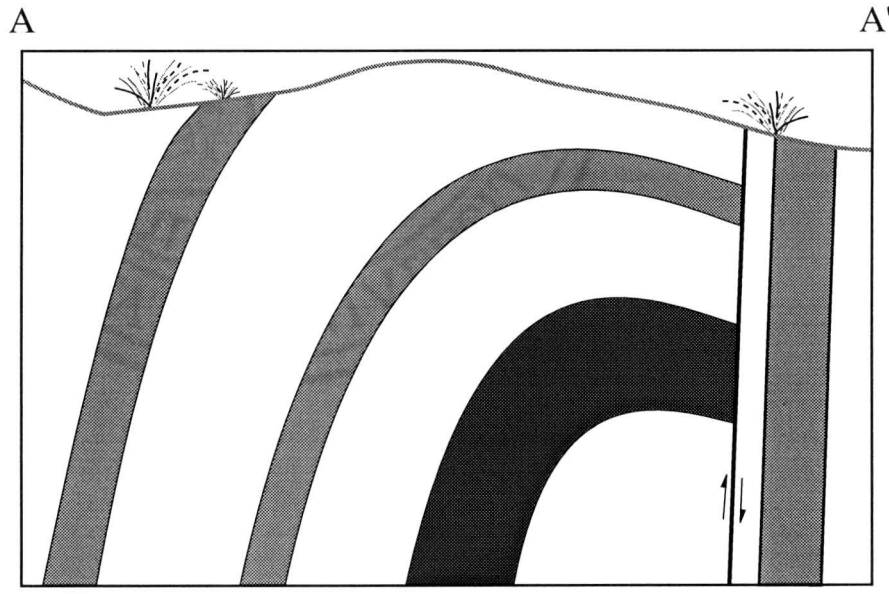

Figure 11. Generalized geologic map and cross-section of a portion of the lower Diligencia Formation. The presence of reverse faulting and development of a thrust culmination in the hangingwall are inferred from bedding orientation relationships.

The contact between basement and sediment on the northern margin of the Diligenica Formation is not well exposed anywhere along its length. Large areas of the northern margin are covered by Quaternary alluvium, masking any evidence of the nature of the marginal structure. A contact between undoubted granitoid basement and definite Diligencia sediment is directly observed only in a single location, on the western end of the northern margin. Along the northwestern-most segment of the approximate basin margin, the contact between basement and sediments of the Diligencia Formation is fairly sinuous (Plate 1). One large arroyo cuts across the contact at a high angle and in the wall of the canyon is exposed a subhorizontal gouge zone separating granitoid basement below from monolithologic granitic breccias above (fig. 12). No fabric is developed within the gouge and no offset markers are apparent. The sense of motion on the fault is therefore constrained only by the observation that the fault emplaces unmetamorphosed Tertiary sediments above Mesozoic crystalline basement. While the observation of this structure, in isolation, is not compelling, it is significant in that it documents the presence of low-angle normal faulting on the northern margin of the Diligencia Basin and strongly resembles similar structural/sedimentological associations observed in Tertiary rift basins in the Colorado River region of the Basin and Range Province(Miller and John, 1988; Fedo and Miller, 1992).

3.2.2 Post-depositional deformation within the Diligencia Basin

3.2.2.1 Clemens Well Fault Zone

The mapped position of the Clemens Well Fault displays a remarkably straight, constant trend of approximately 145°, along the portion of its length where its position is well constrained (Plate 1). While it is nowhere seen in cross-section, its straight map pattern suggests that it is an approximately vertical fault, and it is generally considered to be an oblique slip fault with a large component of dextral strike-slip displacement across it (Crowell, 1975a; Spittler and Arthur, 1982). Topographically, the fault is defined by a

Figure 12. Photograph of low-angle normal fault exposed near western end of northern basin margin.

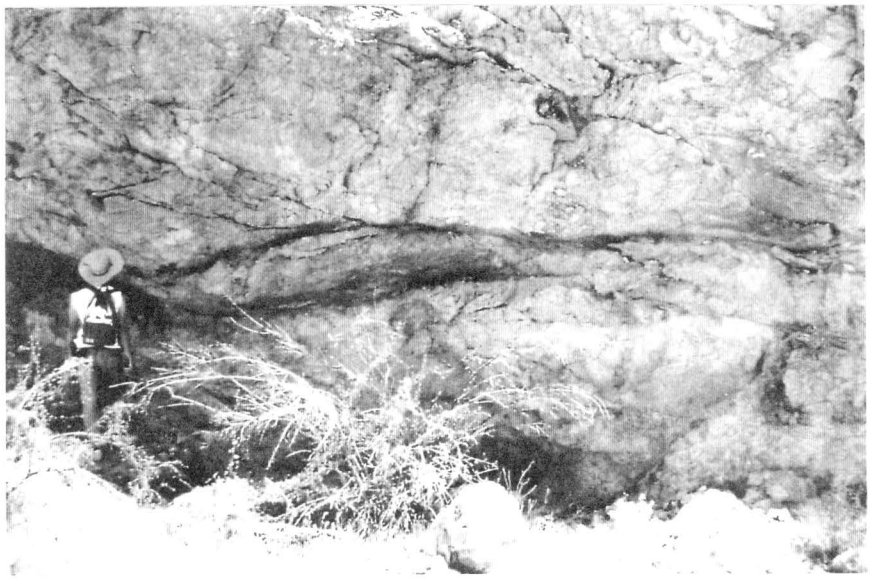

linear canyon 50m-150m wide. The shear zone itself is generally covered by Recent gravel in the canyon bottom, but where it is more readily observable, the zone appears to be fairly discrete, no more than 25m wide. Slivers of basalt associated with the Diligencia Formation have been caught up in the fault zone, and indicate a minimum dextral displacement of 900m across the Clemens Well Fault (Crowell, 1975a; Spittler and Arthur, 1982). Some workers have identified the Clemens Well Fault as a potential proto-San Andreas structure with up to 175km of offset based on correlation of basement terranes (Smith, 1977; Powell, 1981).

Elementary stress theory and numerous experimental studies indicate that brittle faults should form at an angle of approximately 30°-35° to the maximum principal compressive stress direction (Anderson, 1951). Given the trend of the Clemens Well Fault, the inferred maximum principle compressive stress direction was oriented approximately north-south. The stress field under which both the Clemens Well Fault formed and, it will be argued, the Diligencia Basin was deformed, must be a reflection of the middle to late Tertiary stress field in this region of California. The assertion that this inferred stress field may have been regionally important may be supported by the observation that along much of its length, the San Andreas Fault has an orientation which is roughly parallel to the orientation of the Clemens Well Fault. However, the San Andreas Fault system represents a major tectonic plate boundary, and Andersonian Fault theory may not adequately explain its development. Recent analysis of modern stress fields along the San Andreas Fault indicate that currently, the direction of maximum horizontal stress is generally oriented almost perpendicular to the strike of the fault at any point along its length (Mount and Suppe, 1992). These observations suggest that the stress field in this portion of California must have changed significantly since the late Tertiary.

3.2.2.2 Minor Structures

Numerical orientation data were analyzed using standard analytical techniques (Marshak and Mitra, 1988). The result of each aspect of the structural analysis will be discussed in detail in the following sections. Planar structural data were plotted on an equal area stereonet, and the resulting distribution contoured using the program STEREOPLOT (Mancktelow, 1989), on a Macintosh computer. Linear structural data such as fold hinge trace data, and fault trace data were recorded as azimuthal trends. These were taken from field notes where directly observed, and measured from maps where necessary. In areas not covered by the mapping associated with this project, data were collected from the maps of Arthur and Spittler (Arthur, 1974; Spittler, 1974). Azimuthal trend data were plotted on rose diagrams, using an interval of 5° for compilation of segments

Folds

In the southern portion of the Diligencia Basin, the sedimentary fill has been deformed into a series of faulted folds. These structures are dominated by a train of three large folds, two synclines separated by an anticline, and numerous associated minor folds (Plate 1). The three major folds plunge gently to the WNW, and are oriented approximately parallel to the long axis of the basin. The folds are progressively more open and of lower amplitude from south to north. An analysis of the southernmost syncline-anticline pair is shown in fig. 13. For each fold, a least-squares method was used to construct a best-fit great circle through the maxima on the π-plots. Field observations indicate that folding in the Diligencia Formation is approximately cylindrical. In figure 13, the inferred hinge axis for each fold is shown to plunge gently toward the WNW. In addition, the angle, within the fold profile plane, between the contoured maxima of the π-diagram represents the average interlimb angle of each fold.

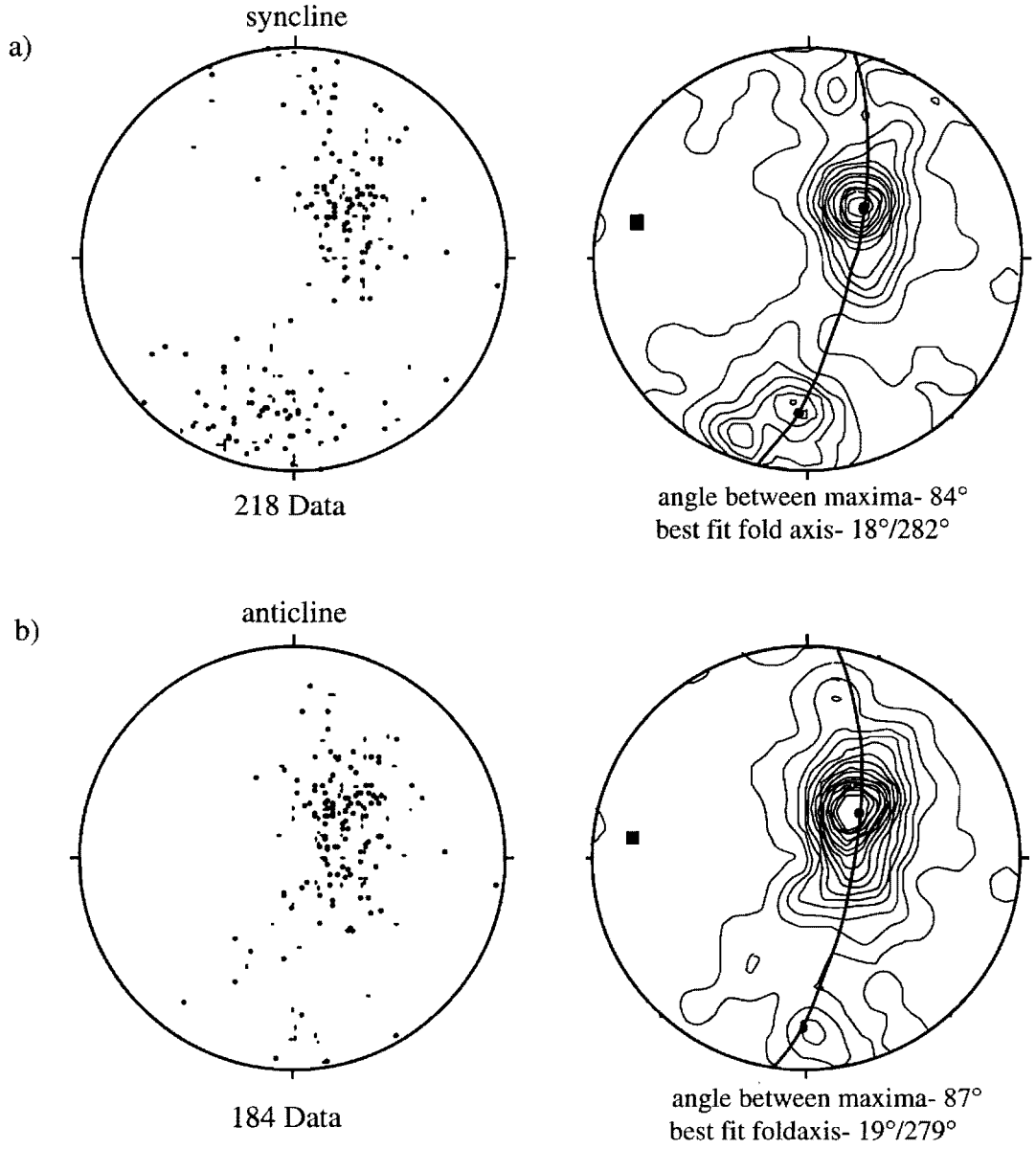

Figure 13. Stereographic analysis of the major syncline-anticline pair located immediately north of the southern basin margin. a) Analysis of southernmost syncline. Figures show poles to bedding orientations from fold and contoured plot of same data. Also shown are best-fit fold profile plane, and fold hinge. b) Analysis of southernmost anticline. Figures show poles to bedding orientations from fold and contoured plot of same data, with best-fit fold profile plane, and fold hinge. See text for discussion.

These analyses support the field observations that the folds are approximately parallel and that the interlimb angle increase (albeit, only modestly) from south to north.

Data related to fold orientation were also analyzed by recording trends of fold hinge traces for all map scale folds in the Diligencia Formation. In cases where the trend of a fold hinge is arcuate, multiple measurements were made in an attempt to avoid averaging out significant data during collection. Azimuthal data of fold hinge trace trends were plotted on rose diagrams. The data are sorted into two groups, those from the southwestern portion of the outcrop belt, and those from the northeastern portion of the outcrop belt. This separation was suggested by the observation that lineaments on the map appear to curve into the Clemens Well Fault as they approach its trace (Plate 1). The vector mean orientation of fold hinge traces in the western part of the outcrop belt is approximately 20° different from the mean trend in the eastern portion (fig. 14). If this difference in orientation is considered to be the result of rotation of passive linear markers into the dextral shear zone of the Clemens Well Fault, then the folds in the eastern portion of the area should give a more satisfactory estimate of maximum compressive stress direction, than do those in the western portion. In fact, the direction of maximum compression inferred from the eastern portion of the area, taken to be perpendicular to the mean fold hinge trend, is 012°, roughly parallel (within about 10 degrees) to that inferred from the orientation of the Clemens Well Fault in the discussion above.

Minor faults

Two broad categories of faults cut across the sediments of the Diligencia Formation. The largest well-exposed faults in the area are long, sigmoidal strike-slip faults in the eastern half of the basin (Plate 1). These faults are remarkable in that the magnitude of displacement across them decreases very suddenly to zero near their ends from a maximum near the middle portion of the fault (Plate 1). Structures commonly observed at wrench fault terminations or points of displacement transfer, such as horsetail

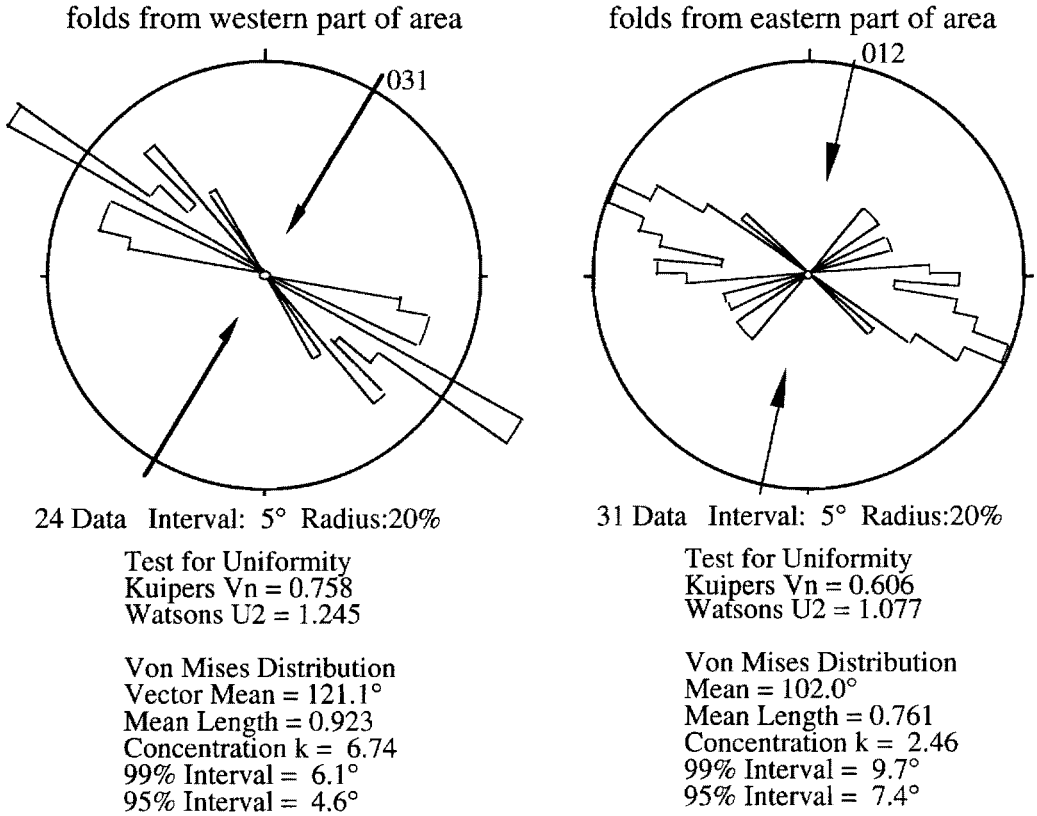

Figure 14. Circular histogram plots of fold hinge trends from different areas of the Diligencia Formation. Direction of maximum compressive stress (represented by arrows) is inferred to be oriented perpendicular to the vector mean of the hinge trends. The inferred maximum compressive stress direction derived for folds from the western portion of the area is rotated with respect to the analogous value for data from the eastern portion of the area. This observation may be explained by rotation of folds into the Clemens Well Fault zone, west of the basin.

splays, overstepping fault arrays or dilational jogs, have not been observed in the field. In the absence of common termination structures, these structures are interpreted as tear faults (fig. 15). If this interpretation is correct, then the faulting must have developed synchronously with folding of the basin fill.

The second category of faults in Diligencia Formation consists of numerous short, dextral and sinistral wrench and oblique slip faults. In general, these faults are either oriented NE-SW, or NW-SE. While exceptions do occur, those faults which strike NW are commonly dextral and those which strike NE are commonly sinistral, based upon observed offset of markers. The arrangement of faults is suggestive of a conjugate pair of fault sets, and this relationship is explored in figure 16. Trends of minor fault traces were collected and plotted on a rose diagram. Data were separated into two groups, those from the northeast portion of the area, furthest from the Clemens Well Fault, and those from the southern portion of the area. Faults trends from the northeast, are observed to form a diffuse spread on the rose diagram (fig. 16). However, both the Kuiper's and Watson's statistical tests indicate that this distribution is less than 95% likely to have been drawn from a uniform distribution. If the faults are separated by sense of offset into dextral and sinistral fault sets, they segregate into one tight cluster with a vector mean of 151°, and one diffuse cluster with a vector mean of 046°. Elementary stress theory predicts that the maximum principal compressive stress axis will bisect the acute angle between conjugate faults. If these two populations of faults are considered a conjugate set, then the inferred stress direction is about 9° east of north, less than 10 degrees away from the stress direction inferred from the Clemens Well Fault and the analysis of folds described above.

The trends of the faults in the southern portion of the field area cluster into one relatively tight grouping (fig. 16). The vector mean trend of these data is approximately 057°, which places the inferred maximum stress direction in an orientation of 022°. This inferred stress direction is oriented approximately 13° clockwise from the stress direction

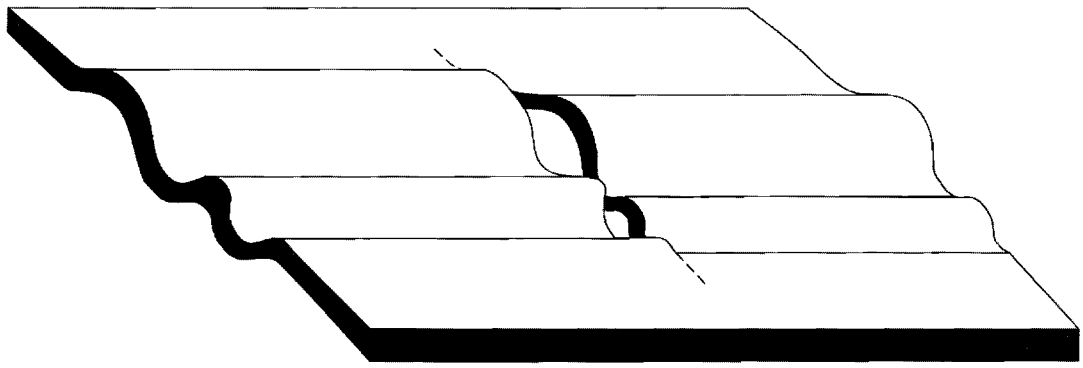

Figure 15. Schematic diagram of the synchronous development of a tear fault during folding. The resulting structure has the greatest magnitude of offset along segments near the middle of the fault, and displacement drops to zero, over a very short distance, near each end.

Figure 16. Circular histogram plots of minor fault trace trends from different portions of the Diligencia Formation. Direction of maximum compressive stress (represented by arrows) is inferred to be oriented at 35° to the vector mean of the fault trends in a), and to bisect the angle between the two means in b). Part b shows the same set of fault orientations, broken into two groups by apparent sense of offset. Sense of offset was determined from field observations where available, and from map pattern where necessary. The inferred maximum compressive stress direction derived for folds from the western portion of the area is rotated with respect to the analogous value for data from the eastern portion of the area. This observation may be explained by rotation of faults into the Clemens Well Fault zone, west of the basin.

a) Faults from western portion of area

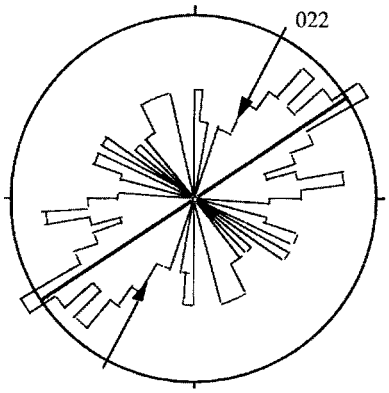

Test for Uniformity
Kuipers Vn = 0.362
Watsons U2 = 0.599

Von Mises Distribution
Vector Mean = 57.4°
Mean Length = 0.402
Concentration k = 0.88
99% Interval = 16.4°
95% Interval = 12.4°

59 Data Interval: 5° Radius:10%

b) Faults from eastern portion of area

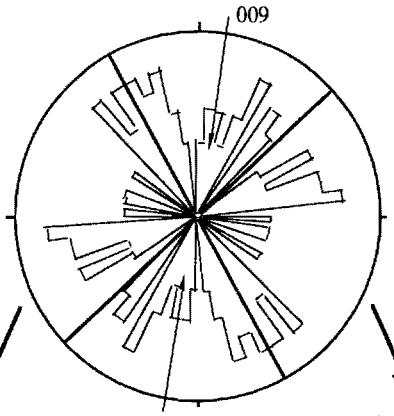

Test for Uniformity
Kuipers Vn = 0.222
Watsons U2 = 0.141

Von Mises Distribution
Vector Mean = 178.1°
Mean Length = 0.136
Concentration k = 0.27

60 Data Interval: 5° Radius:10%

Dextral

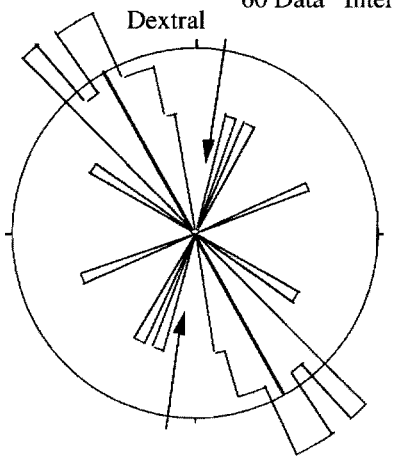

23 Data Interval: 5° Radius:10%

Test for Uniformity
Kuipers Vn = 0.659
Watsons U2 = 0.811

Von Mises Distribution
Vector Mean = 150.5°
Mean Length = 0.745
Concentration k = 2.34
99% Interval = 11.7°
95% Interval = 8.9°

Sinistral

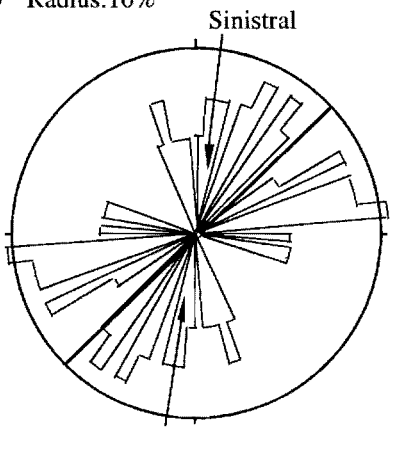

37 Data Interval: 5° Radius:10%

Test for Uniformity
Kuipers Vn = 0.344
Watsons U2 = 0.319

Von Mises Distribution
Vector Mean = 46.4°
Mean Length = 0.383
Concentration k = 0.83
99% Interval = 21.6°
95% Interval = 16.3°

inferred from the faults in the northeastern part of the area. An observation which may explain the difference between stress directions inferred from faults in different parts of the field area is that the minor faults in the western portion of the area curve into the Clemens Well Fault as they approach it (Plate 1). A similar relationship is observed in the trends of fold axes (fig. 14), and in that case, the difference has previously been attributed to rotation of linear elements into a dextral shear zone. The trends of the minor fault traces are interpreted to represent another example of passive linear markers having been rotated by shear along the Clemens Well Fault.

Fracture Analysis

Orientations of fractures, both barren and calcite-filled, were recorded in the field as strike and dip of planes. Data were selectively collected from fractures which did not exhibit evidence of significant shearing across them. Poles to these planes were plotted on an equal area stereonet, and the resulting π-plot contoured (fig. 17). In addition, the strikes of each plane were plotted on a rose diagram, again using an interval of 5° to construct the segments (fig. 17).

The π-plot exhibits two strong maxima with an acute intersection angle of 73° (fig. 17). Also shown in figure 17 is a rose diagram of the strikes of all measured fracture orientations. The modal orientation of the strike of fractures is approximately 010°. It is suggested that these fractures represent extension cracks, rather than shear fractures, and several examples were observed to be filled with concentrically zoned calcite layers, which exhibited no evidence of shearing across the fractures. Extension fractures form by dilation in the direction of the least principal compressive stress. The fracture is then oriented parallel to the plane containing the other two principle stress axes (see discussion in Ramsay and Huber, 1987). The structural data discussed in the previous sections imply remarkably consistent estimates for the orientation of the maximum principle compressive stress direction. The modal strike of the fracture planes across the

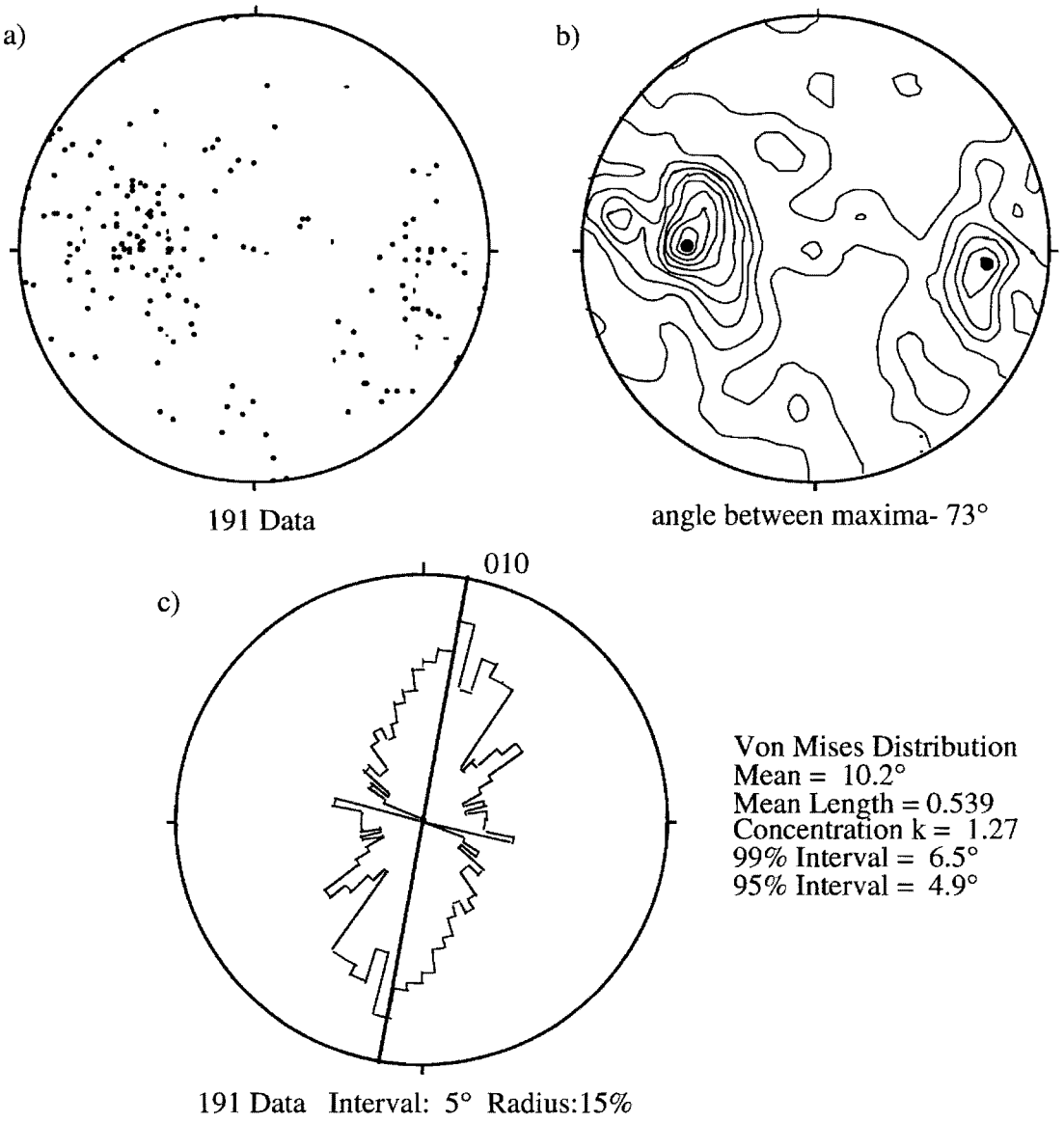

Figure 17. Stereographic analysis of fracture orientations from the Diligencia Formation. Part a) shows a scatter plot of the orientation data, and part b) show the same data contoured and the orientations of the two maxima. A circular histogram plot of strike of extensional fracture planes is given in part c). The inferred direction of maximum compressive stress (010) is taken to be parallel to the vector mean of strike, and is shown by heavy line.

Diligencia basin lies nearly parallel to the maximum compressive stress direction inferred from each of the other sets of structural data. If the interpretation of these fractures as extension features, rather than shear features, is correct, then the two dilational fracture sets cannot consist of a conjugate pair. If two principal compressive stress axes are assumed to be oriented horizontally at all times, there is no readily obvious explanation for the presence of two sets of extensional fractures with similar strikes and opposite dip directions. More data, and more detailed documentation of the natures of the various fractures recorded may clarify this anomaly.

Paleomagnetic Data

The final type of data which may shed light on the post-depositional structural evolution of the Diligencia Basin is paleomagnetic declination data. While this subject is beyond the scope of the present project, this section is the appropriate place to review the geophysical work that has been conducted on the paleomagnetic signatures from the basalts in the Diligencia Formation (Terres, 1984; Hornafius et al., 1986).

Paleomagnetic declinations recorded in basalts of the Diligencia Formation vary systematically with distance from the Clemens Well Fault (fig. 18). Declinations closer to the fault zone are increasingly rotated in a clockwise direction, with respect to those data further from the fault. The difference between the orientations closest to the Clemens Well Fault, and those furthest from the fault is between 80°-115° (Terres, 1984). If the declinations are considered passive linear markers, and the difference in orientation is assumed to be due to rotation into a dextral wrench fault zone, then simple shear must be responsible for up to 100° of clockwise rotation. While both the fold hinge and fault trend data discussed above exhibit apparent rotation into the fault zone, the amount of rotation is more than five times greater in the paleomagnetic data. Terres (1984) proposed a model to explain the discrepancy between rotations observed in the structural data and those observed in the paleomagnetic data. He suggested that early in the

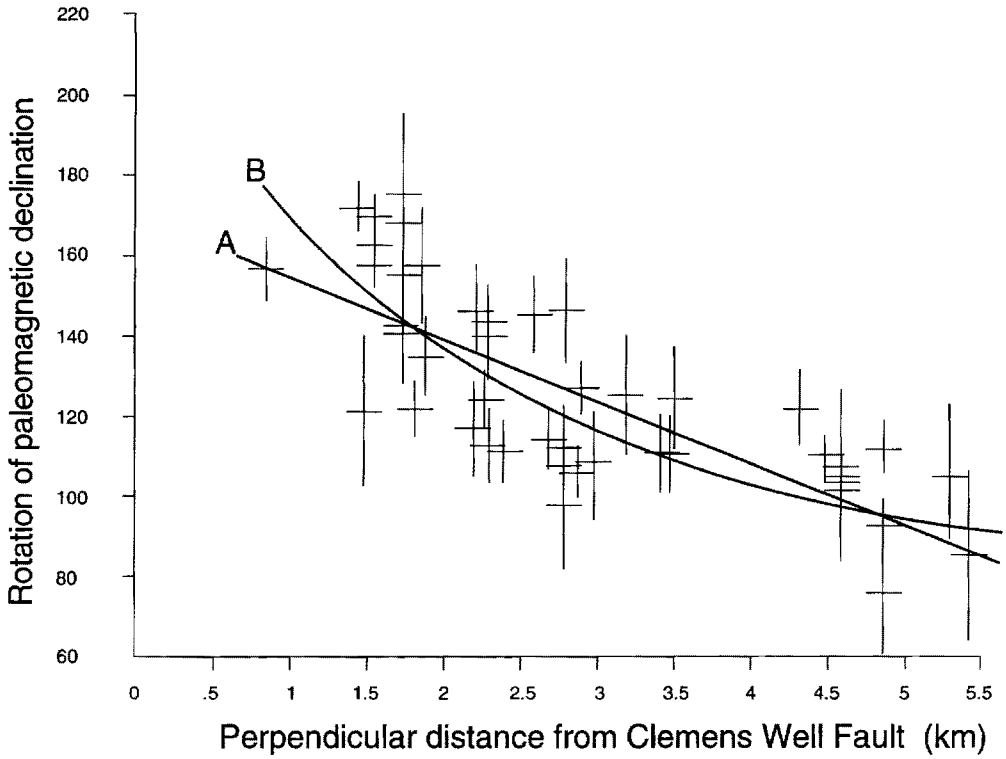

Figure 18. Diagram showing rotation of paleomagnetic declinations, measured from basalts of the Diligencia Formation, plotted with respect to distance from the Clemens Well Fault zone. Rotation of declinations increases with proximity to the fault zone. A and B are linear and non-linear regressions through the data, respectively.

deformational history of the area, a large amount of rotation about a vertical axis, perhaps 40° of clockwise rotation, was taken up by pervasive, ductile-appearing, shear of the basin fill rocks (Terres, 1984). This distributed shear may have taken place at all scales, from intergranular shearing, to pervasive fine fracturing. This hypothesized, 'ductile-appearing' shearing would be responsible for accommodating significant rotation, without the development of discrete deformation structures, including folds and map-scale faults. In Terres' model, the orientations of map-scale structures only record the later stages of deformation associated with motion on the Clemens Well Fault. While this model is basically a hypothetical construction, and there is no clear evidence for Terres' distributed, ductile-appearing shearing, it is interesting to recognize that the paleomagnetic declinations exhibit similar structural trends to the other potential strain markers discussed above.

CHAPTER 4 Sedimentological/Stratigraphic Analysis of the Diligencia Basin

4.1 Methodology

4.1.1 Measurement of Stratigraphic Sections

Five stratigraphic sections were measured through the lower Diligencia Formation (figs. 19, 20a-e). Four of these sections are located along the southern margin of the basin, and one is located on the northern margin (fig. 19). Precise locations of each measured section can be found in Appendix 2. Exposure of the basal units of the Diligencia Formation is discontinuous along the northern margin, where large segments of the margin are covered by Quaternary gravels. Only one section from the base of the Diligencia Formation through the lower units was located along the northern margin. Inspection of all outcrops of the lower Diligencia Formation along the northern margin of the basin indicate that the sedimentary rocks in the measured sections, while not continuous with rocks along strike, are nonetheless, representative of the sedimentary deposits along the northern margin of the basin.

Where possible, each section was measured in a location where the lower Diligencia Formation is observed, in outcrop, to overlie older rocks. The underlying rocks include pre-Tertiary crystalline basement, as well as the Eocene-age Maniobra Formation. Where exposure permitted, sections were measured from the basal contact with underlying rocks, up through the siliciclastic rocks of the lower Diligencia Formation to the first basalt unit greater than 30cm thick. Basalt is spatially widespread throughout the basin, and is therefore useful as an approximately isochronous marker in the Diligencia Formation. The lower Diligencia Formation, as defined here, varies in thickness in the measured sections, between approximately 120m and 400m.

The five measured sections will hereafter be referred to by the names of nearby landmarks. The sections are labeled on figure 19 with the initials of each informal

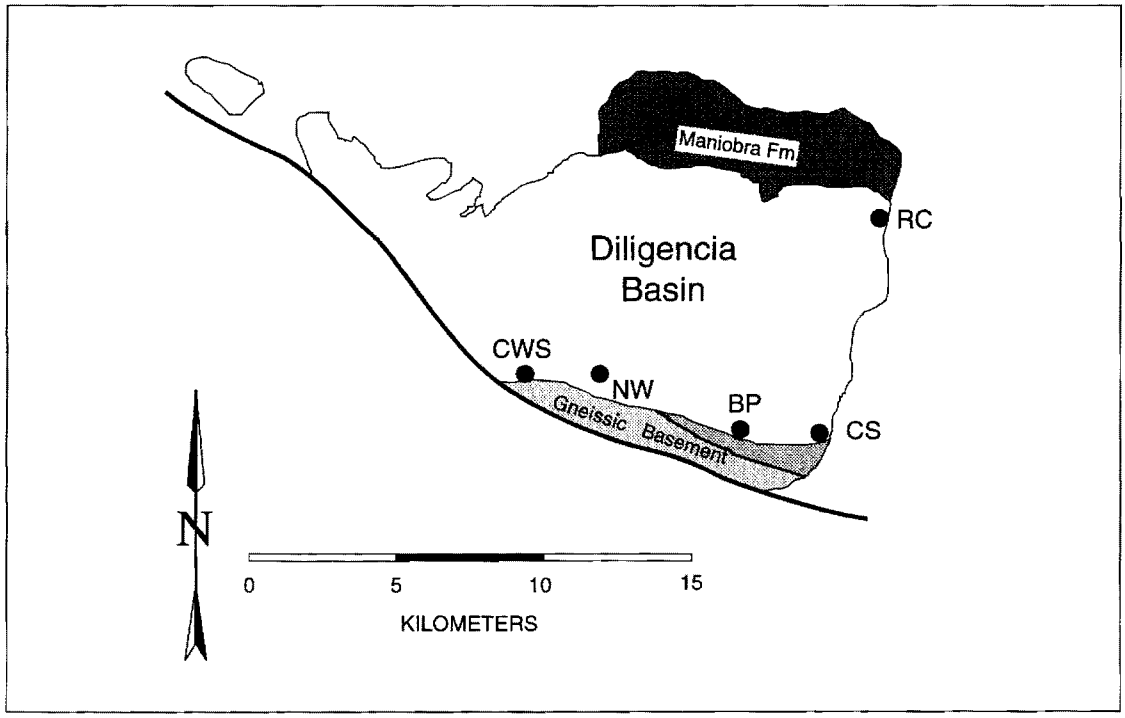

Figure 19. Schematic index map of Diligencia Formation showing locations of the five measured sections discussed in this text. Abbreviated names are: CWS- Clemens Well Saddle, NW- Name Wall, BP- Bullet Peak, CS- Canyon Spring, RC- Red Canyon.

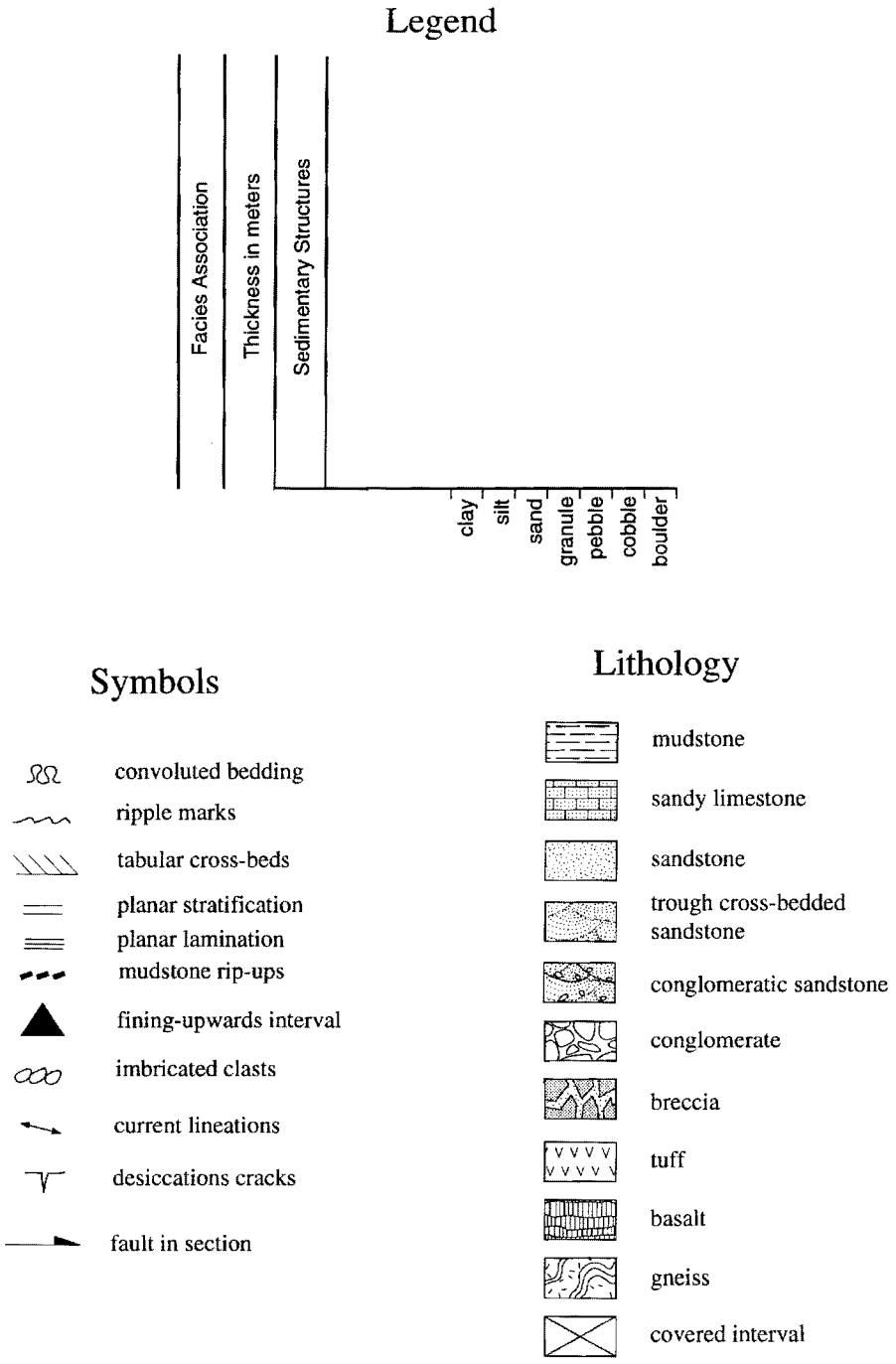

Figure 20. Graphic columns of measured sections described in text. Sections are named as in text, and as in Figure 19. Thicknesses of individual units on columns represent generalized package thickness. See text for description of precise bed thicknesses.

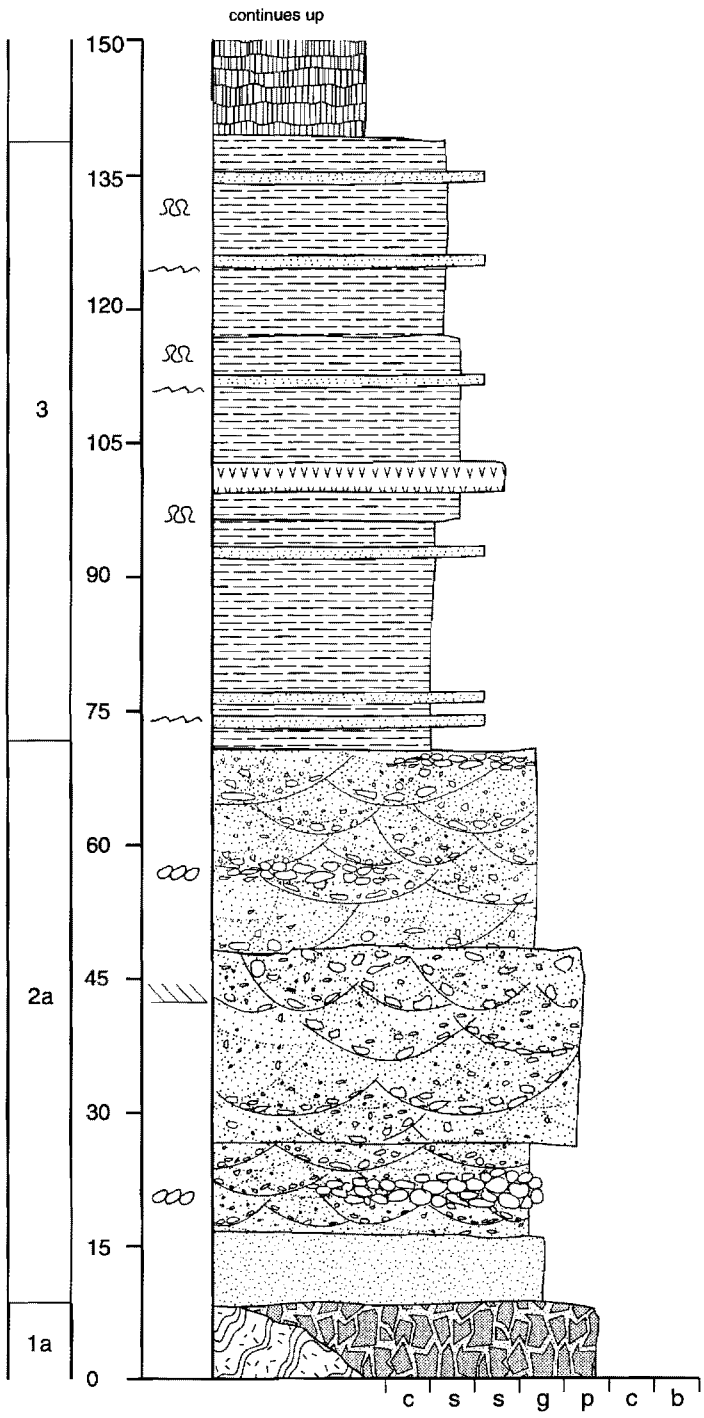

Figure 20a- Clemens Well Saddle Section

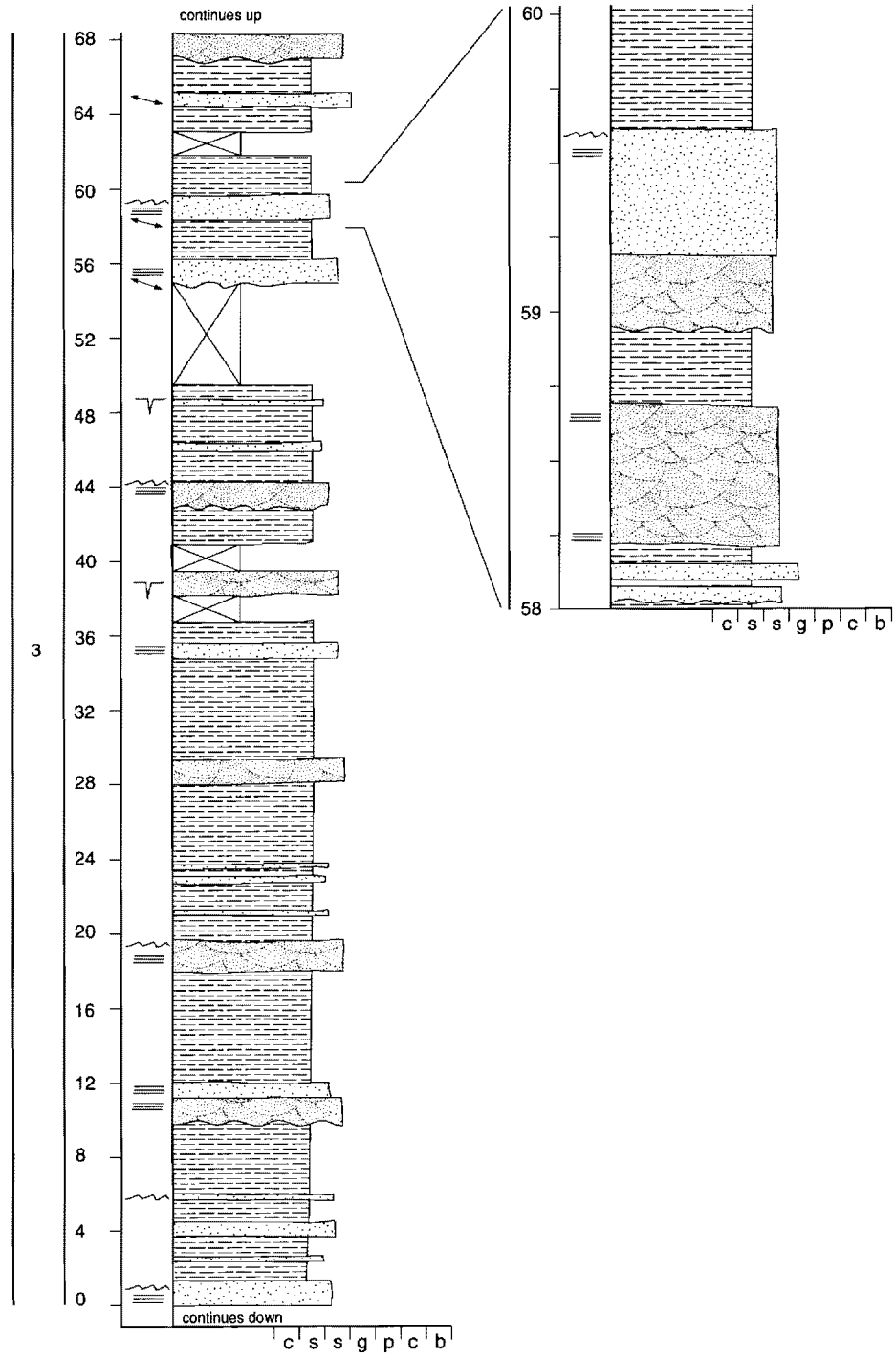

Figure 20b- Name Wall Section

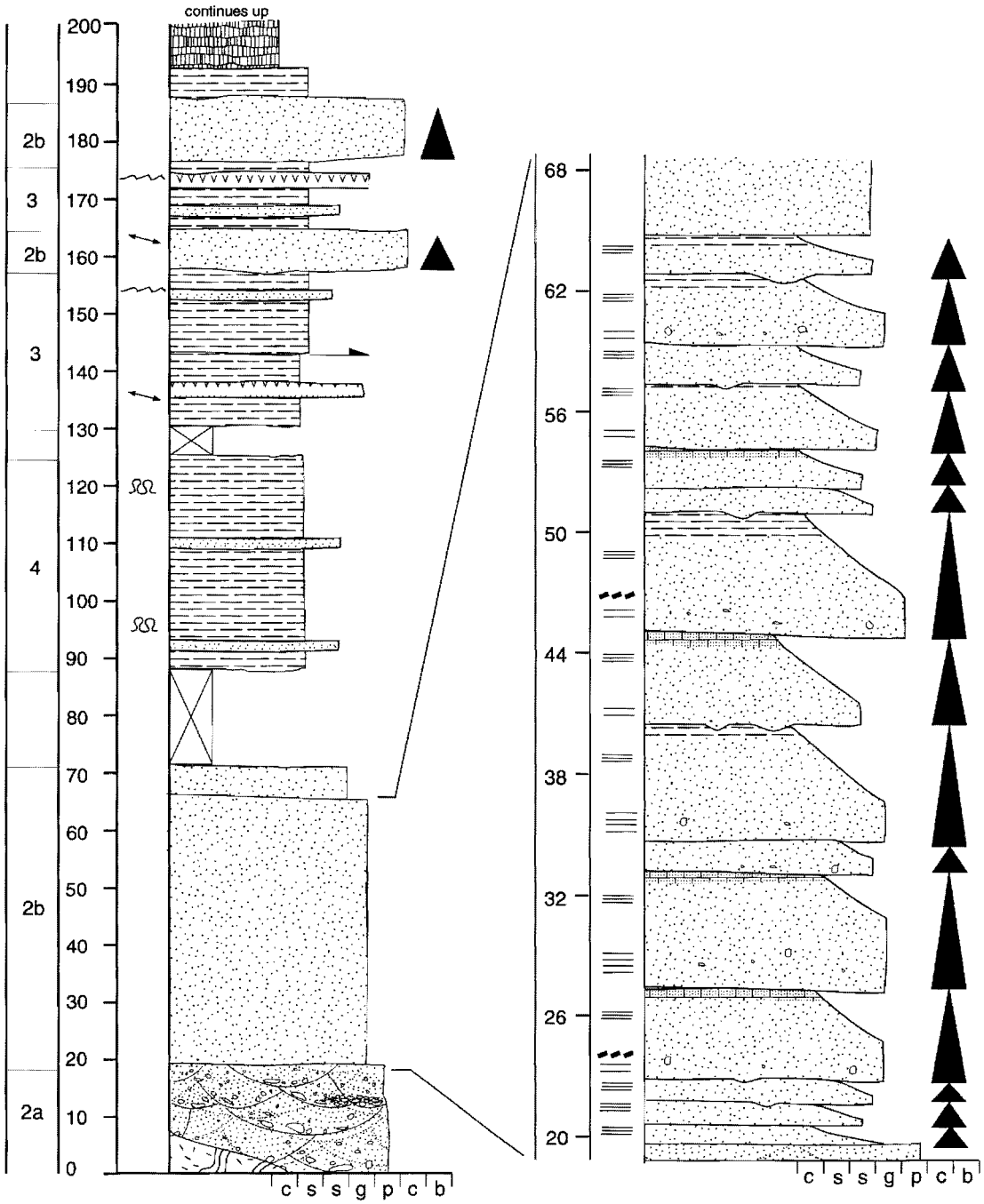

Figure 20c- Bullet Peak Section

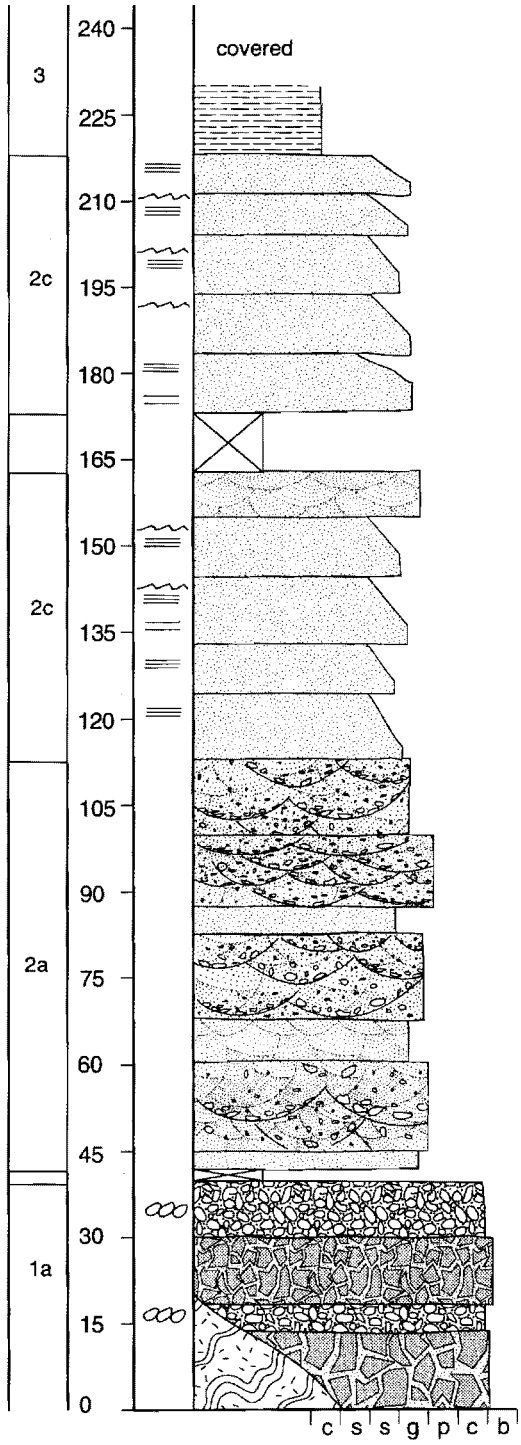

Figure 20d- Canyon Spring Section

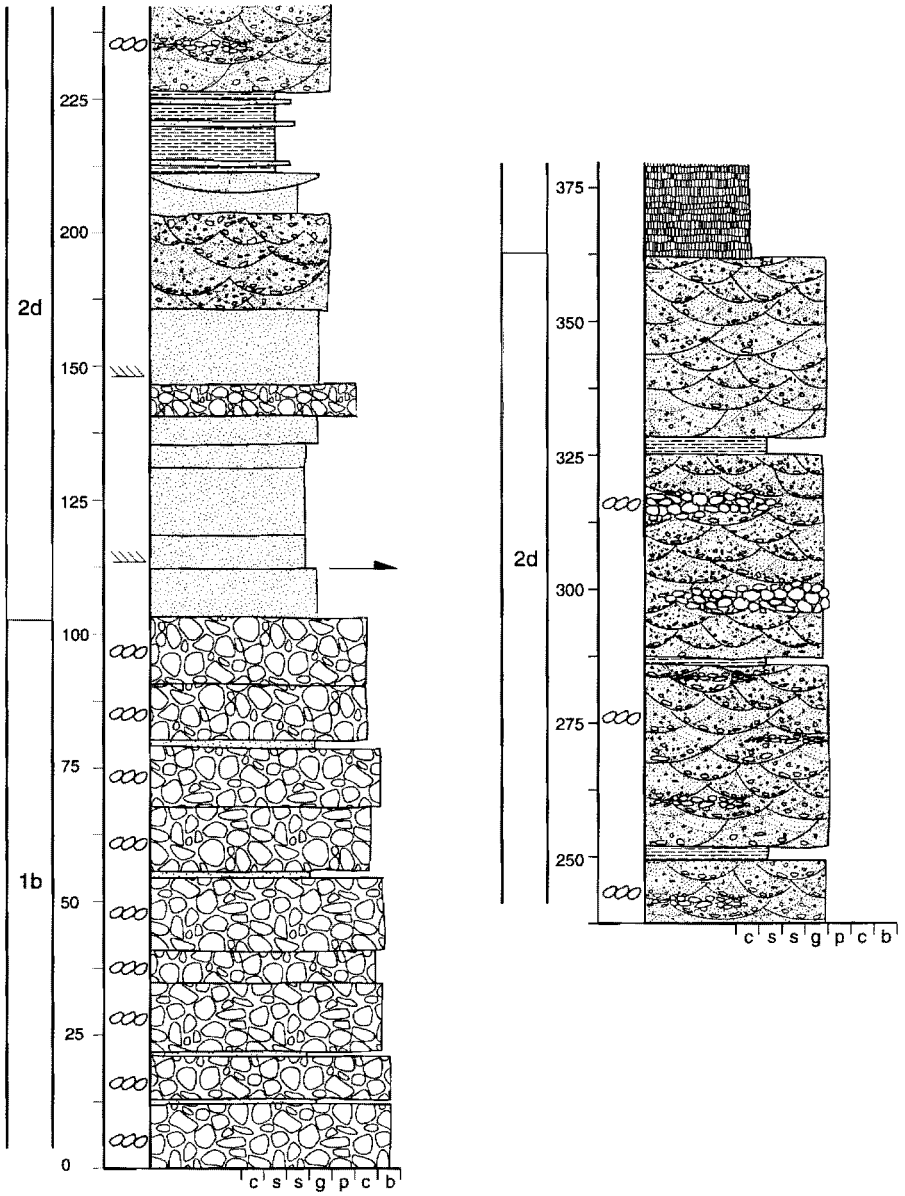

Figure 20e- Red Canyon Section

geographic name. The sections along the southern margin, from west to east are designated: Clemens Well Saddle (CWS), Name Wall (NW), Bullet Peak (BP), and Canyon Spring (CS), respectively (figs. 19, 20a-d). The section on the northern margin is referred to as the Red Canyon (RC) section (figs. 19, 20e). These designations will be used throughout this thesis.

4.2 The Sedimentology and Stratigraphy of the lower Diligencia Formation

The sedimentary rocks of the five measured sections have been separated into three facies associations based on dominant grain size. Two of these facies associations display several variants. The sections in figure 20 have been drawn to emphasize these facies associations.

4.2.1 Breccia/Conglomerate-Dominated Facies Association

The first facies association consists entirely of coarse siliciclastic sedimentary rocks. The deposits are characterized by pebble-to-cobble breccias, and pebble-to-boulder conglomerates. Two variations of this facies association have been identified.

4.2.1.1 Variant 1a

Description

The first variant of this facies association is composed of dark red-brown and tan, matrix-supported pebble and cobble breccias, dark-red and tan, clast-supported pebble and cobble conglomerates, dark-brown pebbly mudstones, and interlayered coarse-grained sandstones. This facies association is present at the base of the Clemens Well Saddle and Canyon Springs sections, where it immediately overlies basement (fig. 20a, d). The majority of clasts can be correlated with lithologies present in the adjacent, underlying basement terrane. However, a small percentage of clasts, primarily of pegmatitic composition, represent basement lithologies which have not been identified in the immediate vicinity of the measured sections. The two sections which contain this

facies association overlie Proterozoic augen gneiss basement, and this lithology is the most common clast type in both occurrences of variant 1a. In addition to augen gneiss, fine-grained quartzofeldspathic gneiss, biotite gneiss, granitic plutonic rocks and milky quartz are present as clast types in significant abundance.

Internal fabric within the breccia is chaotic, and large clasts float in a matrix of sand and dark-red mud (fig. 21a). Within large outcrops, there is a suggestion of very crude, thick layering, which may represent amalgamation of several similar units. However, most outcrops appear massive. Some sedimentary intervals exhibit a more strongly developed internal fabric defined by crude alignment of clasts. Conglomerates have more well-defined internal fabrics, most commonly exhibiting broad lensoidal units and channel-form beds, with strongly erosive bases. The conglomerates are framework supported, with some examples containing little or no matrix between adjacent clasts (fig. 21b).

The coarsest deposits described above are commonly interlayered with and overlain by finer-grained, coarse siliciclastic rocks of two primary types. The first type consists of rare dark-brown mudstone with floating, small pebbles and very-coarse, sand-sized grains. The clasts are primarily quartz and feldspar, but gneissic and granitoid rock fragments are also present. The second interlayered sediment type is composed of dark-red and tan, very coarse- and coarse-grained sandstone. These deposits are generally thickly bedded, with little discernible fabric.

Interpretation of Depositional Environments

The matrix-supported breccias of this facies association are comparable to debris flow deposits described by Fisher (1971) and Lowe (1979). The associated pebbly mudstones are also interpreted to represent gravity-dominated depositional processes. Conglomerates, and breccias that exhibit crude layering and/or clast alignment, may represent internal organization developed by laminar flow during deposition, or later

Figure 21. Photographs of features of deposits of facies association 1a. Part a) shows matrix supported pebble/cobble breccias, interpreted as debris flow deposits. Scale graduations are 10 cm. Part b) shows tabular bed of clast supported cobble conglomerate, interpreted as representing fluvial reworking of previously deposited debris flow material.

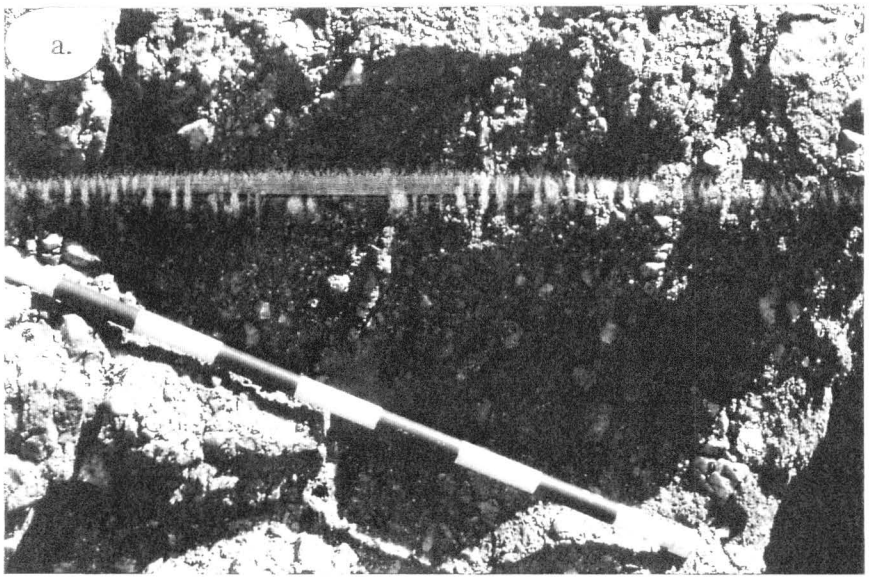
a.


b.

reworking of flow tops by streambed traction processes (Fisher, 1971; Nemec and Steel, 1984). Intercalated sandstones are also interpreted to record periods of stream reworking, between mass flow events.

Although debris flow deposits do not make up a large volume of the total sedimentary package, they are widespread along the southern basin margin and, thus, are potentially significant. Paleobotanical studies (Axelrod, 1950; Wolfe, 1986) indicate that the Miocene climate in this region was semi-arid. Vegetation on hill slopes was probably quite sparse, and precipitation episodic. Both of these factors would promote the development of gravity-driven mass flows (Fisher, 1971).

4.2.1.2 Variant 1b

Description

Variant 1b of the breccia/conglomerate-dominated facies association consists of crudely defined layers, several to tens of meters thick, composed of boulder conglomerate. Interlayered with these conglomerates, are thin, discontinuous, tan and gray coarse- to very coarse-grained sandstones. These deposits are present at the base of the Red Canyon section (figs. 19, 20e). The boulder conglomerates are composed of clasts of several locally-derived basement lithologies, but consist predominantly of granitic rock. In addition, rare banded gneiss, quartz/feldspar pegmatite, and sandstone clasts are present. Of these clast lithologies, the igneous and metamorphic rocks are similar to rocks that presently outcrop in the Hayfield Mountains (see fig. 2), and the sandstone is similar in composition and color to sandstones of the Maniobra Formation in the Hayfield and Orocopia mountains. Deposits of this facies association variant outcrop along a low ridge line, approximately five kilometers long, in the northeast corner of the study area. Similar deposits are not observed elsewhere along the northern margin of the basin.

The conglomerates are exposed on tall cliffs and steep hillsides around Red Canyon (fig. 22a). Clasts are generally well-rounded, and the average clast diameter is approximately 50cm. The largest clasts, however, can be up to 15m long (fig 22b). Mean clast size appears to decrease slightly toward the south; however very large clasts are observed everywhere within this unit. The deposits are clast-supported, and the space between clasts is commonly either filled with coarse sand having the composition of gruss, or is open, possibly due to recent weathering. Because clasts are commonly sub-spherical, the internal fabric of the deposits is not well-defined. Uncommon elongate clasts do exhibit imbrication where long axes of clasts plunge to the north (fig. 22c).

Within extensive outcrops, primarily large cliff faces in Red Canyon, these deposits exhibit crude, discontinuous layering. The layering is defined by the presence of 5-30 cm thick, discontinuous, gray sandstone beds (fig 22c). The sandstone beds have wavy bases, which appear to drape over the boulder clasts below the bed, and the tops are strongly eroded, and commonly breached, by the overlying conglomerates. The internal fabric is typically cryptic, although some sandstone units exhibit planar stratification.

Interpretation of Depositional Environment

Boulder conglomerates and interbedded sandstones in the Red Canyon section are interpreted to have been deposited in a very high-energy, braided-stream system. Erosion at the base of boulder units, well-rounded boulders in a framework supported array, and the presence of stratified sandstones indicate the operation of traction flow processes.

The conglomerates are most similar to those observed in modern, gravelly, braided-river systems and coarse-grained alluvial fans such as the Scott Glacier, and Donjek River (Boothroyd and Ashley, 1975; Miall, 1977). By analogy to modern, gravelly, braided-fluvial systems in glacial outwash fans, these conglomerates and sandstones may represent massive-bedded, longitudinal bar deposits. Boothroyd and Ashley (1975), found that bar morphology in Alaskan outwash fans changes

Figure 22. Photographs of features of facies association 1b. Part a) shows a typical cliff-face outcrop of boulder conglomerates in the Red Canyon area. Part b) shows a close-up of a cliff outcrop, exhibiting boulder conglomerates with imbricated elongate clasts yielding transport direction toward the right (south). Thin, discontinuous sandstone unit can be observed near the upper right-hand corner of the photograph. See text for description and interpretation. Part c) shows an example of an outsize clast from deposits of facies association 1b. This boulder is approximately 15 meters long, note that hat near front of boulder is approximately 2.5 feet in diameter.

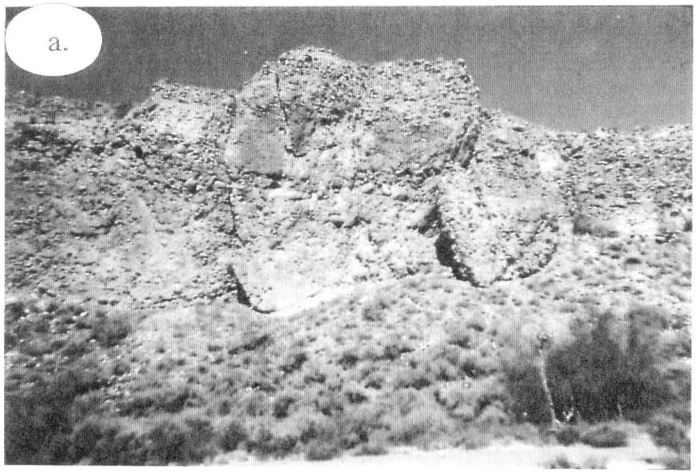

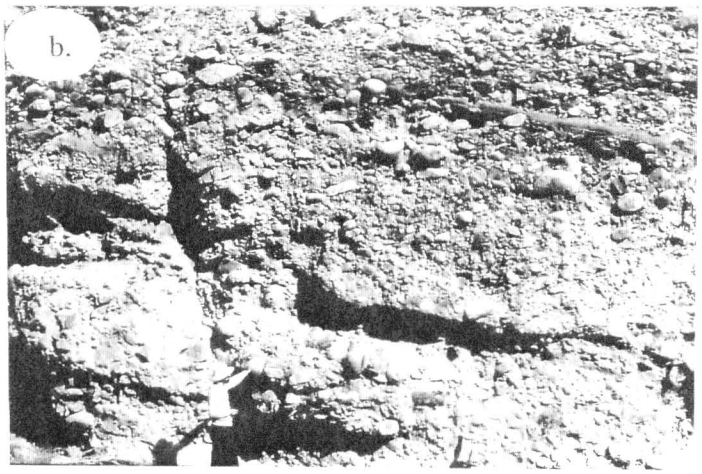

c.

systematically downslope. The most proximal bars are composed of the coarsest-grained gravel, arranged in relatively low-relief bedforms. Mid-fan bars are composed of higher-relief bedforms of finer-grained gravel. Individual gravel longitudinal bars in these settings tend to exhibit decreasing clast size downslope, and sandy slipfaces are typically present on the downslope face (Boothroyd and Ashley, 1975).

Flume experiments indicate that this type of bar deposit forms as a lag during the initial waning stage of a flood (Miall, 1977). Material is deposited in the lee of the gravel sheet, and growth continues as the flood wanes. Successive events may deposit multistory conglomerate units, with no internal fabric other than imbrication of clasts (Miall, 1977).

Because the paleoclimate during deposition was semi-arid, the analogy to processes on glacial outwash fans is somewhat strained. However, even in the perennial river systems of the outwash fans, the coarsest, most proximal, longitudinal bars initially move only during 'rare high flood' events (Boothroyd and Ashley, 1975). The superposition of episodic floods upon the background perennial flow may make the analogy to semi-arid region alluvial fans less tenuous.

The very high energy sedimentation indicated by this variant of the conglomeratic facies association is likely to have taken place on the medial portions of a high-gradient alluvial fan, where flow was confined to active channels, and the slope was great enough to promote transport of very large boulders. Although flooding must have been episodic, these deposits are not envisaged to represent day-long events, but may record lengthier, less frequent events on the order of twenty or one-hundred year floods, for example.

4.2.2 Sand-Dominated Facies Association

The second facies association is characterized by relatively coarse sandstones. However, both conglomeratic and fine-grained siliciclastic deposits are present in these units. Four variations of this facies association are recognized.

4.2.2.1 Variant 2a

Description

The first variant of the sandy facies association is dominated by pervasively cross-stratified, pink and gray, very coarse-grained and pebbly arkosic sandstones. Interbedded with these are very coarse- to medium-grained sandstone units with internal fabrics ranging from massive to planar laminated. In addition, rare muddy and limey units are observed, primarily near the top of the interval. This variant of the sandy facies association occurs in greatest abundance in the Clemens Well Saddle section, and to a lesser degree in the Bullet Peak section and at the base of the Canyon Springs section (fig. 20a, c, d).

Clast composition can generally be correlated directly with lithologies in the nearby basement terrane. The most abundant clast types include augen gneiss, granitic rock, milky quartz, and large feldspar grains probably derived from the augen gneiss. Pebbles are typically localized into stringers or lenses of clast-supported conglomerate, although individual pebbles surrounded by sand also are common (fig. 23a). The sandstones exhibit well-developed internal organization, and trough cross-stratification is abundant (fig. 23b). Troughs are erosive into underlying deposits , and the bases of troughs are commonly defined by thin pebble layers. Foresets are generally defined by color variation, occurring as pink streaks in gray sandstone, although, foresets defined by thin, black, heavy mineral concentrations are also common. Also observed in conjunction with trough cross-stratification are packages of tabular cross-stratified sandstone and planar-laminated sandstone.

Interbedded with the dominant coarse sandstones are less common medium- to fine-grained sandstones, siltstones and sandy, oolitic limestones. The finer-grained sandstones are present, within the main portion of the section, as thin interbeds, which separate large thicknesses of coarse-grained sandstone. The finer sandstones are

generally dark-red and brown, and thinly bedded to laminated. Siltstones and limestones occur only in the Clemens Well Saddle section, and there, only in the upper part of the section, forming a transition into the overlying facies association.

Paleocurrent measurements from units of this facies association were collected in the Clemens Well Saddle area (fig. 24). Paleocurrent indicators have been separated by type of structure. Non-directional indicators include channels in plan view, and small-scale linear scours and yield only a sense of flow (for example, north *or* south). Directional indicators yield an azimuth of flow, and include tabular cross-strata foresets, and limbs of troughs. All paleocurrent measurements presented in this thesis have been corrected for post-depositional deformation. Where possible, this was accomplished by rotation about axes parallel to nearby fold hinges. Where minor folds were not observed nearby, measurements were rotated about horizontal axes. A complete listing of paleocurrent data is presented in Appendix 3.

Interpretation of Depositional Environment

Planar stratified and cross-stratified coarse-grained sandstones, and pebble conglomerates of this variant of the sandy facies association are comparable to deposits described from modern and ancient braided-fluvial systems (McKee et al., 1967; Miall, 1977; Nilsen, 1982). In comparison to the contemporaneous system depositing braided-fluvial conglomerates in the Red Canyon area (facies association 1b), the relatively small average clast size, and the small thickness of individual sediment packages indicates that the system in which these sediments were deposited was a relatively low energy one. The channelized and cross-laminated deposits of this facies association indicate confined flow in some form of braided fluvial system (Picard and High, 1973; Boothroyd and Ashley, 1975). The deposition of planar laminated, very coarse-grained sandstone units, however, indicates unconfined flow (Hardie et al., 1978; Tunbridge, 1981). Periodically,

Figure 23. Photographs of features of facies association 2a. Part a) shows an outcrop of thinly flat bedded very coarse-grained sandstones, with pebbles localized into stringers. Part b) shows a more typical outcrop of trough cross laminated very coarse-grained sandstone with pebbles localized into lensoidal packages at bases of troughs.

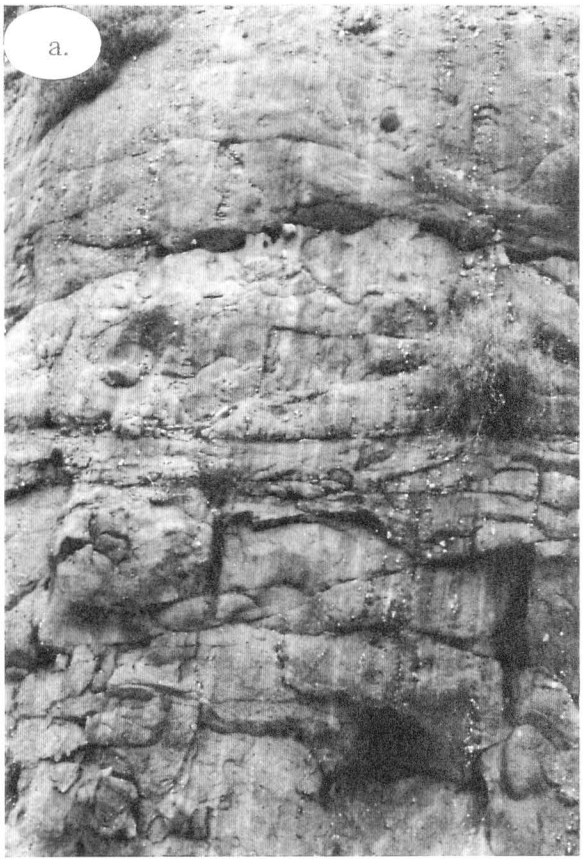
a.

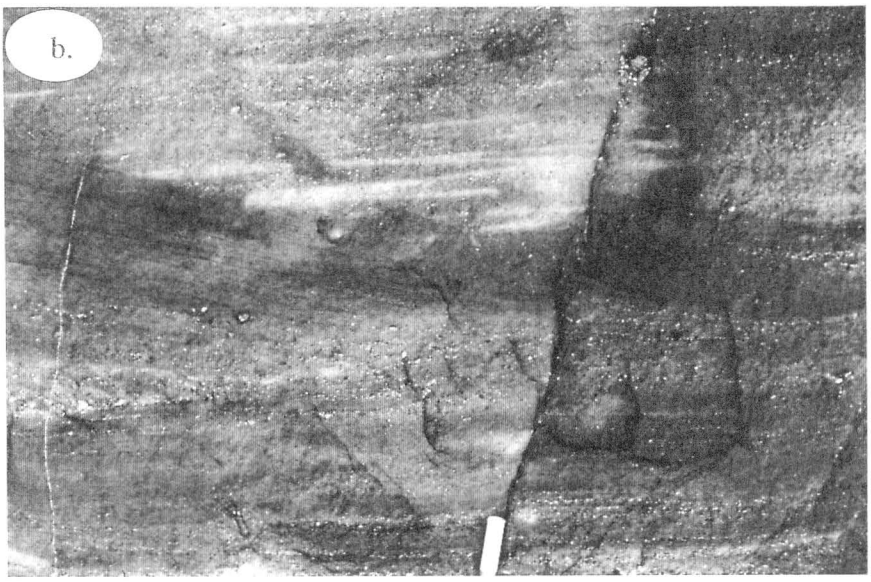
b.

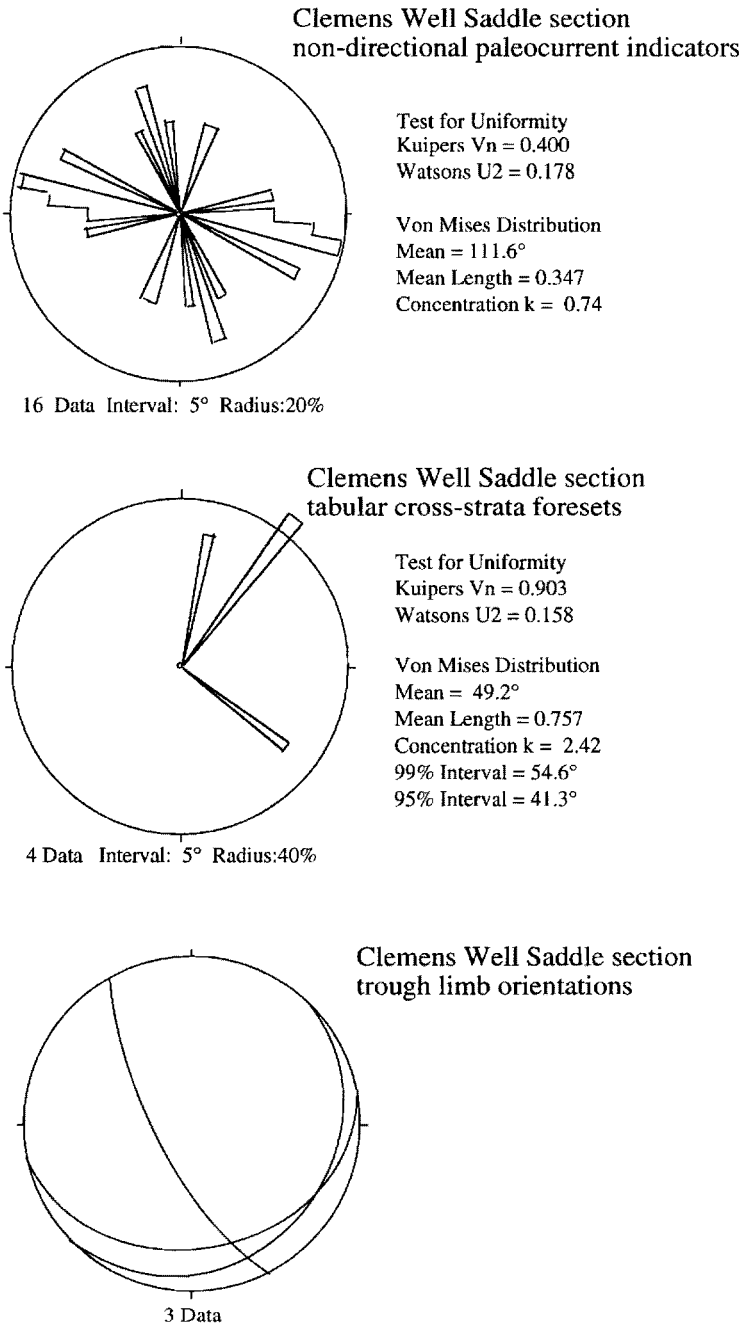

Figure 24. Paleocurrent measurements from deposits of facies association 2a in the Clemens Well Saddle area. Measurements have been separated by type of structure.

storms must have overwhelmed the channel system, and resulted in unconfined sheetflow.

Fine-grained siliciclastic rocks in this facies association may represent settling deposits that formed during abatement of periodic flood events. Waning flow of turbid waters may have draped muddy sediment over bedforms deposited during the higher-energy stages of the flood. Oolitic limestone units are more difficult to explain. They occur in this facies association near the top of the section, in proximity to deposits of the mud-dominated facies association, and will be discussed in more detail in a later section.

All types of paleocurrent indicators present in these deposits, exhibit paleoflow directions in a roughly northward direction, or flow sense oriented approximately northwest-southeast. The fluvial system within which facies association 2b in the Clemens Well Saddle area was deposited flowed primarily toward the north, with a strong component of flow toward the west.

4.2.2.2 Variant 2b

Description

The second variant of the sandy facies association is composed of very coarse- to medium-grained, gray and tan sandstones, gray mudstones and brown and orange sandy limestones. This facies association makes up much of the lower half of the section at Bullet Peak, on the downthrown side of a growth fault (figs. 19, 20c; plate 1).

Facies association 2b is composed primarily of a series of 1-3m thick, fining-upward packages. Each package consists of a thick basal deposit of massive or crudely layered, very coarse-grained, gray or tan sandstone (fig. 25a). These sandstones commonly exhibit erosive bases. The basal sandstones contain rare pebbles, which generally float in sand, but which rarely are aligned into stringers. Rare mud chip horizons are observed in the coarse sandstones at the bases of two packages (fig. 25b).

Rare examples of trough cross-stratification are present in these coarse-grained, basal sandstones.

Basal, very coarse-grained sandstones commonly fine gradually upward into medium- and fine-grained sandstones. These finer sandstone intervals exhibit thin-bedded to planar laminated internal fabric, with rare ripple cross-laminated intervals. Above the laminated fine sandstones, the package is capped by either a 30-80 cm thick interval of pale gray siltstone, or more commonly by a 20-50 cm thick orange-brown, sandy, oolitic limestone bed. The capping siltstones are finely laminated, and generally are eroded into by the coarse-grained sandstone at the base of the overlying package. Capping limestones do not exhibit any obvious internal fabric, and are not observed to be eroded by overlying sandstones.

No interpretable paleocurrent indicators were identified in deposits of this facies association.

Interpretation of Depositional Environment

The fining-upward packages of facies association 2b represent ephemeral, braided-fluvial deposits. Each fining-upward package may record deposition in response to a single, waning, storm event. Very heavy, episodic precipitation is recorded by the massive, very coarse-grained sandstones with floating pebbles, suggesting deposition from gravity-driven grain flows. Such flows are induced by sudden elevation of pore fluid pressure in the sediments on a slope, perhaps by heavy rains (Hooke, 1967). Traction flow processes, associated with initial waning of flood conditions, may have modified the tops of the flows, as indicated by clast alignment and rare cross-stratification. As flow velocity decreased, finer sands would have been deposited under upper flow regime conditions as parallel-laminated sandstones, and finally, rare ripple cross-laminated sandstones as flow velocity dropped further. Capping mudstones may represent settling out of suspended fines in the wake of flood events, and their presence,

Figure 25. Photographs of features of facies association 2b. Part a) shows the parallel laminated fine-grained sandstone and massive sandy limestone at the top of one fining-up sequence, overlain by the massive, very coarse-grained sandstone at the base of the next. Stratigraphic facing direction is toward the right (north). Part b) shows layers of aligned, intraformational mud clasts, in the crudely stratified base of a fining-up sequence. Scale increments are 10 cm.

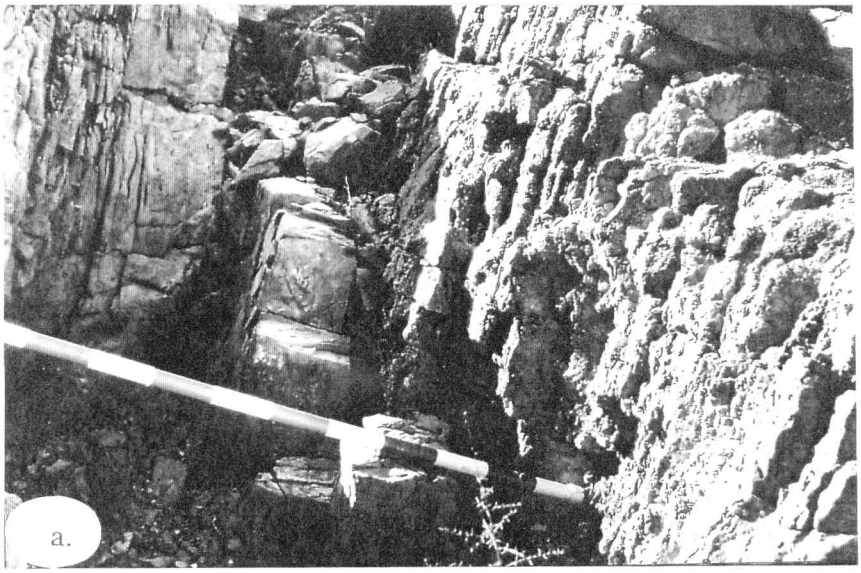
a.


b.

as well as the presence of oolitic limestones, suggest that these rocks may represent deposition into a local topographic low, which collected standing water for indeterminate periods of time between flood events.

Alternatively, each apparent fining-upward interval may represent a particularly intense storm event, separated by some period of time during which sedimentation proceeded by ephemeral streamflow modifying the preexisting sediments, locally eroding the fine grained caps from the underlying sequence, and forming very coarse sand bodies with a weakly-defined internal fabric. These deposits would then be overlain by subsequent flood events, giving rise to the thick based packages observed, many of which are bounded by demonstrably erosive surfaces. Such a scenario would, most likely, result in a package of deposits characterized by massive flood deposits separated by stratified interflood deposits. However, two distinct families of deposits are not observed. Rather, the sediments appear to have been deposited in a series of roughly similar packages. If this alternate interpretation is appropriate, though, then boundaries between flood and interflood deposits must be cryptic, because such surfaces are not observed.

4.2.2.3 Variant 2c

Description

The third variant of the sandy facies association is dominated by orange-tan, planar- laminated, medium- and fine-grained sandstone. Associated with these deposits are significant amounts of tan, planar stratified and cross-stratified, coarse-grained sandstone, and orange-tan, ripple cross-laminated, fine-grained sandstone. This variant of the sandy facies association makes up a major portion of the Canyon Springs section (fig. 20d).

Facies association 2c is composed, in part, of poorly defined, and commonly incomplete, fining-upward packages. Complete packages consist of less than one meter of coarse- to medium-grained sandstone at the base, which is thinly planar stratified

and/or trough cross-stratified. The basal deposits grade sharply into an interval of medium- to fine-grained, planar laminated sandstone, which generally makes up most of the thickness of the package (fig. 26a). The package is capped by a 5-40cm thick interval of fine grained sandstone which commonly preserves climbing ripples and less commonly, convoluted bedding, and dish-and-pillar structures (fig. 26b).

Typically, though, the packages are incomplete. The coarse-grained, basal sandstone may be thin or absent. Rippled tops also are commonly absent. The overall effect is of a deposit dominated by fine-grained, planar laminated sandstone.

In the upper portion of the Canyon Spring section the sedimentary rocks described above are succeeded by an interval of parallel-laminated, fine-grained, yellow-white, sandstone. Bedded, silicified tuffs are present in the Diligencia Formation, and form useful marker horizons in the upper portion of the basin fill (Spittler and Arthur, 1982). This deposit may represent an occurrence of a tuffaceous unit at a relatively low stratigraphic level in the Diligencia Formation.

Paleocurrent indicators were measured in facies association 2c in the Canyon Spring area (fig. 27). All of the interpretable structures examined are symmetrical ripple marks in fine- and medium-grained sandstones near the top of the section near Canyon Spring.

Interpretation of Depositional Environment

The sedimentary rocks which make up facies association 2c probably represent another example of deposition induced by episodic, intense rainfall. The deposits are composed of sequences and partial sequences in which basal sedimentation represents high-velocity flow deposition of coarse sand by traction currents. Above these coarse basal deposits, lower-velocity flow deposits finer-grained sand by upper-flow-regime processes (Picard and High, 1973). Above the laminated fine sands, fine sands

Figure 26. Photographs of features of facies association 2c. Part a) shows typical outcrop of incomplete sequences. Coarse-grained sandstone at base of one sequence is visible at right, overlain by very finely laminated medium- to fine-grained sandstone. Stratigraphic facing direction is toward the left (north). Note compass for scale (lower portion of photo, left of center). Part b) shows ripple cross-laminated top of a sequence that has been extensively eroded by the coarse-grained sandstone at the base of the overlying sequence. Stratigraphic facing direction is toward top of page.

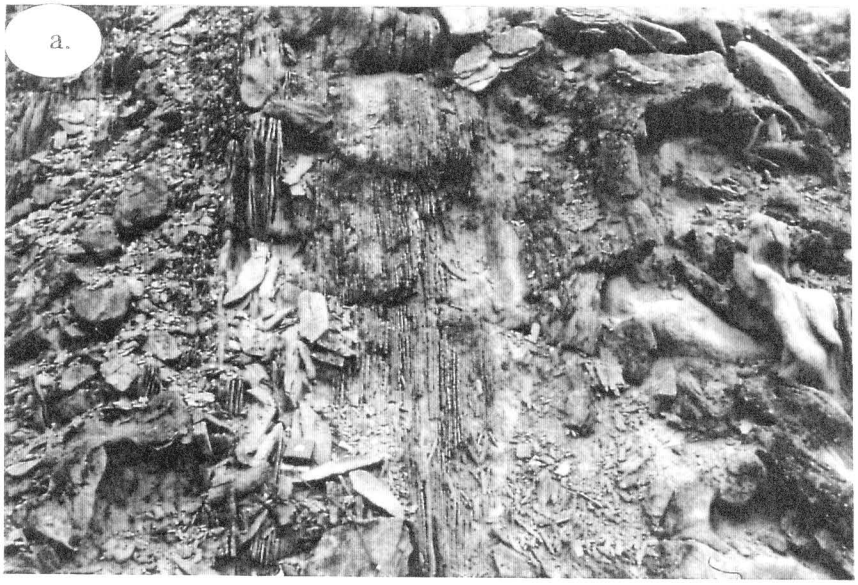
a.

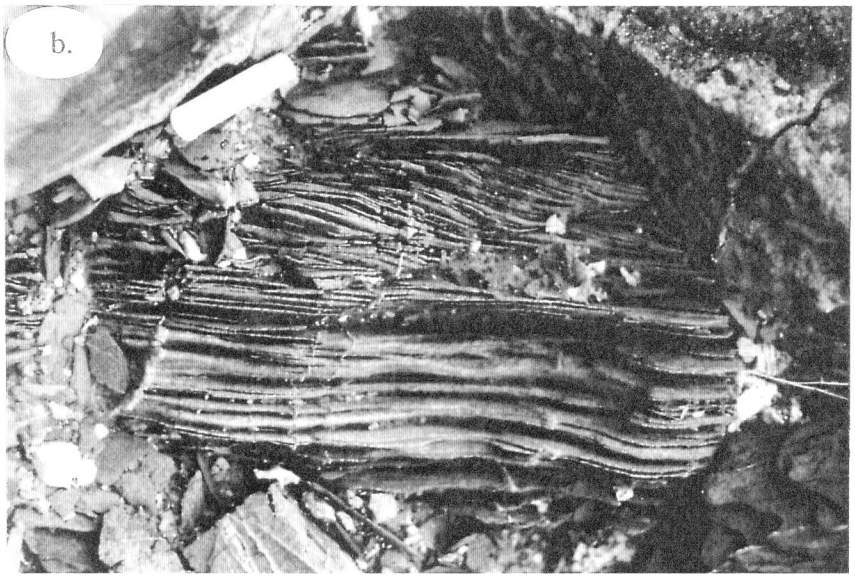
b.

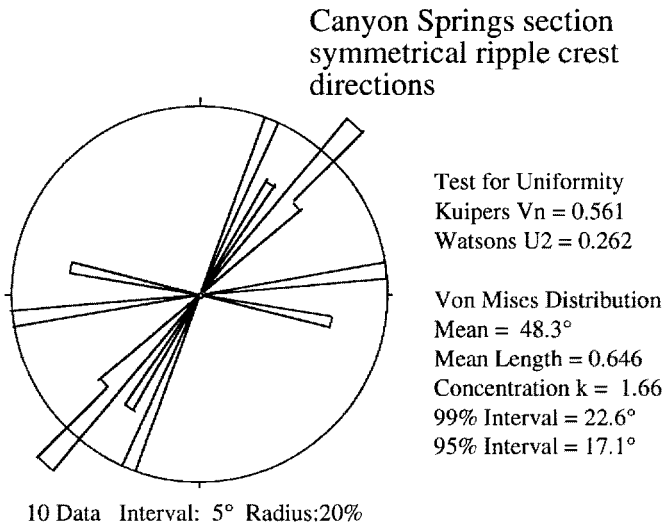

Figure 27. Paleocurrent measurements from deposits of facies association 2c in the Canyon Spring area.

containing abundant climbing ripples record waning flood stages and deposition under lower-flow-regime conditions (Picard and High, 1973).

The processes described above may be active over large portions of a fluvial braidplain. During flood events, flow is often great enough to overwhelm the active system of channels, and deposition occurs from unconfined sheetflow (Picard and High, 1973). The same processes are active on arid region alluvial fans (Hardie et al., 1978; Nilsen, 1982). The remarkable abundance of planar laminated sandstone, suggests deposition below the intersection point of a fan, where stream channelization is poorly developed, and unconfined flow is promoted (Hooke, 1967; Nilsen, 1982).

Paleocurrent indicators measured from these deposits are composed entirely of symmetrical ripples that are present near the top of the section. Because these structures yield oscillation direction, rather than some indication of paleoflow, it is unclear how to integrate these data into a picture of flow patterns along the southern margin.

4.2.2.4 Variant 2d

Description

The final variant of the sand-dominated facies association comprises very coarse- and coarse-grained, dark-red and tan sandstones, and cobble conglomerates. Interlayered with the predominant coarse-grained sandstones and conglomerates are minor medium- and fine-grained sandstone, and siltstone intervals. This variant of the sandy facies association is present on the northern side of the basin, and composes the upper two-thirds of the Red Canyon section (fig. 20e). These units are distinguished from similar deposits elsewhere in the Diligencia Formation by the overall coarseness of the deposits, the large average clast size of the conglomeratic units, and the presence of minor, fine-grained, siliciclastic deposits within the section.

In the Red Canyon section, the deposits which compose facies association 2d can be subdivided into two different package types. The lower half of the interval is

dominated by gray and tan, very coarse-grained sandstones which exhibit planar lamination or tabular and trough cross-stratification. These sandstones commonly form 1-4m thick tabular bodies and broad, lensoidal, channel-form bodies (fig. 28a). The conglomeratic units have highly erosive bases which commonly truncate stratification in the underlying, very coarse-grained sandstones. Clast composition of the conglomeratic units is oligomictic, and clast lithologies match those of the thick conglomerate unit which forms the base of the Red Canyon section. Interlayered with these coarse-grained sandstones and conglomerates are minor, thinly-bedded, dark-red and green, fine-grained sandstones and sandy siltstones. The fine-grained deposits, while distinctive within a large thickness of coarse -grained sediments, make up a small volumetric proportion of the total deposit.

The upper half of this interval of the Red Canyon section is characterized by stacked packages of pervasively cross-stratified, dark-red, very coarse-grained sandstone, and lenses of cobble conglomerate (fig. 28b). Superficially, these deposits resemble the cross-stratified sandstones and pebble conglomerates of facies association 2a, but average grain size, clast size and bed thickness are generally greater than in the units on the southern margin. Individual 3-8m thick packages of trough cross-stratified sandstone and cobble conglomerate are generally separated from one another by 1-3m thick intervals of dark-red, fine-grained sandstone and siltstone. The fine-grained deposits are present in greater abundance than they are lower in this section; however the sediments are still predominantly very coarse-grained siliciclastics. At the top of this section, siltstones make-up a more significant portion of the section, and are overlain by basalt.

Paleocurrent indicators were examined from facies association 2d, in the Red Canyon area and are shown in figure 29. Interpretable structures are distinguished according to type, and position within the section. Directional indicators of paleoflow consist of trough and tabular cross-strata, whereas, nondirectional paleoflow indicators

Figure 28. Photographs of features of facies association 2d. Part a) shows a fairly typical outcrop of very coarse and coarse-grained sandstones in the lower half of the Red Canyon section. Part b) shows outcrop of very coarse-grained sandstone and cobble conglomerate lenses in the upper half of the Red Canyon section. Stratigraphic facing direction is toward the top of the page in both photographs.


a.

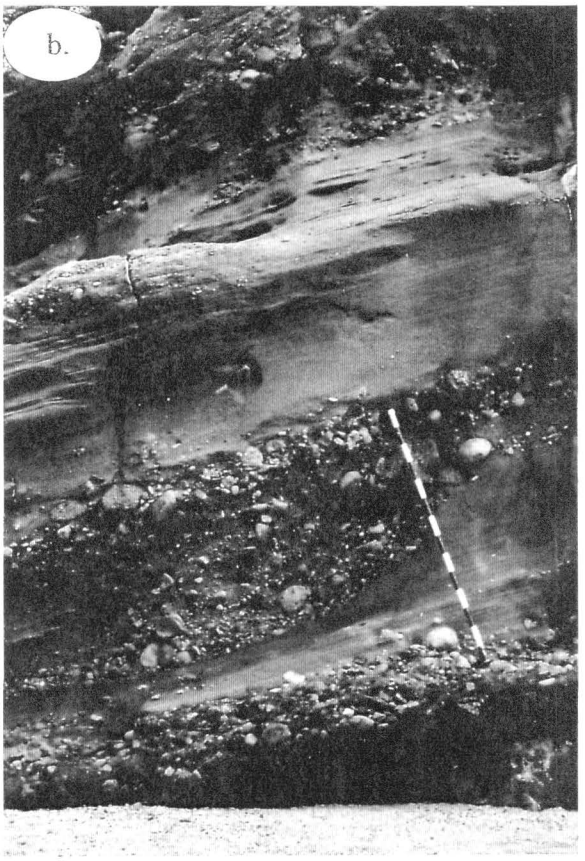
b.

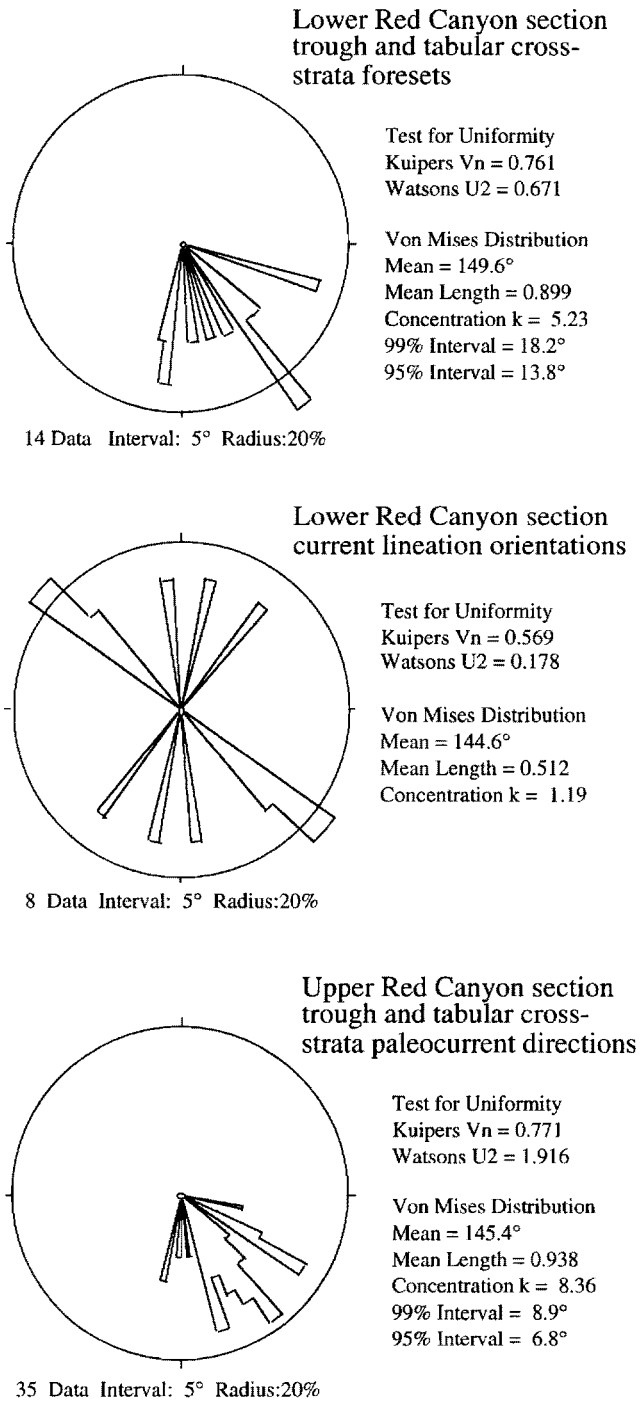

Figure 29. Paleocurrent measurements from deposits of facies association 2d in the Red Canyon area. Measurements have been separated by type of structure and position in the section.

are composed of current lineations. All current lineation measurements were made in the lower portion of the sandy deposits in Red Canyon.

Interpretation of Depositional Environment

Facies association 2d reflects the same processes active in variant 2a, that is, sandstones and conglomerates deposited in a gravelly, braided-fluvial system. These deposits are comparable to the Donjek-type depositional profile of Miall (1977), and also resemble midfan and lower fan deposits of the Scott Glacier outwash fan (Boothroyd and Ashley, 1975). The sandstones and conglomerates of this facies association overlie the boulder conglomerates at the base of the Red Canyon section, which are interpreted to represent the proximal deposits of a braided fluvial system.

In terms of scale, the fluvial system in which these sediments were deposited was demonstrably different from that associated with variant 2a. The thickness of individual sediment packages, and consistently large clast size of the conglomeratic units, as well as the association of these rocks with the conglomerates that underlie them, indicate episodic, very high energy discharge, that moved large volumes of very coarse sediment. During individual depositional events, flow was probably localized into restricted, active channel systems, leaving nearby channels abandoned. Finer-grained deposits between large sandstone packages, may represent deposition from overbank splays of nearby active channels, or perhaps form from some sort of flood abatement or inter-flood depositional processes.

Directional paleocurrent indicators yield a constant direction toward the southeast, for measurements taken at all positions in the section, and non-directional indicators yield northwest-southeast sense of flow.

4.2.3 Mud-Dominated Facies Associations

Description

The third facies association is dominated by fine-grained siliciclastic sedimentary rocks. These deposits consist primarily of dark-red and gray-green, and less commonly tan, gypsiferous siltstone and minor claystone. Interlayered with the mudstones are common 1-20 cm thick tan sandstone beds, less common, meter-scale sandstone beds and rare sandy limestone beds. Deposits of this facies association cap the Clemens Well Saddle, Bullet Peak, and Canyon Springs sections (fig. 20 a,c,d), and comprise the entire thickness of the Name Wall section (fig. 20b).

The fine-grained siliciclastic rocks of this facies association are primarily silty. Claystone is present in small proportions and does not appear to be localized in any regular way. The mudstones are generally not well-laminated, and weather into blocky, or rarely spheroidal, outcrops (fig. 30a). These deposits also contain a remarkable amount of gypsum. The evaporitic material commonly occurs as sheets of selenite forming parallel to bedding or at a high angle to bedding (fig. 30b). In addition, fibrous gypsum commonly fills fractures.

Bedding is typically defined by the presence of thin (10-30 cm), sandstone interbeds. These sandstone beds have complex internal organization which include: a flat or wavy base; coarse- to medium-grained massive or, uncommonly, trough cross-stratified sandstone making up approximately one third to one half of the thickness of sand; planar-laminated, medium- to fine-grained sandstone; and common asymmetric or symmetric rippled intervals composing the upper one half to two thirds of the sand package. Each sand package is capped by overlying mudstone (fig. 30c).

Less common, meter-scale sandstone units are demonstrably different. They are considerably thicker, on average, but in addition, all observed examples have erosive bases overlain by trough cross-stratified, coarse-grained sandstone. These units may also

contain parallel-laminated intervals with well developed current lineation, asymmetric ripple horizons, loading features, mammal tracks, and abundant desiccation features at the bases (fig. 30d-e).

Rare, thin, orange-brown sandy, oolitic limestones are present near the bottom of this facies association in the Clemens Well Saddle section (fig. 20a). These limestone beds have no recognizable internal fabric. Exposure of bedding surfaces exhibit internally structured bodies which may represent algal mat material (fig. 30f). Additionally, during fieldwork for this thesis, a single macrofossil was discovered, the distal portion of the humerous of an unidentified, sheep-sized, mammal (A. Wyss, pers. comm.).

Paleocurrent indicators for this facies association were recorded from the southern margin of the basin, in the Bullet Peak, and Name Wall areas (figs. 31, 32). Directional indicators in both areas consist of trough axes, and yield paleoflow direction toward the west-northwest. In the Name Wall area, current lineations yield a northwest-southeast sense of paleoflow. Structures measured in both locations are present in fine- and medium-grained sandstone interbeds, within the mudstones.

Interpretation

The relatively fine-grained siliciclastic rocks of this facies association are interpreted to represent deposition both into, and marginal to, a playa lake system. Mudstones in this assemblage represent accumulation of fine-grained siliciclastic material by settling in quiet waters. Sediment input was probably ephemeral and contingent upon precipitation during episodic storms. The presence of significant volumes of evaporitic material, animal tracks and abundant desiccation features including mudcracks, in conjunction with the inferred, semiarid paleoclimate, indicate that the lake system was probably ephemeral. Oolitic limestones similar to those present in this facies association

Figure 30. Photographs of features of facies association 3. Part a) shows a typical outcrop of mudstones with thin, intercalated fine-grained sandstone beds. Part b) shows a gypsum-rich interval, where gypsum occurs primarily as thin sheets of selenite, parallel to bedding. Parts c) and d) show evidence of subaerial exposure. These photos show mammal footprints (camel?) and mudcracks a the base of a thin sandstone bed, respectively. Part e) exhibits the internal structure of a thin sandstone bed that is interpreted as a possible turbidite. The bed has a cross-laminated base, overlain by a parallel laminated interval, a symmetrically rippled top, and capped by mudstone. See text for further description, and interpretation. Part f) shows algal mat material from a sandy limestone bed near the base of a mudstone unit, where these deposits interfinger with fluvial deposits of facies association 2a.

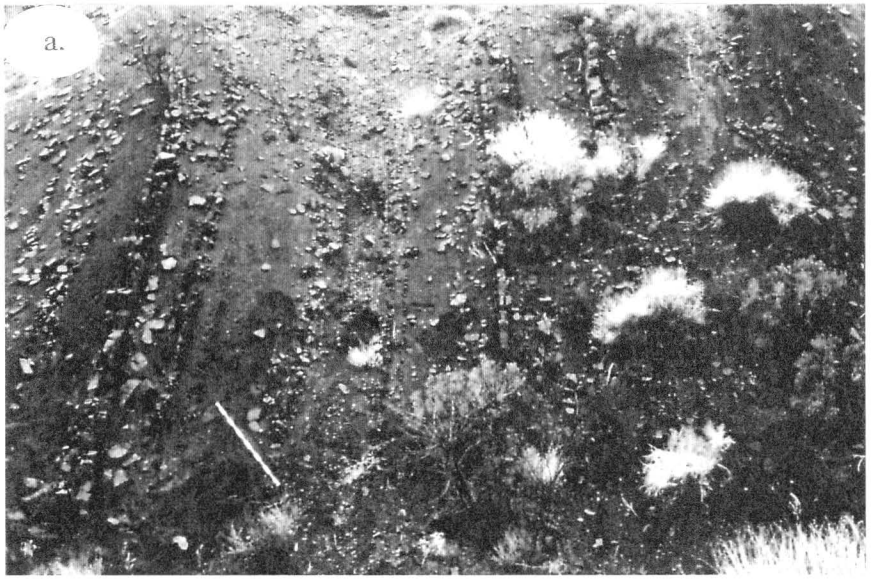
a.

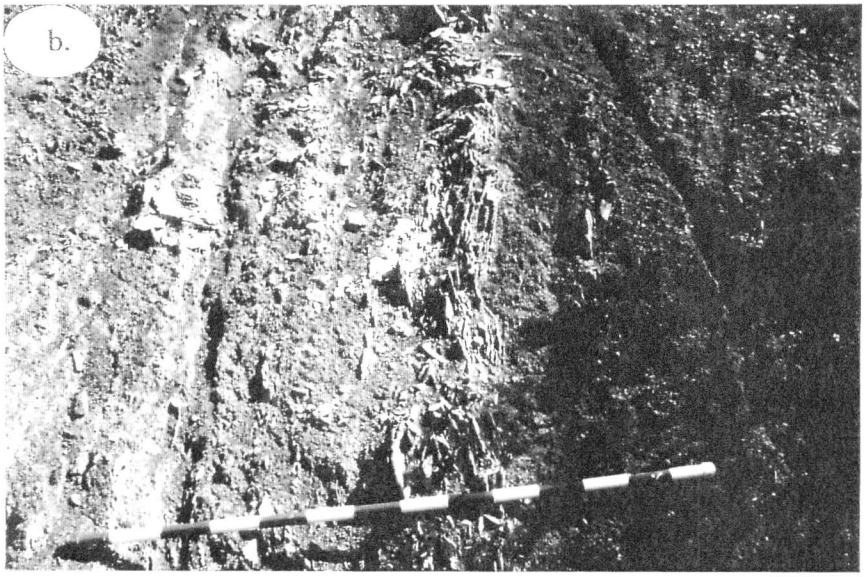
b.


c.


d.

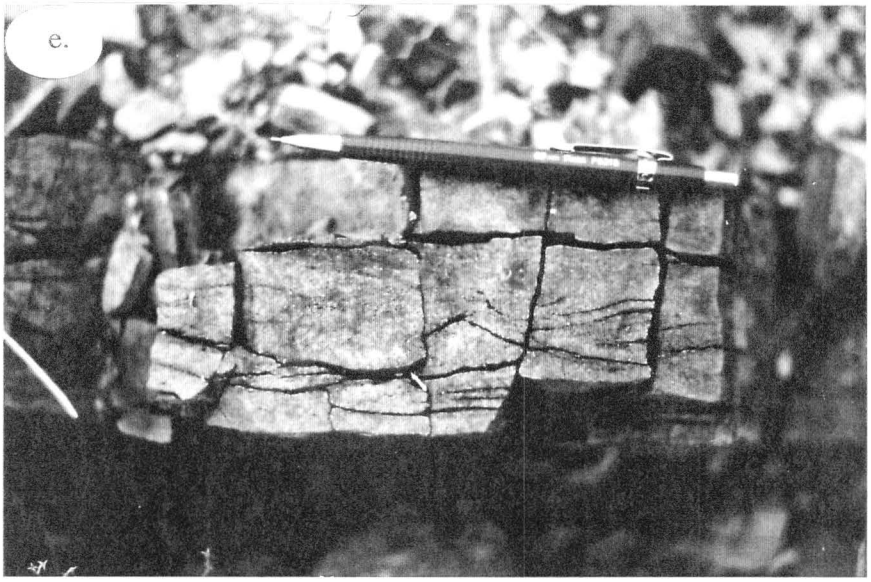
e.

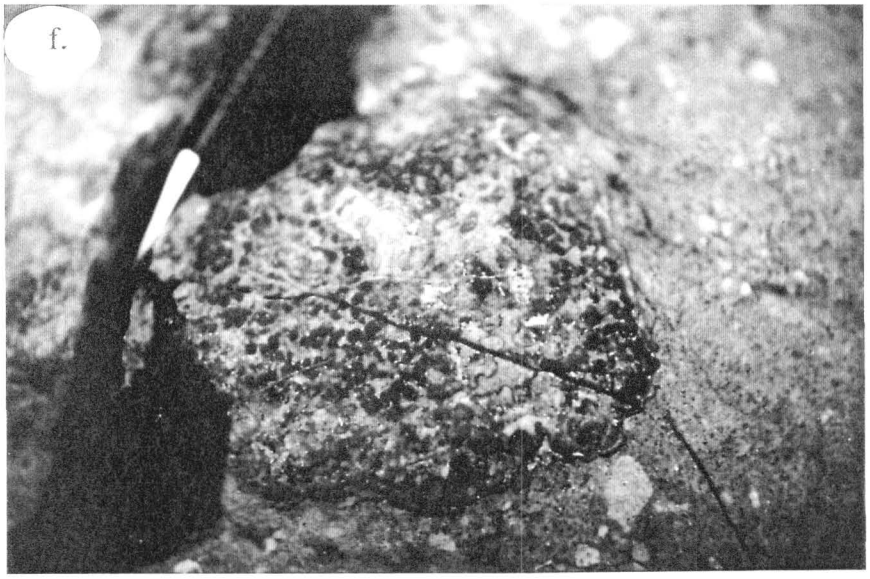
f.

have been reported from nearby basins of similar age (Fedo and Miller, 1992). These limestones may represent primary fluvial deposition of carbonate (McGannon, 1975), or lacustrine oolite formation near the lake margin (Swirydczuk et al., 1979). Formation of carbonate from lake water requires an unusually high ratio of dissolved bicarbonate to calcium and magnesium in the groundwater (Hardie and Eugster, 1970; Hardie et al., 1978). As carbonate is formed, though, the process removes bicarbonate from the system until the ratio is too low for further carbonate precipitation. Thereafter, calcium and/or magnesium sulfates commonly form (Hardie and Eugster, 1970; Hardie et al., 1978). This brine evolution scheme suggests that the carbonates are likely to form near the margin of the lacustrine deposit, and sediments nearer the center should contain the majority of the sulfate evaporites. This prediction is born out by the observation that the carbonate beds are intimately interfingered with the sandstones of the marginal fan/fluvial system.

The relatively thick sandstone units in this facies association are interpreted to represent lacustrine margin deposition in response to episodic flooding, during which fluvial sands prograded out onto the playa surface. Erosive bases and cross-stratification of coarse sandstones indicate relatively high-energy traction flow. Parallel laminated fine sandstone overlain by ripple cross-laminated fine sandstone records waning flood deposition whereby upper flow regime traction processes are succeeded by lower flow regime formation of sand waves (Picard and High, 1973). The associations of sedimentary structures, as well as the interpretation of flow evolution are comparable to those of low-discharge flash-flood events described from Israel (Karcz, 1972). The similarity of these ancient deposits to deposits from small flood events suggests either that they too are the result of small, low-volume floods, or that they represent the most distal reaches of major flood deposits in which flow energy has decreased significantly, and flow is distibuted over a relatively large area of braidplain.

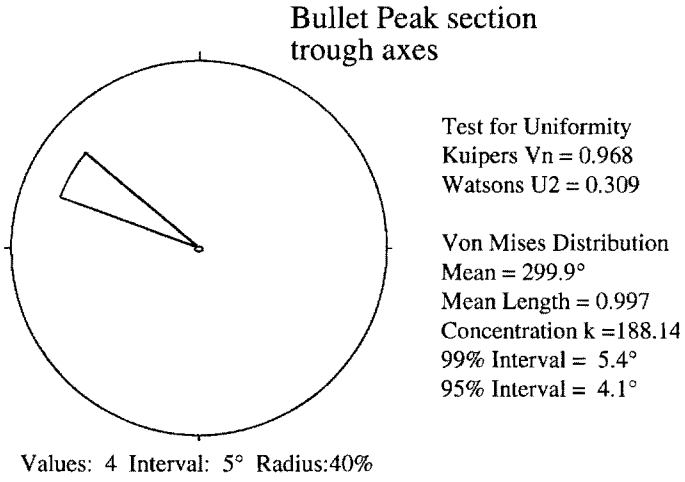

Figure 31. Paleocurrent measurements from deposits of facies association 3 in the Bullet Peak area.

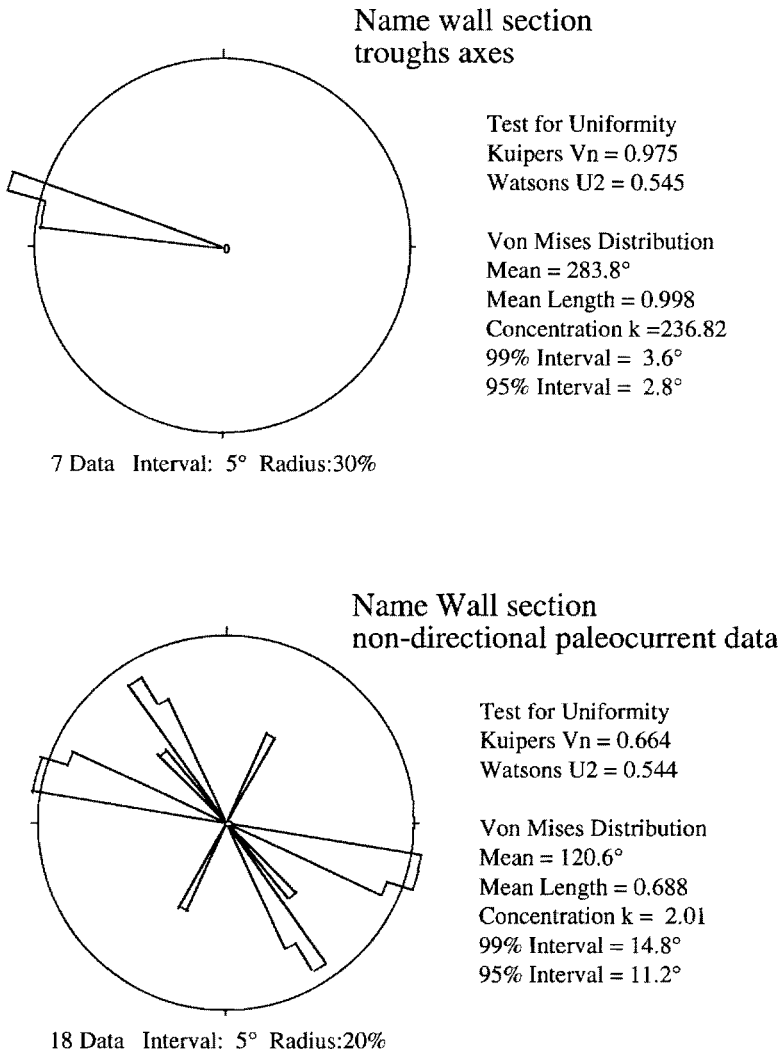

Figure 32. Paleocurrent measurements from deposits of facies association 3 in the Name Wall area. Measurements have been separated by type of structure.

Thin sandstone beds with complex internal fabric successions described above are interpreted as partial Bouma sequences, indicating deposition by sediment gravity flows. Probable turbidites have been identified in association with similar rocks in the Whipple and Sacramento mountains of California (Fedo and Miller, 1992), and Hardie et al. (1978) have indicated that sheetflows may enter saline lakes as 'a waning turbid underflow.' In ephemeral saline lakes, salinity is generally very high, and formation of density currents may be rather limited. However, during periods of increased rainfall, salinity would decrease, while lake area and sediment supply to the lake would increase. These factors, in concert, would favor the formation of turbid density flows, and the deposition of turbidite units. Lowe (1982) has described high-density turbidite deposits which exhibit erosive bases and cross-stratified lower divisions. The thin sandstones in this facies association may represent an occurrence of such Bouma sequence variants, containing divisions which include the modified Ta of Lowe (1982), overlain by Tb, and Tc, and capped by the Te mudstones of a traditional Bouma sequence (Blatt et al., 1980, p. 145).

Paleocurrent analysis of structures present in sandstone interbeds of this facies association along the southern margin of the basin suggests that those units were deposited in systems which flowed toward the northwest. Flow directions are parallel in both localities, and no difference is observed between data from thin sandstone units and thick sandstone units.

CHAPTER 5. Basin Reconstruction

5.1 Areal Distribution of Depositional Systems

5.1.1 Depositional Systems on Southern Margin

The southern margin of the Diligencia Basin is dominated by bedload deposits that locally overlie relatively thin packages of facies produced by gravity-dominated processes. These fluvial rocks are subsequently overlain by, and interfinger with rocks of lacustrine origin (see Chapter 4). The arrangement of these facies associations suggests that the deposition along the southern margin was dominated by a system of relatively low-gradient alluvial fans that extended into a playa-lacustrine basin. These fans are characterized by small volumes of debris-flow deposits with relatively small average clast size (cobble or smaller), and the predominance of very coarse-grained and pebbly sandstones of braided fluvial/alluvial origin.

Debris-flow deposits are a common component of arid-region alluvial fans. Gravity-flow deposition may occur at any position on an alluvial fan surface (Hooke, 1967), however, it is most abundant on the proximal and medial portions (Nilsen, 1982). The scarcity of gravity flow deposits in these fans may be accounted for in two ways. The fans may have been deposited on a low-gradient depositional surface such that the medial and distal portions of the fans had particularly large areal extents, and deposition was dominated by fluvial processes, as reported in similar systems by Nilsen (1982). In this situation, gravity-flow deposits would have been most common only in the areally-restricted updip portions of the fans. Another possible explanation is that the present outcrop exposes more distal reaches of the fan system and deformation and erosion have removed the gravity flow deposits that once composed the proximal portions of the fans. Perhaps most likely is that some combination of these factors has contributed to the predominance of fluvially deposited sedimentary rocks along the southern margin.

The facies association which makes up the greatest thickness of section along the southern margin is sand dominated. As discussed in Chapter 4, the variants of the sand dominated facies association were probably deposited by different processes active on a fluvial braidplain. Braided-rivers commonly are intimately associated with arid-region alluvial fans, and such fans typically grade down-dip into braidplains (Nilsen, 1982). Facies association 2a represents fairly typical braided fluvial deposits and probably made up a significant portion of the original sedimentary package. Even in the present outcrop, facies association 2a is significant both in terms of the volume of these deposits and their wide distribution across the entire southern margin. The rocks of facies association 2c are interpreted to represent sheet-flood deposits, which probably formed during flash floods. Such floods may overwhelm the channel systems on the surface of the fans, resulting in unconfined flow (see Chapter 4). Below the intersection point on an alluvial fan, channels are not deeply incised and flood events, where discharge is still high in the distal reaches of the fan, may result in well developed sheet-flood deposits at the toes of the fans (Hooke, 1967; Nilsen, 1982). Facies association 2b reflects the influence of small-scale (relative to the entire basin), synsedimentary normal faulting superimposed on the alluvial fan/fluvial braidplain developed on the southern margin. The bullet peak section (see Fig. 20c) is located on the downthrown side of a fault, across which the lower Diligencia Formation thickens considerably (see Plate 1). This growth fault formed a small sub-basin within the Diligencia Basin into which characteristic sediments were shed. The sediments of facies association 2b in the Bullet Peak measured section are interpreted to represent flood deposition into this growth-faulted sub-basin in the form of decelerating grain flows overlain by traction deposited sediments, recording waning flood conditions (see Chapter 4).

Analysis of paleocurrent indicators in the sediments of the southern margin indicates that paleoflow was primarily from southeast to northwest (see fig. 33). Clast

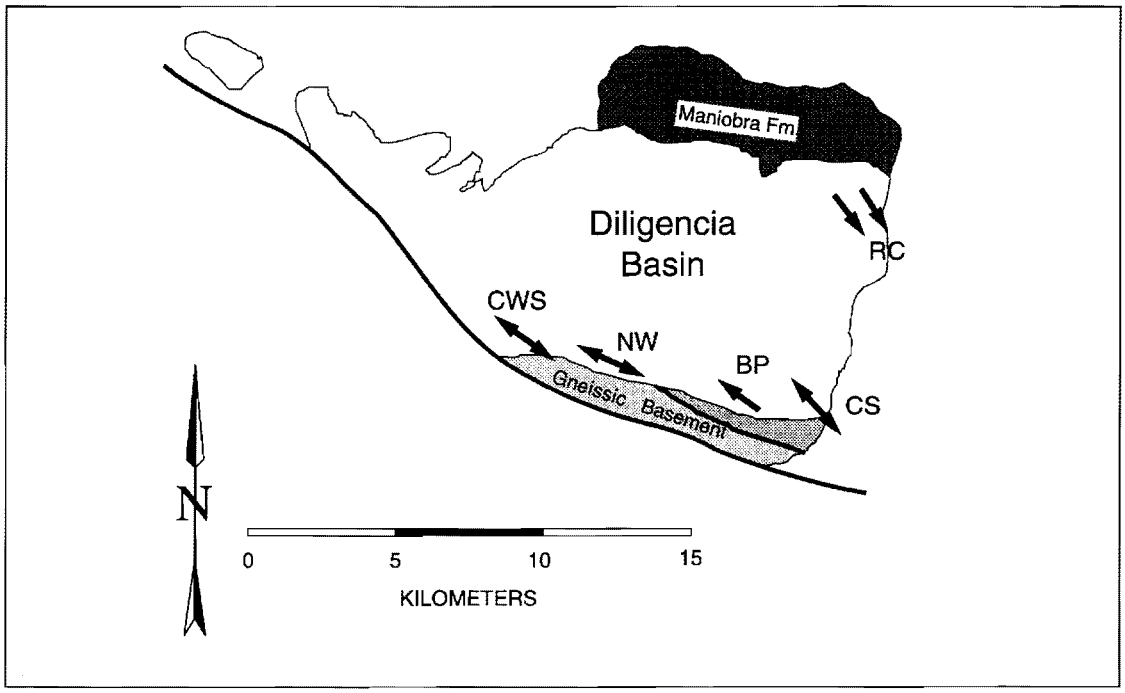

Figure 33. Schematic index map of the Diligencia Formation showing mean paleocurrent orientations at the locations of the five measured sections. See text for discussions of individual examples.

composition of the conglomerates and pebbly sandstones indicates that these sediments were probably locally sourced, and material was primarily derived from basement terranes which outcrop south and west of the basin margin. These observations, integrated with the interpretation of a low-gradient alluvial fan system along the southern margin yield a reconstruction of the southern margin as a fluvially dominated, probably areally extensive, system of alluvial fans forming on a low-gradient depositional surface by erosion of the basement highland presently located to the south of the basin. The strong component of axial flow along the southern margin may be related to local depositional gradients imposed by the formation of tilted basement surfaces in the hangingwalls of growth faults along the margin (see Chapter 4, section 4.2.2.2, for discussion of these faults).

5.1.2 Depositional Systems on Northern Margin

The facies on the northern margin are interpreted to have been deposited in a very high-energy braided fluvial system (see Chapter 4). The remarkably large clast size observed in rocks of facies association 1b, as well as the relatively large clast size in the conglomeratic sandstones of facies association 2d indicate that the sedimentary rocks on the northern margin were deposited in high-gradient systems. These sediments are interpreted to be the remains of a system of steep alluvial fans which developed against the northern edge of the Diligencia Basin.

No major mass-flow deposits, which can be definitively assigned to the Diligencia Formation, are present on the northern margin of the basin. Debris-flow deposits, with meter-scale average clast size, do occur in abundance on the northern side of the basin. These deposits, however, have been assigned to the Eocene-age Maniobra Formation (Advocate, 1983), and field investigations for this thesis were not able to conclusively show that this assignment is in error. These deposits occupy the same structural position as the lower Diligencia sediments. They overlie sandstone and siltstone of definite

Maniobra affinity, although the nature of the contact is uncertain. The contact has been interpreted as a facies transition by Advocate (1983), however, the possibility that it represents a low-angle unconformity between the Maniobra and Diligencia formations deserves further consideration in the field. These mass-flow deposits are nowhere observed in direct contact with definitive Diligencia Formation sediments, but are separated by tens or hundreds of meters of Quaternary alluvium in the bottom of Red Canyon. If these deposits are actually of Miocene age, then they may represent the proximal portion of a series of high-gradient alluvial fans which developed along the northern margin of the Diligencia Basin. If these deposits are truly part of the Maniobra Formation, then there may be few mass-flow deposits of Diligencia-age present along the northern margin of the basin.

The alluvial fans which formed along the northern margin of the Diligencia basin were deposited upon a more steeply sloping surface, and probably covered a much smaller area than the contemporaneous fans which formed along the southern margin. It is possible that the proximal portions of the northern alluvial fan complex on the eastern end of the margin were erosionally removed by the formation of Red Canyon, which now separates the rocks of the Diligencia Formation from the Maniobra Formation and the crystalline rocks of the Hayfield Mountains.

The sediments of facies association 1b are interpreted to represent the medial portion of the high-gradient alluvial fan complex on the northern margin of the Diligencia Basin. These boulder conglomerates and very coarse-grained sandstones are interpreted to have been deposited in an energetic braided fluvial system as longitudinal bar complexes (see Chapter 4). While these particular deposits are rather larger scale than many similar occurrences reported in geological literature, the processes that they represent are commonly reported from similar basins (e.g., Beratan, 1991; Cole and Stanley, 1992; Fedo and Miller, 1992). Similarly, the sediments of facies association 2d

are interpreted to represent the medial and distal reaches of the northern alluvial fan complex. These deposits are remarkably coarse-grained in comparison to the contemporaneous deposits on the southern margin.

Paleocurrent indicators observed within sediments of facies association 2d from the Red Canyon area record paleoflow directions from north to south (see fig. 33) as does imbrication of elongate clasts in facies association 1b (see Chapter 4). Clast compositions observed in conglomerates of facies association 1b, and in conglomeratic sandstones of facies association 2d suggest that these deposits were locally sourced, and that the sediment was derived from crystalline basement terranes presently exposed in the Hayfield Mountains to the north (see fig. 2). These observations suggest that transport of sediment during deposition was directed primarily from basement highlands to the north, southward into the Diligencia Basin. Together, the deposits discussed above lend considerable credence to the reconstruction of a system of high-gradient alluvial fans along the present northern margin of the Diligencia Basin.

5.1.3 Depositional Systems in Central Part of Basin

Deposits of the lower Diligencia Formation from the center of the basin are not exposed anywhere in the study area. These deposits are overlain by several hundred meters of coarse- and fine-grained siliciclastic rocks and basalt which make up the upper Diligencia Formation.

Sediments of facies association 3 make up the upper portion of the lower Diligencia Formation along the southern margin (see fig. 20). These sediments comprise predominately evaporitic mudstones and turbidite sandstones which are interpreted to have been deposited in an ephemeral lake. Associated with these mudstones are distinctive fluvially-derived sandstone and limestone units which are interpreted to represent marginal lacustrine deposition (see Chapter 4). Paleocurrent indicators from the fluvial sandstone units and the turbidite sandstone units within this facies association, in

the name wall area, indicate a strong component of paleoflow along the axis of the basin (see fig. 33). This observed axial flow may reflect the topographic effect of the growth fault in the Bullet Peak area. A family of minor normal faults at high angles to the basin margin (one of which has been identified in the Bullet Peak area), may have formed a series of local topographic highs. These topographic highs would have superimposed a component of axial flow upon the dominant transport system.

The sedimentary rocks of facies association 3 indicate the presence of a playa lake system in the depocentral portion of the Diligencia Basin. The lake bed deposits are intimately associated with sandy and gravelly rocks of the low-gradient alluvial fan system along the southern margin (see fig. 20). Although mudstone is fairly common on the northern margin, the characteristic gypsiferous siltstone observed on the southern margin, is not observed.

5.2 Basin Geometry: Synthesis

If the Diligencia Basin had formed as a horst and graben structure, then certain ramifications of this geometry should be observed. In a graben, normal faulting along both margins should produce fault escarpments, development of alluvial fan systems, and an overall approximate symmetry of facies distributions across the axis of the basin. In addition, some evidence of normal faulting should be observed on both trough margins where the basement/sediment contact is exposed.

This thesis has demonstrated that there is a fundamental asymmetry of facies distribution across the axis of the Diligencia Basin. The basement/sediment contact along the southern margin is of depositional origin along its entire length, except where it has been activated as a reverse fault by later, compressional deformation. Evidence of normal faulting is observed in outcrop only along the northern margin of the trough. For

these reasons, it is evident that a symmetric horst and graben model is inadequate to explain the evolution of the early Diligencia Basin.

The Diligencia Basin is presently an east-west. trending, elongate trough. The orientation during formation, however, may have been different, and the implications of this fact have been discussed in Chapter 3. In its present orientation, the early Diligencia Basin may be reconstructed as an asymmetric half-graben basin, which formed in response to north-south directed extension.

Leeder and Gawthorpe (1987) developed a model of the patterns of sedimentation into an internally-drained, continental half-graben basin. Subsequently, this model has been successfully applied to the reconstruction of such basins in the Basin and Range, and elsewhere (e.g., Hamblin and Rust, 1989; Fedo and Miller, 1992; Karpeta, 1993). In an internally-drained half-graben basin, contemporaneous sediment packages will be demonstrably different in different parts of the basin. Facies against the relatively steep relief of the detachment fault escarpment will be dominated by thick, high-gradient alluvial fan deposits, of limited areal extent (Leeder and Gawthorpe, 1987). In contrast, upon the gently dipping surface of the hinged hangingwall block, facies will be dominated by thin, low-gradient alluvial fans (cones), which may show well-developed braided fluvial influence (Leeder and Gawthorpe, 1987; Fedo and Miller, 1992). Each of these basin margin sedimentary systems interfinger in the basin interior with lacustrine deposits. The locus of greatest subsidence within the basin is located at the foot of the detachment fault escarpment, on the hangingwall block. The lacustrine depocenter should be located as close to the locus of subsidence as the high-gradient fans will allow (Leeder and Gawthorpe, 1987).

The depositional systems described above from the lower Diligencia Formation can be interpreted within the framework provided by Leeder and Gawthorpe (1987) to reconstruct the original basin geometry. The low-gradient fans along the southern margin

are interpreted to have formed upon the gently-dipping hangingwall block of the half-graben. The high-gradient fans along the northern margin are interpreted to have formed against the relatively steep slope of the detachment fault escarpment. The lacustrine deposits are interpreted to record the presence of a playa lake complex in the basin interior (see fig. 34).

Lacustrine deposits in the lower Diligencia Formation are observed along the southern margin only. The locus of maximum extension in the basin should be at the foot of the detachment fault escarpment. Thus, in the case of the Diligencia Basin, the lacustrine depocenter is expected to be closer to the northern basin edge than to the southern, in plan view (see fig. 35a). In fact, though, lake-bed deposits are most closely associated with the southern margin of the basin. Similar observations have been reported in Paleozoic rift basins of Nova Scotia (Hamblin and Rust, 1989). Hamblin and Rust report the widespread occurrence of lacustrine deposits in the Upper Craignish Formation and identifies multiple playa lake depocenters located well up on the hangingwall ramp (see Hamblin and Rust, fig. 4).

The displacement of the lacustrine depocenter(s) up the hangingwall ramp from the locus of maximum subsidence is most satisfactorily explained by the behavior of the footwall-sourced alluvial fans. These high-gradient fans are likely to have a high rate of progradation, and accumulation rates higher than those for the lacustrine system. As these fans prograde across the basin, the active playa is pushed up the hangingwall ramp. Motion on the fault causes an incremental increase in subsidence. Immediately following the fault motion, the lake will move back toward the foot of the fault escarpment. After some lag period, progradation of fans will again displace the playa up the ramp (Blair and Bilodeau, 1988). This zone of tectonically induced cyclothems is not exposed on the northern margin, however the intertonguing of facies association 3 with variants of facies association 2, on the southern side of the basin, is interpreted to represent the record of

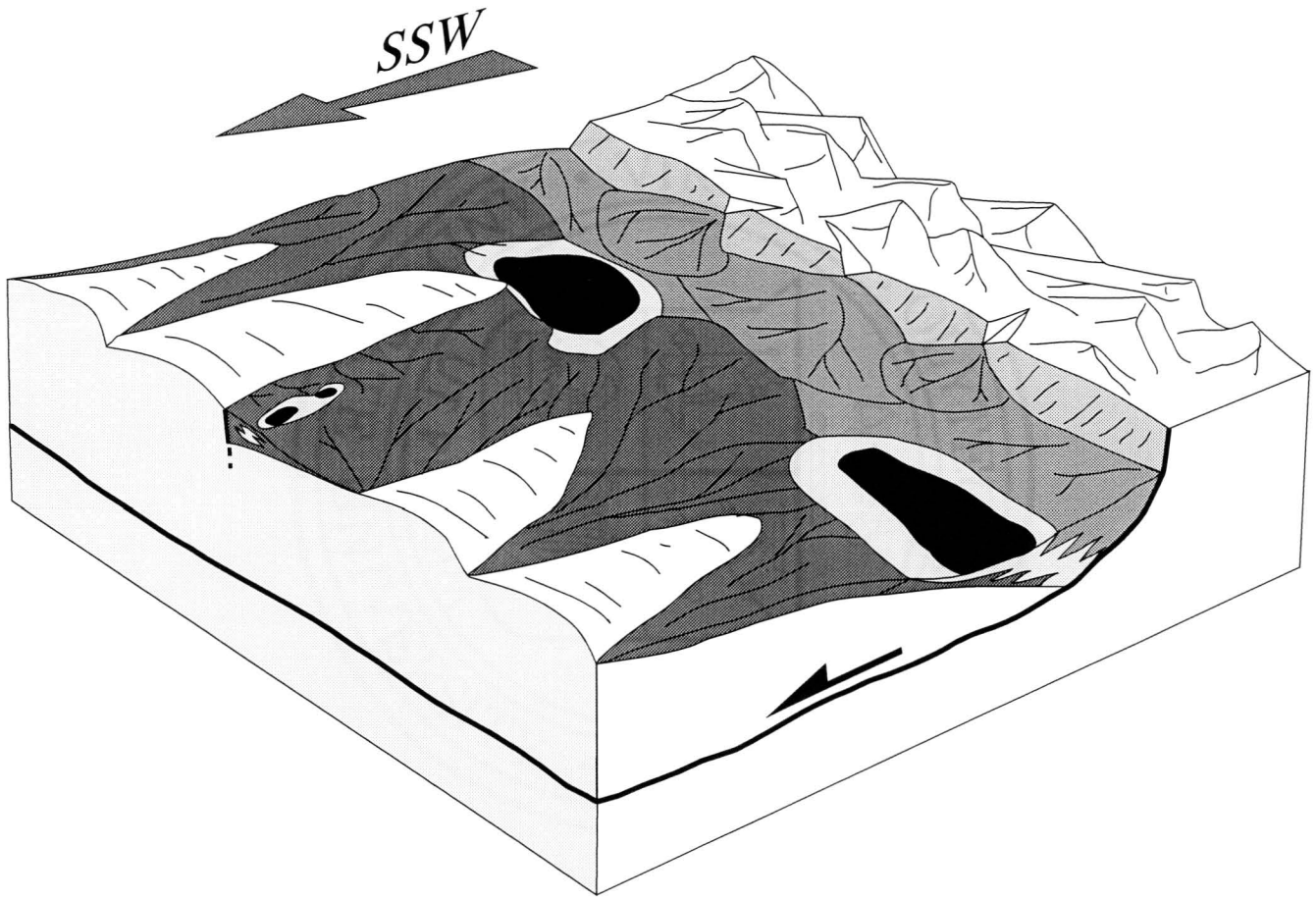

Figure 34. Block diagram illustrating the proposed paleogeographic reconstruction of the early Diligencia Basin. See text for discussion and description of sedimentary units. Not to scale.

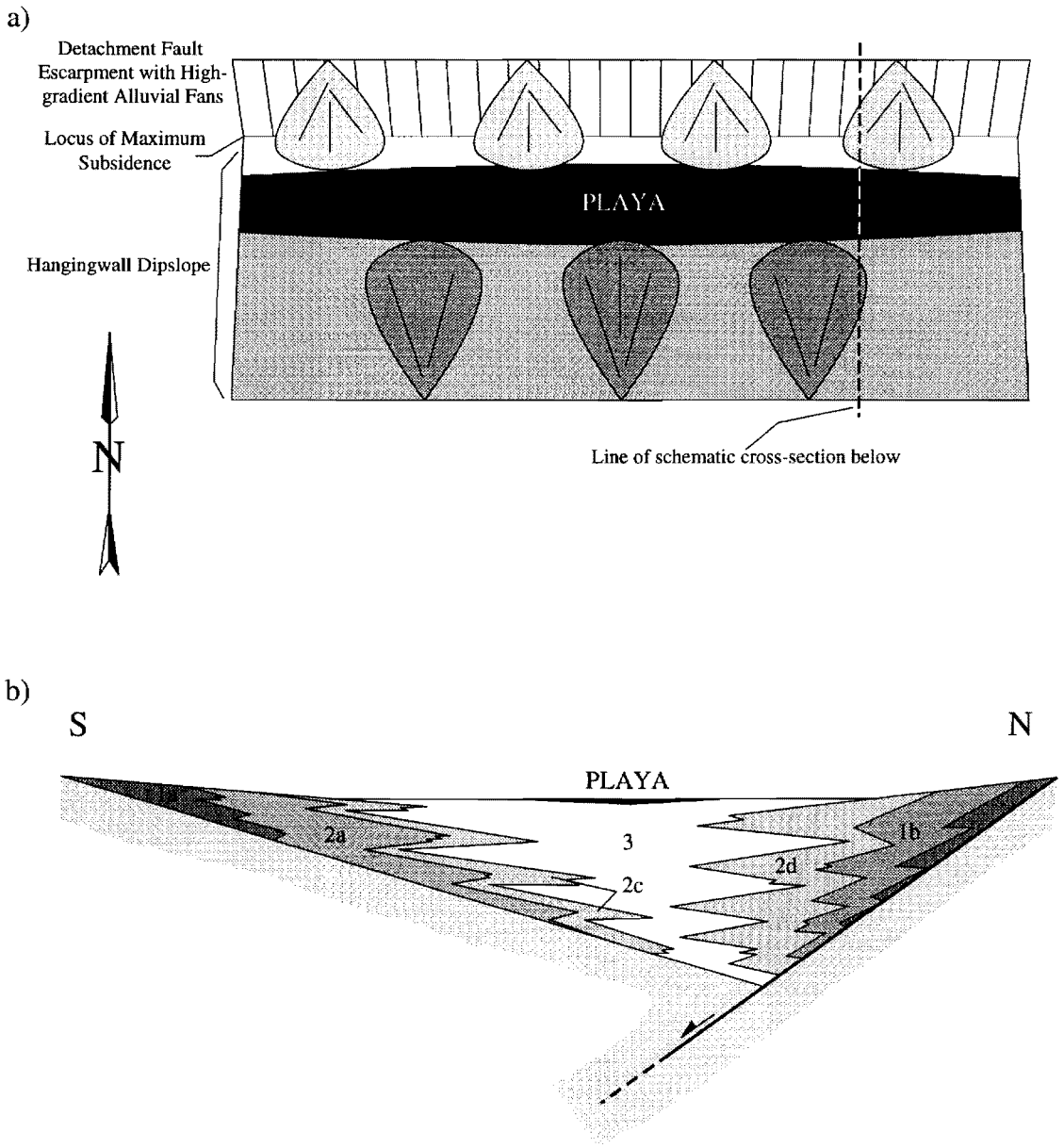

Figure 35. Generalized map of, and profile across a half-graben rift basin, similar to the early Diligencia Basin. Part a) shows a schematic map of the basin, and displays the asymmetric distribution of depositional systems across the basin. Part b) shows a cross-section, where packages are labeled with numbers of corresponding facies associations within Diligencia Formation (e.g. 1a, 2b, 3).

this phenomenon on the updip portion of the hangingwall ramp (see Fig. 35b). An added aspect of this phenomenon is the effect of the dip of the detachment fault. If the basin bounding fault has a low angle of dip, then the distance, in the transport direction, covered by the footwall-sourced alluvial fans will be greater than for a system with a high-angle normal fault (see Fig. 36). In a low-angle fault system, the locus of maximum subsidence will be relatively far inboard from the surface expression of the footwall escarpment (see Fig. 36).

The only definitive evidence of normal displacement across a fault striking parallel to the length of the basin, is observed near the western end of the northern margin (see Plate 1). At this location, a thick gouge zone is observed to separate granitic basement in the footwall from breccia containing granitic clasts, in the hangingwall (see Chapter 3). The fault surface is nearly horizontal with a gentle apparent dip toward the south, into the basin. The association of normal faulting with the northern margin strengthens the interpretation, from sedimentological evidence, that the basin-forming fault ran along the northern margin, and dipped toward the south.

The sedimentary package on the northern margin of the Diligencia Basin indicates that the fault escarpment against which the high-gradient alluvial fans formed, had a steep dip relative to the depositional surface on the southern margin. The presence of low-angle normal faults along this margin, in concert with the inference of a high-angle fault escarpment suggests that the basin bounding fault system may have had a listric geometry (see Fig. 36).

5.3 Discussion

This thesis has demonstrated that the sedimentology of the deposits of the Diligencia Formation, as well as the deformation observed therein, indicate that the Diligencia Basin formed as an asymmetric half-graben in response to presently north-

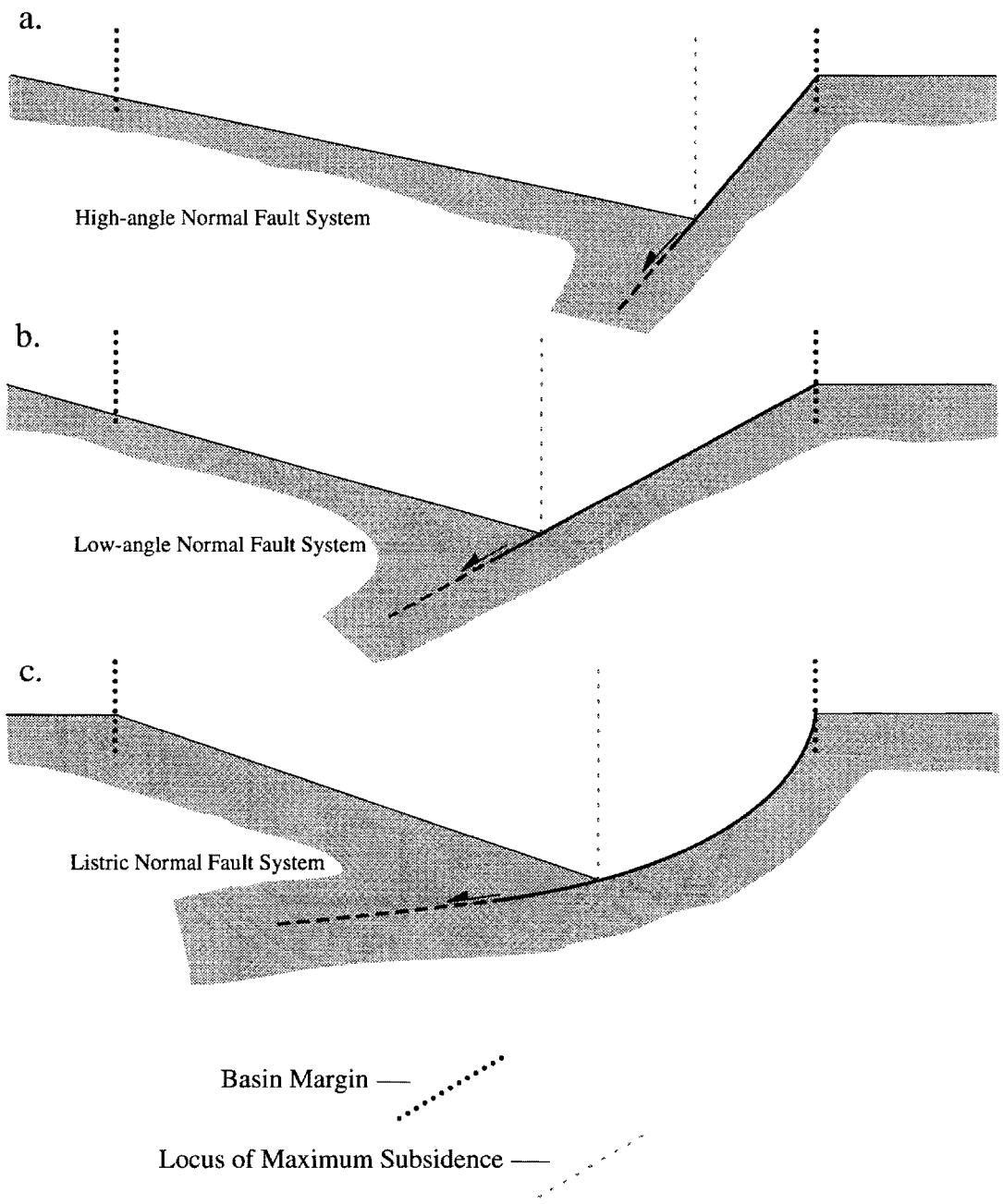

Figure 36. Diagrammatic profiles across half-graben basins, showing the effect of detachment fault geometry on position of the locus of maximum subsidence with respect to basin margins.

south extension. Folds and faults observed in the basin fill are consistent with deformation associated dextral wrenching, rather than syn-sedimentary extension. Robinson and Frost (1989, 1991) have modeled the Diligencia Basin as an asymmetric half-graben which formed along an east-dipping detachment in response to east-west extension (see Chapter 1). This geometry would yield several features of the basin which one might expect to observe. Most fundamental, extension along a north-south striking detachment should yield a north-south elongate trough. The sedimentary fill of this basin should exhibit an asymmetrical distribution of facies as described above, with high-gradient alluvial fans along the western edge, and low-gradient alluvial fans along the eastern margin. In fact, though, the Diligencia Basin is an east-west elongate trough, and this thesis demonstrates that the sense of asymmetry of facies distribution is from north to south, across the long axis of the basin.

Another implication of the model of Robinson and Frost involves sediment composition. If the Diligencia Basin formed by motion across a detachment fault which progressively unroofed a metamorphic core comprising the Orocopia Schist body in the western Orocopia Mountains (see Fig. 2), then the history of this unroofing should be recorded in the clast composition of the Diligencia Formation. The Orocopia Thrust Fault emplaces the anorthosite/syenite/gneiss complex of the central Orocopia Mountains, structurally above the Orocopia Schist to the west (see Fig. 2). If detachment faulting unroofed the Orocopia Schist body during the active lifetime of the Diligencia Basin, then it is to be expected that the clasts in the Diligencia Formation would reflect the distinctive lithologies of the eroded basement terrane. Spittler and Arthur (1982) reported only a single unit containing anorthositic clasts in the Diligencia Formation. In the main, however, clast compositions in the Diligencia Formation suggest that the anorthosite/syenite/gneiss complex did not act as a source terrane. Similarly, the Orocopia Schist is not represented as clasts anywhere within the Diligencia Basin,

although it forms the dominant clast lithology of the Quaternary sediments in the area. The fact that neither the Orocopia Schist, nor those rocks which structurally overlie it are present as clasts in the Diligencia Formation suggests that these rock units were not exposed in proximity to the developing Diligencia Basin. Instead, it is suggested here that the interpretation of Crowell (1975), wherein the Clemens Well Fault has juxtaposed the Diligencia Basin against the rocks to the west (sometime after deposition into the basin had ceased), is more compatible with the observations of this study. This study, therefore, indicates that the Diligencia Basin did not form by the action of a north-south striking, east-dipping detachment fault, in response to east-west directed extension. Rather, the Diligencia Basin is an asymmetric half-graben which formed along a south-dipping detachment in response to presently north-south directed extension.

CHAPTER 6. Summary of Basin Evolution

6.1 Basin Opening and Early Fill

The Diligencia Basin is an asymmetric half-graben rift basin that, with reference to present day geographic coordinates, formed in response to north-south oriented extension. It is suggested that a normal fault along which tectonic subsidence was localized formed the northern margin of the basin. The sedimentary rocks which are present along this margin comprise very coarse conglomerates and sandstones and are interpreted to have been deposited in a high-gradient alluvial/fluvial system that formed on the steeply sloping detachment fault escarpment (see fig. 34). The observed presence of a low-angle normal fault on the northern margin of the outcrop belt, in close association with the high-angle faulting, inferred from the very coarse sediments deposited along the northern margin escarpment, suggests that the fault system which controlled basin formation may have had a listric geometry.

The southern margin of the basin is inferred to lie within the hangingwall of the listric detachment fault system. Sediments were deposited nonconformably on the crystalline basement similar to that from which they were derived. The tilted basement block in the hangingwall of the detachment fault formed a gently-dipping depositional surface on the southern side of the basin, on which a system of low-gradient alluvial fans/fluvial braidplain developed (see fig. 34). A minor component of extension parallel to the axis of the basin resulted in the formation of at least one small, syn-depositional growth fault, at a high angle to the southern basin margin (in the Bullet Peak area).

The central portion of the early Diligencia Basin comprised an ephemeral playa lake complex, wherein lacustrine and lacustrine margin sediments interfingered with alluvial and braided-fluvial deposits from the fan systems along the northern and southern margins of the basin. Within the outcrop area, lacustrine sedimentary rocks are observed

in association with alluvial and fluvial rocks along the southern margin, but the contact with contemporaneous rocks along the northern margin is not exposed. This observation may be explained by the displacement of the lacustrine complex updip onto the hangingwall by the rapid progradation of northern-margin alluvial fans. This effect is enhanced by the role of post-depositional deformation in determining the level of erosional exposure across the basin. Because the rocks have been tilted prior to erosion, the most distal deposits are exposed along the southern margin of the outcrop area, whereas, only relatively more proximal deposits are exposed along the northern margin.

Crustal extension beneath the developing Diligencia Basin was sufficient to permit basaltic volcanism within the basin. This resulted in the extrusion of a greater than one hundred meter thick package of amalgamated basalt flows distributed basinwide. Above the basaltic lavas, approximately 1000 meters of Miocene-age sediments were deposited. These basin fill rocks of the upper Diligencia Formation record two successive pulses of siliciclastic sedimentation into the Diligencia Basin which postdate the deposits which have been discussed in this thesis (Spittler and Arthur, 1982).

6.2 Basin Closure and Block Rotation

6.2.1 Minor Structures

The Diligencia Basin is partially inverted, and the basin-fill package is deformed into a series of faulted folds. Structural analysis of this deformation indicates that the various families of minor structures yield internally consistent estimates of the paleostress field within which they formed. The stress field indicated by structural analysis is not consistent with syndepositional drape folding and normal faulting, as has been suggested by some workers (Robinson and Frost, 1991).

Macro- and meso-scale folds and faults affect the rocks of the Diligencia but are not observed to affect the younger, Quaternary gravels which are present in the area.

However, stress field estimates from these minor scale structural data are consistent with estimates from extensional fracture sets that are observed to cross-cut gravels of Pliocene age (see discussion, sec. 2.3.3), and all paleostress estimates indicate deformation under an imposed compressive stress field. These observations clearly indicate that the deformation observed in the eastern Orocopia Mountains postdates deposition of the lower Miocene Diligencia sediments, and must have progressed at least into the Pliocene.

Analysis of the various post-depositional structures in the Diligencia (e.g. faults, folds, fractures) yield consistent estimates of the orientation of the paleostress field. This stress field is also closely similar to that expected for formation of the Clemens Well Fault. Minor structures in the Diligencia Formation occur in average orientations that are remarkably consistent with those predicted in association with dextral wrench faulting. If these orientations are plotted with respect to the Clemens Well Fault, they compare favorably with ideal orientations predicted from modeling studies (Harding, 1974) (see fig. 37). The greatest deviation from predicted values is the fact that observed structures have formed at a consistently smaller angle to the wrench fault than those in the experimental data set. The modelling study from which these ideal orientations are derived used a clay-cake material to simulate the deforming rock. The wrench fault forms at an angle of 45° to the maximum principal compressive stress axis in such a ductile material. The fact that each family of data from the Diligencia Formation, as well as the Clemens Well Fault itself, lie at less than 45° to the inferred σ_1 suggests that these rocks deformed in a more nearly brittle fashion, thereby following Andersonian geometry more closely.

6.2.2 Paleomagnetic Evidence

Paleomagnetic studies of the basalts in the Diligencia Formation indicate that these rocks may have been rotated through a clockwise angle greater than 90° (to a maximum estimate of approximately 140°) about a vertical axis (Terres, 1984).

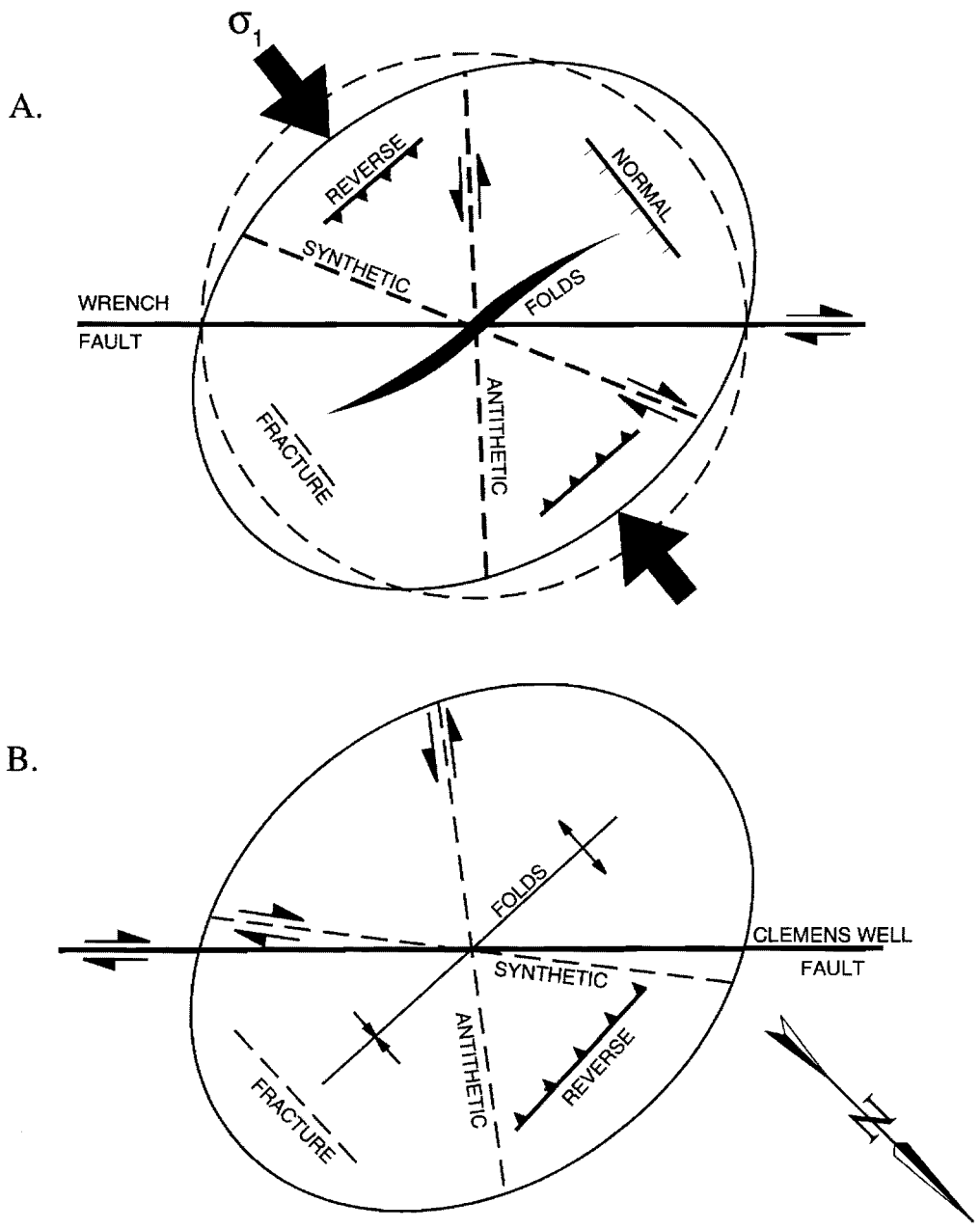

Figure 37. Comparison of ideal average orientations of minor structures with respect to a major dextral wrench fault (part A) (from Sylvester and Smith, 1976, after Harding, 1974), to average orientations of minor structures observed in the Diligencia Formation with respect to the Clemens Well Fault (part B).

This result suggests that, although the Diligencia Basin is presently an east-west elongate trough, the present-day orientation may not accurately reflect the orientation during basin formation. If the block containing the Diligencia basin has been rotated approximately 90°, then the basin may have formed as a north-south elongate trough, along an east-dipping detachment, in response to extension oriented east-west, and may have been subsequently rotated into its present orientation. In addition, regional palinspastic reconstructions, based on paleomagnetic studies, suggest that, in the Miocene, the block containing the Diligencia Basin may have been hundreds of kilometers north and east of its present position (Luyendyk et al., 1985). Since the mid-Tertiary, therefore, the basin may have been moved to its present location by rotation of crustal blocks in response to motion along a complex array of intersecting wrench faults.

6.3 Synthesis

In the past, workers have struggled to place the rocks of the Orocopia Mountains into a tectonic context. Most often, attempts have been made to genetically link these rocks to similar rocks in the Transverse Ranges Province of southern California, or to similar rocks in the Colorado River Extensional Corridor of the Basin and Range. These attempts have not been entirely successful, largely because while the rocks of the Orocopia Mountains share characteristics with rocks in both tectonic settings, they are not similar enough to make either correlation unequivocal. This thesis has demonstrated that the rocks of the eastern Orocopia Mountains share an array of features with comparable basins of the same age in the western Basin and Range. In addition, paleomagnetic reconstructions suggest that the Diligencia Basin may, in the Miocene, have been more closely associated spatially with these basins in the Basin and Range. Therefore, the Diligencia Basin may indeed be genetically related to similar basins in the Basin and Range, and may have been subsequently removed from them by deformation associated

with the development of the dextral strike-slip tectonic regime which has characterized the late Tertiary and Quaternary history of California.

The relatively recent deformation features observed in the rocks of the Diligencia Formation are consistent with a paleostress field associated with a dextral strike-slip fault. Such wrench faults play a singularly important role in the late Tertiary and Quaternary tectonic history of southern California. Two large-scale, dextral, wrench faults are present in close proximity to the Orocopia Mountains: the San Andreas Fault zone, and the related (and potential precursor) Clemens Well Fault. The presence of large, dextral, strike-slip faults, and the characteristic deformation associated with them is one of the defining characteristics of the Transverse Ranges. The associations of distinctive basement lithologies and San Andreas-style structures, give good reason to link the Orocopia Mountains to similar complexes in the Transverse Ranges.

This thesis has demonstrated that the Diligencia Basin, and associated rocks of the Orocopia Mountains share tectonic and lithologic characteristics with rocks of both the western Basin and Range and the Transverse Ranges. However, these features and events are separated in time. The formation of the basin, and subsequent filling, may be closely related to mid-Tertiary extension which also formed rift basins in the Colorado River Extensional Corridor. Subsequently, the rocks of the Diligencia Formation were deformed by the action of detral wrench faulting, and placed in proximity to distinctive crystalline rocks which tie the complex to the Transverse Ranges. Enough information now exists to indicate that processes associated with both Basin and Range tectonics and Transverse Ranges tectonics have been important in the development of the rocks of the Orocopia Mountains, but at different times in the history of the basin.

Appendix 1

Structural Data

All structural data used in this thesis are presented in this appendix. The data are separated into four groups by type. These groups are:

A) Bedding orientations measured from the first syncline/anticline fold set north of the southern basin margin. These data are presented as dip azimuth and dip angle.

B) Minor fold hinge traces. These data are presented as trend azimuth.

C) Minor fault trace trends. These data are presented as trend azimuth.

D) Orientation of extensional fractures. These data are presented as dip azimuth and dip angle.

A) Bedding Orientations of first syncline north of southern basin margin

Dip Azimuth	Dip Angle	Dip Azimuth	Dip Angle	Dip Azimuth	Dip Angle
000	082	018	055	172	036
000	057	018	061	175	086
000	057	018	027	175	062
000	084	020	085	178	020
001	072	020	077	179	086
001	053	020	078	182	075
001	085	020	072	184	059
002	072	020	077	186	079
002	063	021	080	186	025
003	053	021	069	186	070
003	064	021	083	187	068
003	079	022	084	189	071
004	061	023	046	189	063
005	024	026	076	192	084
006	062	026	067	192	040
007	046	027	078	193	073
008	073	028	058	193	068
009	057	030	090	194	060
009	075	031	079	194	068
010	047	031	081	194	021
011	080	031	070	195	053
011	056	032	053	195	048
011	061	033	086	197	022
012	077	034	051	197	030
012	061	036	067	198	027
012	062	036	039	200	044
013	090	046	088	203	031
013	064	048	058	204	030
014	084	056	062	204	042
014	090	056	070	206	034
015	035	138	061	206	036
015	036	152	073	206	034
015	045	155	035	207	018
016	060	156	085	208	071
018	078	156	089	208	028

A) Bedding Orientations of first syncline (cont.)

Dip Azimuth	Dip Angle
209	059
209	048
210	070
211	055
211	026
213	034
213	042
216	032
216	026
216	026
216	041
217	026
217	030
218	051
218	020
218	051
218	062
220	070
220	021
220	052
220	024
221	051
221	037
221	064
222	031
223	018
223	032
223	023
224	022
225	014
225	034
225	035
225	041
226	036
227	031
227	028
227	030
227	042
229	027

Dip Azimuth	Dip Angle
229	039
230	033
232	040
233	029
233	034
234	025
234	023
234	034
234	042
235	034
235	037
235	025
236	024
237	022
237	043
239	023
239	031
240	031
241	025
241	033
244	030
245	056
246	012
247	040
247	050
250	022
255	014
256	034
257	030
259	029
261	029
262	038
263	028
263	026
267	061
268	043
269	020
270	015
271	012

Dip Azimuth	Dip Angle
274	026
274	013
277	032
278	085
282	020
288	027
290	022
292	021
292	029
298	033
301	030
309	081
313	063
317	022
327	079
328	069
331	011
332	079
335	050
343	071
346	064
347	075
348	053
348	089
351	076
351	045
352	059
352	059
352	077
352	090
355	065
355	070
358	062
358	061
359	086

A) Bedding Orientations from first anticline north of southern basin margin

Dip Azimuth	Dip angle	Dip Azimuth	Dip angle	Dip Azimuth	Dip angle
000	61	198	27	218	62
001	74	200	44	220	21
005	83	203	31	220	52
005	20	203	43	220	24
006	40	204	30	221	51
016	15	204	42	221	37
016	14	205	44	221	64
018	27	206	34	222	31
023	46	206	36	223	18
024	40	206	34	223	32
025	54	206	19	223	23
036	39	207	18	224	22
037	74	208	28	225	14
150	11	209	48	225	34
155	35	211	55	225	35
172	36	211	26	225	41
173	34	211	25	226	36
178	20	213	34	226	25
181	15	213	42	227	31
184	59	213	18	227	28
185	30	214	23	227	30
186	25	215	49	227	42
186	70	215	24	228	54
192	40	216	32	229	27
193	68	216	26	229	39
194	60	216	26	230	33
194	68	216	41	231	15
194	21	217	26	232	40
195	53	217	30	232	12
195	48	218	51	233	29
197	22	218	20	233	34
197	30	218	51	234	25

A) Bedding Orientations from first anticline (cont.)

Dip Azimuth	Dip Angle	Dip Azimuth	Dip Angle	Dip Azimuth	Dip Angle
234	23	254	18	301	30
234	34	255	14	301	40
234	42	256	34	301	22
234	40	256	35	303	48
235	34	257	30	305	37
235	37	259	29	309	18
235	25	261	29	317	22
236	24	262	38	317	14
236	15	263	28	319	15
237	22	263	26	321	37
237	43	267	61	321	24
237	40	268	43	321	36
238	56	269	20	323	36
239	23	271	12	324	18
239	31	274	26	330	86
240	31	274	13	331	11
240	15	277	32	331	63
241	25	278	85	337	27
241	33	282	20	343	12
241	11	282	22	350	86
243	21	283	14	351	87
244	30	286	30	352	76
244	21	287	23	352	73
245	56	288	27	355	35
246	12	290	22	356	63
247	40	290	29	359	69
247	50	292	29	359	73
250	22	292	18	359	18
250	14	294	16		
253	17	298	33		

B) Minor Fold Hinge Traces

These data include minor folds mapped during the fieldwork for this thesis, as well as those measured directly from the geologic map of Arthur (1974).

Western Minor Fold Hinge Traces
044
045
051
068
074
085
089
091
094
094
098
100
102
103
106
106
108
109
110
110
110
110
112
114
116
117
117
117
120
121
134

Eastern Minor Fold Hinge Traces
103
104
106
108
109
112
113
114
120
120
121
121
121
121
122
122
124
126
129
130
138
138
139
148

C) Minor Fault Trace Trends

These data include minor faults mapped during the fieldwork for this thesis, as well as those measured directly from the geologic map of Arthur (1974).

Western Minor Fault Trace Trends

001	064
006	066
023	066
029	070
031	078
034	079
035	081
038	081
039	082
040	084
042	089
042	089
043	091
044	108
045	114
048	114
049	122
050	124
051	130
052	143
053	149
054	150
055	152
056	156
056	159
057	160
057	161
058	
059	
061	
062	

Eastern Minor Fault Trace Trends

001	082
005	084
006	090
011	102
014	105
018	122
021	136
022	138
026	139
027	139
029	140
029	141
036	145
037	146
039	146
040	148
044	150
056	150
060	152
062	154
064	156
066	158
070	159
072	162
074	164
075	164
078	164
079	166
082	168
082	174

D) Fracture Orientations

Dip Azimuth	Dip Angle
000	55
005	60
010	50
010	58
010	70
025	70
030	70
035	37
040	35
040	55
040	45
045	45
046	29
050	45
052	31
055	71
058	45
059	80
060	35
063	42
065	85
069	29
070	35
070	65
070	35
070	55
072	33
075	19

Dip Azimuth	Dip Angle
075	60
075	30
075	40
077	37
080	85
080	50
080	45
080	70
081	89
081	61
085	51
085	49
090	50
090	65
091	40
091	25
091	30
092	68
093	48
093	62
093	41
095	40
097	64
097	30
097	45
097	42
099	35
099	80

Dip Azimuth	Dip Angle
099	55
100	76
100	50
100	70
100	75
100	70
100	75
100	70
100	90
100	75
100	90
101	50
102	40
110	60
110	80
111	35
113	50
115	38
115	49
115	55
117	50
118	92
118	81
119	50
120	46
120	48
120	40
120	80

D) Fracture Orientations continued

Dip Azimuth	Dip Angle
120	60
120	40
120	70
120	60
122	88
124	40
125	70
126	32
135	65
135	65
140	50
140	50
144	62
237	20

Dip Azimuth	Dip Angle
240	22
242	18
243	65
245	75
247	71
255	70
259	58
260	55
264	28
265	55
267	50
270	60
270	70
270	65

Dip Azimuth	Dip Angle
271	65
272	79
275	75
275	65
275	60
275	55
275	45
277	80
280	60
280	60
280	60
280	0
285	60

Appendix 2

Localities of Measured Sections

The following appendix presents details of the topographic base maps of the eastern Orocopia Mountains, and the precise locations of the measured stratigraphic sections presented in Chapter 4, figure 20. The index on this page shows the locations of the following maps on Plate 1.

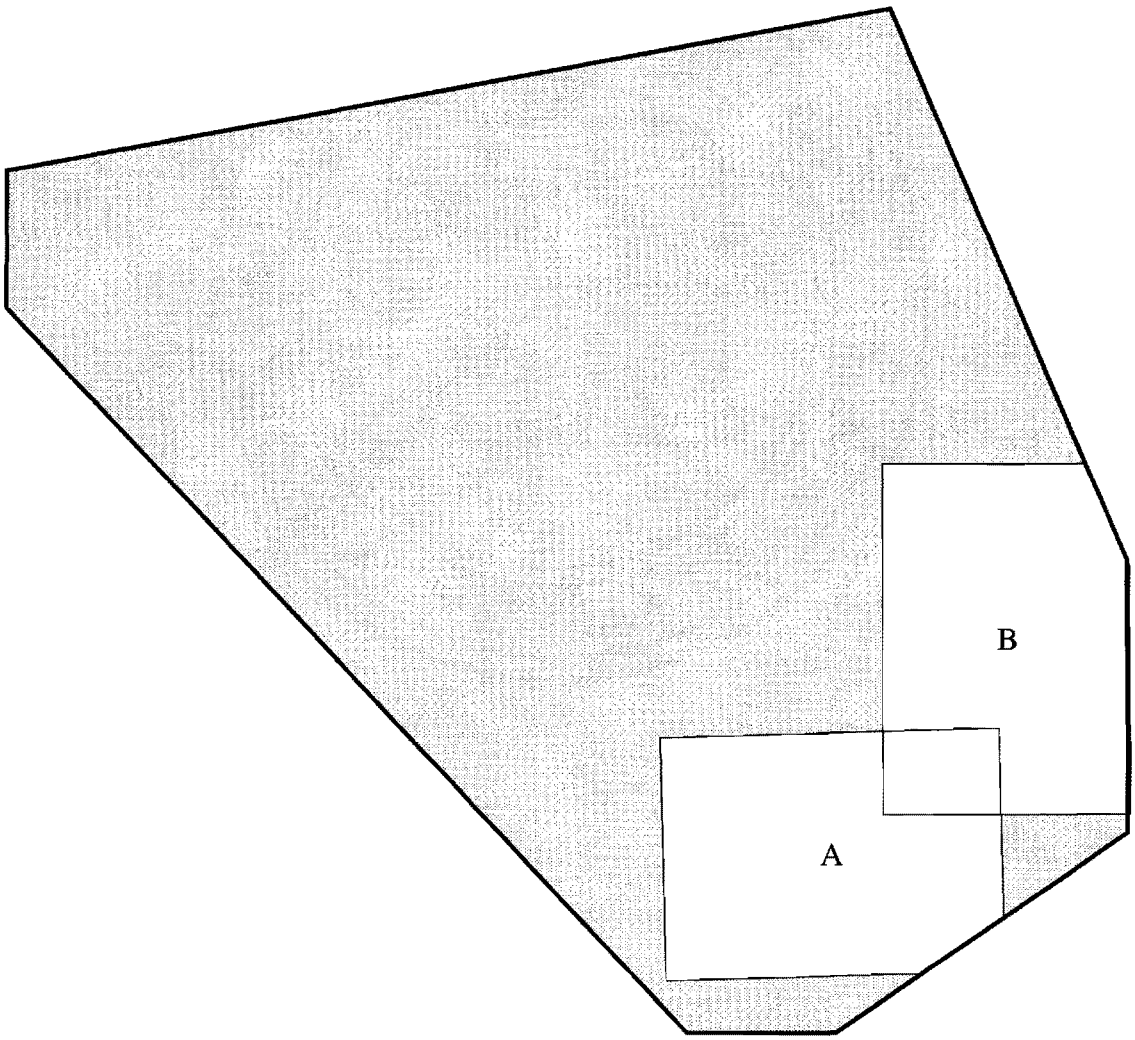

A
Canyon Spring Section
Bullet Peak Section
Name Wall Section
Saddle Section
Clemens Well

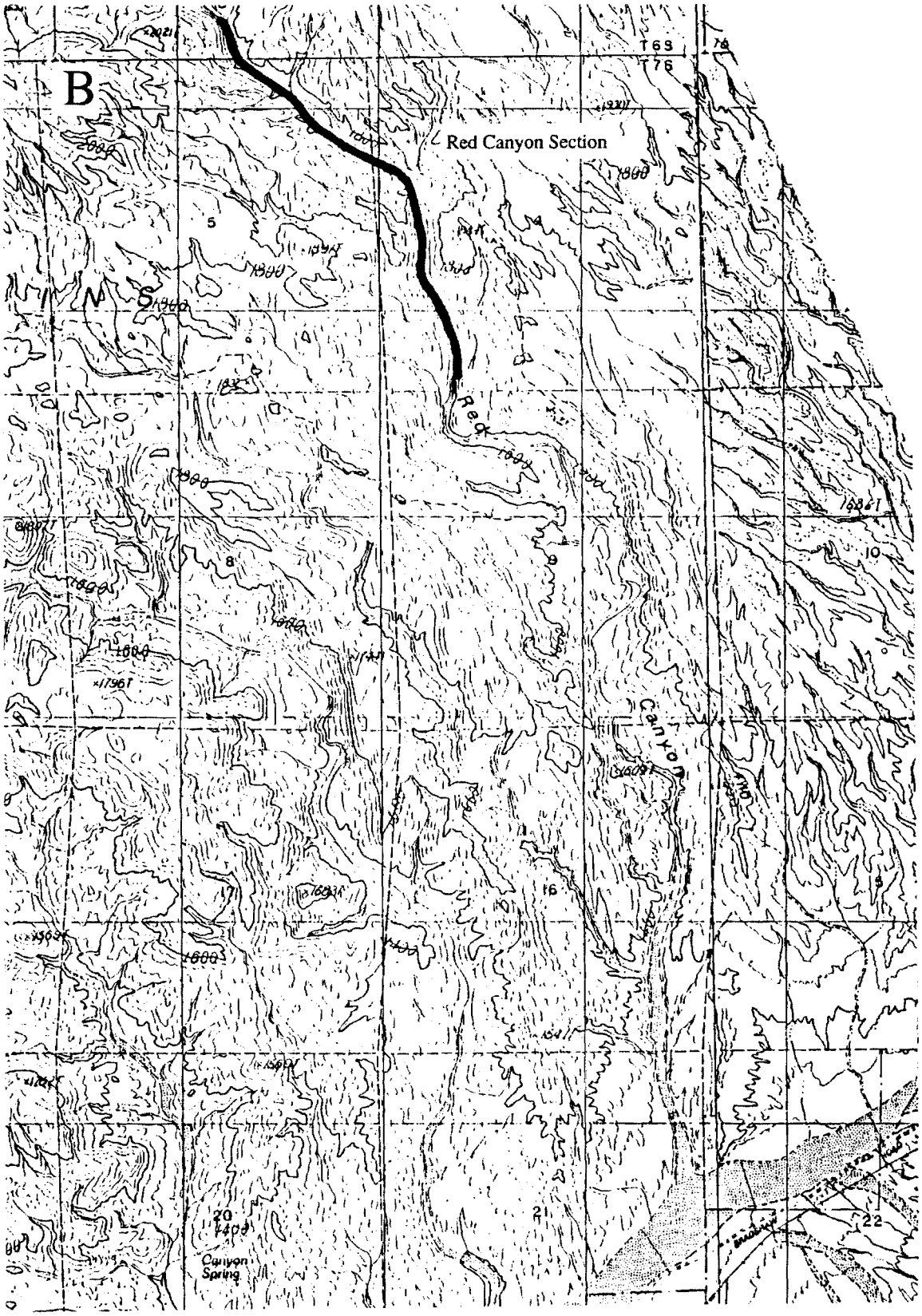
B
Red Canyon Section
T63
T76
Canyon Spring

Appendix 3

Paleocurrent Data

All paleocurrent measurements taken from sedimentary rocks of the lower Diligencia Formation are presented in this appendix. Measurements have been rotated into approximate horizontality about axes parallel to nearby fold hinges. Note that this rotation has resulted in very gently plunging linear orientations in most cases, rather than ideal horizontal azimuths. Planar structures (trough limbs and tabular crossbed foresets) are presented as dip azimuth and dip angle. Linear structures (trough axes, sole marks, current lineations, ripple crest and oscillations directions) are presented as trend azimuth and plunge angle (where greater than 0°).

NAME WALL PALEOCURRENTS

Trough Axes

290	3
109	6
288	3
280	2
282	2
280	2
282	2

Sole Marks and Current Lineations

295	4
290	3
290	3
292	4
292	4
289	3
288	3
282	2
284	2
282	2
284	2

Symmetrical Ripple Crests

235	8
229	8
237	10
060	5
062	5
058	5
298	5

Oscillation Directions

145
139
147
150
152
148
208

CLEMENS WELL SADDLE PALEOCURRENTS

Channels and Sole Marks

343	4
335	5
021	3
019	4
117	2
091	2
098	2
102	7
098	5
281	6
283	7
295	12
077	0
088	0

Trough Limbs

079	27
045	19
152	74

Tabular Crossbed Foresets

015	27
039	39
037	27
125	80

Clemens Well Saddle ripples

081	16
251	6

Oscillation Directions

171
161

BULLET PEAK PALEOCURRENTS

Trough Axes

294	9
306	9
302	9
300	9

Symmetrical Ripples

179	12

Oscillation Direction

089

CANYON SPRING PALEOCURRENT

Trough Axis

203	17

Symmetrical Ripples

292	7
304	14
312	11
313	3
316	21
313	12
291	9
354	10
350	21
012	25

Oscillation Direction

202
214
222
223
226
222
201
264
260
102

RED CANYON PALEOCURRENTS

LOWER PORTION OF SECTION

Trough Axes

160
106
108
170
188
140
140
142
144
136
132
188
192
150

Current Lineations

132
130
126
136
172
190
128
038

UPPER PORTION OF SECTION

Trough Axes

130
124
158
140
160
164
152
190
142
164
148
154
138
146
119

Trough Axes (cont.)

142
118
120
122
100
160
140
142
152
146
164
170
120
136
120

Tabular Crossbed Foresets

156
140
190
146
180

References Cited

Advocate, D. M., 1983, Depositional Environments of the Eocene Maniobra Formation, Northeastern Orocopia Mountains, Riverside County, Southern California [M.S. Thesis]: California State University at Northridge, 112 pp.

Anderson, E. M., 1951, *The Dynamics of Faulting*, Oliver and Boyd, Edinburgh, 206 pp.

Armstrong, R. L. and J. Suppe, 1973, Potassium-argon geochronometry of Mesozoic igneous rocks in Nevada, Utah, and southern California: v. 84, (4), p. 1375-1392.

Arthur, M. A., 1974, Stratigraphy and sedimentation of Lower Miocene non-marine strata of the Orocopia Mountains: constraints for late Tertiary slip on the San Andreas fault system in southern Califonia [M. S. Thesis]: University of California, Riverside, 200 pp.

Atwater, T., 1970, Implications of plate tectonics for the Cenozoic evolution of western North America: Geological Society of America Bulletin, v. 81, p. 3513-3536.

Axelrod, D. I., 1950, *Studies in Late Tertiary Paleobotany*, Contributions to Paleontology, Carnegie Institute of Washington, Washington, D.C., 323 pp.

Blair, T. C. and W. L. Bilodeau, 1988, Development of tectonic cyclothems in rift, pull-apart, and foreland basins: sedimentary response to episodic tectonism.: Geology, v. 16, p. 517-520.

Blatt, H., G. Middleton and R. Murray, 1980, *Origin of Sedimentary Rocks*, Prentice-Hall, Inc, Englewood Cliffs, NJ, 781 pp.

Bohannon, R. G., 1976, Mid-Tertiary along the San Andreas Fault in southern California [PhD Dissertation]: University of California, Santa Barbara, 311 pp.

Boothroyd, J. C. and G. M. Ashley, 1975, Processes, Bar Morphology, and Sedimentary Structures on Braided Outwash Fans, Northeastern Gulf of Alaska, *In:* Jopling, A. V. and B. C. McDonald, eds., *Glaciofluvial and Glaciolacustrine Sedimentation*, Society of Economic Paleontologists and Mineralogists, Tulsa, OK, p. 193-222.

Carter, J. N., B. P. Luyendyk and R. R. Terres, 1987, Neogene clockwise tectonic rotation of the eastern Transverse Ranges, California, suggested by paleomagnetic vectors: Geological Society of America Bulletin, v. 98, p. 199-206.

Cole, R. B. and R. G. Stanley, 1992, Alluvial-fan and Lacustrine Fan-delta Sedimentation in West-central California During the Middle Tertiary Transition from Subduction to Transform Tectonics, Geological Society of America, Abstracts with Programs, v. 24, p. A51.

Coney, P. J., 1987, The regional tectonic setting and possible causes of Cenozoic extension in the North American Cordillera, *In:* Coward, M. P., J. F. Dewey and P. L. Hancock, eds., *Continental Extensional Tectonics*, Geological Society Special Publication No. 28, p. 177-186.

Coney, P. J. and T. A. Harms, 1984, Cordilleran metamorphic core complexes: Cenozoic extensional relics of Mesozoic compression: Geology, v. 12, p. 550-554.

Crowell, J. C., 1957, Structure of the Orocopia Mountains, southeastern California: Geological Society of America Bulletin, v. 68, (12), p. 1712.

Crowell, J. C., 1974, The Orocopia thrust, southeastern California, Geological Society of America, Abstracts with Programs, v. 6, p. 159.

Crowell, J. C., 1975a, Geologic Sketch of the Orocopia Mountains, Southeastern California, *In:* Crowell, J. C., ed., *San Andreas Fault in Southern California: A guide to San Andreas Fault from Mexico to Carrizo Plain*, California Division of Mines and Geology, Special Report 118, Sacremento, Ca, p. 99-110.

Crowell, J. C., 1975b, The San Andreas Fault in Southern California, *In:* Crowell, J. C., ed., *San Andreas Fault in Southern California, A guide to San Andreas Fault from Mexico to Carrizo Plain*, California Division of Mines and Geology, Special Report 118, Sacremento, CA, p. 7-27.

Crowell, J. C., 1981, An Outline of the Tectonic History of Southeastern California, *In:* Ernst, W. G., ed., *The Geotectonic Development of California*, Prentice-Hall, Englewood Cliffs, NJ, p. 583-600.

Crowell, J. C. and T. Susuki, 1959, Eocene stratigraphy and paleontology, Orocopia Mountains, southeastern California: Geological Society of America Bulletin, v. 70, p. 581-592.

Crowell, J. C. and J. W. R. Walker, 1962, Anorthosite and related rocks along the San Andreas fault, southern California: California University Publications in the Geological Sciences, v. 40, (4), p. 219-288.

Davis, G. A. and G. S. Lister. 1988. *Detachment faulting in continental extension; Perspectives from the Southwestern U.S. Cordillera.* Geological Society of America, Special Paper 218, p. 133-159 .

Ehlig, P. L., 1981, Origin and Tectonic History of the Basement Terrane of the San Gabriel Mountians, Central Transverse Ranges, *In:* Ernst, W. G., ed., *The Geotectonic Development of California*, Prentice-Hall, Englewood Cliffs, NJ, p. 253-283.

Ehlig, P. L., T. E. Davis and R. L. Conrad, 1975, Tectonic implications of the cooling age of the Pelona Schist, Geological Society of America, Abstracts with Programs, v. 7, p. 314-315.

Ehlig, P. L. and K. W. Ehlert, 1972, Offset of Miocene Mint Canyon Formation from Volcanic Source along San Andreas Fault, Southern California, Geological Society of America, Abstracts with Programs, v. 4, p. 154.

Ehlig, P. L., K. W. Ehlert and B. M. Crowe, 1975, Offset of the Upper Miocene Caliente and Mint Canyon Formations along the San Gabriel and San Andreas Faults, *In:* Crowell, J. C., ed., *The San Andreas Fault in Southern California: A guide to the San*

Andreas Fault from Mexico to Carrizo Plain, California Division of Mines and Geology, Special Report 118, Sacramento, CA, p. 83-92.

Fedo, C. M. and J. M. G. Miller, 1992, Evolution of a Miocene half-graben basin, Colorado River extensional corridor, southeastern California: Geological Society of America Bulletin, v. 104, p. 481-493.

Fisher, R. V., 1971, Features of coarse-grained, high-concentration fluids and their deposits.: Journal of Sedimentary Petrology, v. 41, p. 916-927.

Frost, E. G., T. E. Cameron, D. Krummenacher and D. L. Martin, 1981, Possible regional interaction of mid-Tertiary detachment faulting with the San Andreas Fault and the Vincent-Orocopia thrust system, Arizona and California, Geological Society of America, Abstracts with Program, v. 13, p. 455.

Frost, E. G., T. E. Cameron and D. L. Martin, 1982, Comparison of Mezoic tectonics with mid-Tertiary detachment faulting in the Colorado River area, California, Arizona and Nevada, *In:* Cooper, J. D., ed., *Geologic Excusions in the California Desert*, Geological Society of America, Boulder CO, p. 111-159.

Frost, E. G. and D. L. Martin, 1983, Overprint of Tertiary detachment deformation on the Mesozoic Orocopia Schist and Chocolate Mtns. thrust, Geological Society of America, Abstracts with Program, v. 15, p. 577.

Frost, E. G., D. L. Martin and D. Krummanacher, 1982, Mid-Tertiary detachment faulting in southwestern Arizona and southeastern California and its overprint on the Vincent thrust system, Geological Society of America, Abstracts with Program, v. 14, p. 164.

Frost, E. G. and J. K. Otton, 1981, Mid-Tertiary stratigraphic record produced during regional detachment faulting and development of extensional arches and basins, southwest of the Colorado Plateau, Geological Society of America, Abstracts with Program, v. 13, p. 197.

Gans, P. B., 1987, An open-system, two-layer crustal stretching model for the eastern Great Basin: Tectonics, v. 6, (1), p. 1-12.

Goodmacher, J., L. Barnett, G. Buckner, L. Ouachrif, A. Vidigal and E. G. Frost, 1989, The Clemens Well Fault in the Orocopia Mountains of Southern California; a Strike-slip or Normal Fault Structure?, Geological Society of America, Abstracts with Programs, v. 21, p. 85.

Hamblin, A. P. and B. R. Rust, 1989, Tectono-sedimentary analysis of alternate-polarity half-graben basin-fill successions: Late Devonian-Early Carboniferous Horton Group, Cape Breton Island, Nova Scotia: Basin Research, v. 2, p. 239-255.

Hardie, L. A. and H. P. Eugster, 1970, *The Evolution of Closed Basin Brines*, Special Publication No. 3, Mineralogical Society of America, 273-290 pp.

Hardie, L. A., J. P. Smoot and H. P. Eugster, 1978, Saline lakes and their deposits: a sedimentological approach, *In:* Matter, A. and M. E. Tucker, eds., *Modern and ancient*

lake sediments, Special Publications of the International Association of Sedimentologists, No. 2, p. 7-41.

Harding, T. P., 1974, Petroleum Traps Associated with Wrench Faults: The American Association of Petroleum Geologists Bulletin, v. 58, (7), p. 1290-1304.

Haxel, G. and J. Dillon, 1978, The Pelona-Orocopia Schist and Vincent-Chocolate Mountain thrust system, southern California, *In:* Howell, D. G. and K. McDougall, eds., *Mesozoic paleogeography of the western United States*, Pacific Coast Paleogeography Symposium, Sacremento, CA, p. 453-469.

Hornafius, J. S., B. P. Luyendyk, R. R. Terres and M. J. Kamerling, 1986, Timing and extent of Neogene tectonic rotation in the western Transverse Ranges, California: Geological Society of America Bulletin, v. 97, p. 1476-1487.

Karcz, I., 1972, Sedimentary Structures Formed by Flash Floods in Southern Israel: Sedimentary Geology, v. 7, p. 161-182.

Karpeta, W. P., 1993, Volcanism and Sedimentation in Part of a Late Archaean Rift: the Hartbeesfontein Basin, Transvaal, South Africa: Basin Research, v. 5, (1), p. 1-19.

Leeder, M. R. and R. L. Gawthorpe, 1987, Sedimentary models for extensional tilt-block/half-graben basins, *In:* Coward, M. P., J. F. Dewey and P. L. Hancock, eds., *Continental Extensional Tectonics*, Geological Society Special Publication Number 28, p. 139-152.

Lister, G. S. and G. A. Davis, 1989, The origin of metamorphic core complexes and detachment faults formed during Tertiary continental extension in the northern Colorado River region, U.S.A.: Journal of Structural Geology, v. 11, (1/2), p. 65-94.

Lowe, D. R., 1979, Sediment gravity flows: their classification and some problems of application to natural flows and deposits, *In:* Doyle, L. J. and O. H. Pilkey, eds., *Geology of continental slopes*, Society of Economic Paleontologists and Mineralogists, Special Publication No. 27, p. 75-82.

Lowe, D. R., 1982, Sediment Gravity Flows: II. Depositional Models with Special Reference to the Deposits of High-density Turbidity Currents: Journal of Sedimentary Petrology, v. 52, (1), p. 279-297.

Luyendyk, B. P., M. J. Kamerling, R. R. Terres and J. S. Hornafius, 1985, Simple Shear of Southern California During Neogene Time Suggested by Paleomagnetic Declinations: Journal of Geophysical Research, v. 90, (B14), p. 12,454-12,466.

Mancktelow, N., 1989, Stereoplot, v. 1.2, Stereographic Analysis Software for the Macintosh System.

Marshak, S. and G. Mitra, 1988, *Basic Methods of Structural Geology*, Prentice-Hall, Inc., Englewood Cliffs, NJ, 446 pp.

McGannon, D. E., Jr., 1975, Primary Fluvial Oolites: Journal of Sedimentary Petrology, v. 45, p. 719-727.

McKee, E. D., E. J. Crosby and H. L. J. Berryhill, 1967, Flood Deposits, Bijou Creek Colorado, June 1965: Journal of Sedimentary Petrology, v. 37, (3), p. 829-851.

Miall, A. D., 1977, A review of the braided-river depositional environment: Earth Sciences Reviews, v. 13, p. 1-62.

Miller, J. M. G. and B. E. John, 1988, Detached strata in a Tertiary low-angle normal fault terrane: a sedimentary record of unroofing, breaching, and continued slip: Geology, v. 16, p. 645-648.

Miller, W. J., 1944, Geology of Palm Springs-Blythe Strip, Riverside County, California: California Journal of Mines and Geology, v. 40, p. 11-72.

Misch, P. H., 1960, West Cordilleran metamorphic and granitic evolution: Geological Society of America Bulletin, v. 71, (12), p. 2069.

Morris, R. S. and D. A. Okaya, 1986, Crustal Geometry of Detachment Faulting--Structural Analysis of Seismic-Reflection Data in SE California, Geological Society of America, Abstracts with Programs, v. 18, p. 160.

Morris, R. S., D. A. Okaya, E. G. Frost and P. E. Malin, 1986, Base of the Orocopia Schist as Imaged on Seismic Reflection Data in the Chocolate and Cargo Muchacho Mtns. Region of SE Calif., and the Sierra Pelona Region Near Palmdale , Calif., Geological Society of America, Abstracts with Programs, v. 18, p. 160.

Mount, V. S. and J. Suppe, 1992, Present-Day Stress Orientations Adjacent to Active Strike-Slip Faults: California and Sumatra: Journal of Geophysical Research, v. 97, (B8), p. 11,995-12,013.

Neilson, J. E. and K. K. Beratan, 1990, Tertiary basin development and tectonic implications, Whipple detachment system, Colorado River extensional corridor, California and Arizona: Journal of Geophysical Research, v. 95, p. 599-614.

Nelson, C. A., 1981, Basin and Range Province, *In:* Ernst, W. G., ed., *The Geotectonic Development of California*, Prentice-Hall, Englewood Cliffs, NJ, p. 203-216.

Nemec, W. and R. J. Steel, 1984, Alluvial and coastal conglomerates: their significant features and some comments on gravelly mass-flow deposits, *In:* Koster, E. H. and R. J. Steel, ed., *Sedimentology of gravels and conglomerates*, Canadian Society of Petroleum Geologists, Memoir 10, p. 1-34.

Nilsen, T. H., 1982, Alluvial fan deposits, *In:* Scholle, P. A. and D. Spearing, ed., *Sandstone Depositional Environments*, American Association of Petroleum Geologists, p. 49-86.

Norris, R. M. and R. W. Webb, 1976, *Geology of California*, John Wiley &Sons, New York, 541 pp.

Okaya, D. A. and E. G. Frost, 1987, Three-dimensional geometry of regional seismic character terranes derived from seismic reflection profiles, Colorado Plateau to Salton

Trough crustal transect, Geological Society of America, Abstracts with Program, v. 19, p. 793.

Picard, M. D. and L. R. High, 1973, *Sedimentary Structures of Ephemeral Streams*, Developments in Sedimentology, Elsevier Scientific Publishing Co., Amsterdam, 223 pp.

Powell, R. E., 1981, Geology of the Crystalline Basement Complex, Eastern Transverse Ranges, Southern California: Constraints on Regional Tectonic Interpretations [Ph.D. Dissertation]: Cal Tech, 441 pp.

Powell, R. E., 1982, Crystalline Basement Terranes in the Southern Eastern Transverse Ranges, California, *In:* Cooper, J. D., ed., *Geologic Excursion in the Transverse Ranges, Southern California: Field Trip Guide Book*, Geological Society of America, p. 109-151.

Pridmore, C. L. and E. G. Frost, 1992, Detachment Faults: California's Extended Past: California Geology, v. 45, (1), p. 3-17.

Ramsay, J. G. and M. I. Huber, 1987, *The Techniques of Modern Structural Geology: Volume 2: Folds and Fractures*, Academic Press, London, 700 pp.

Rehrig, W. A., 1982, Metamorphic Core Complexes of the Southwestern United States, *In:* Frost, E. G. and D. L. Martin, eds., *Mesozoic-Cenozoic Evolution of the Colorado River Region, California, Arizona, and Nevada*, Cordilleran Publishers, San Diego, CA, p. 551-560.

Robinson, K. L. and E. G. Frost, 1989, Orocopia Mountains detachment system; progressive ductile to brittle development of a tilted crustal slab during regional extension, Geological Society of America, Abstracts with Program, v. 21, p. 135.

Robinson, K. L. and E. G. Frost, 1991, Tertiary Extension and Basin Development in Southern California: The Temporal Similarity, Style of Deformation and Crustal Geometry in the Orocopia Mountains and the San Joaquin Hills, Geological Society of America, Abstracts with Programs, v. 23, p. A132-A133.

Silver, L. T., 1971, Problems of Crystalline Rocks of the Transverse Ranges, Geological Society of America, Abstracts with Programs, v. 3, p. 193-194.

Smith, D. P. 1977. *San Juan-St. Francis fault- Hypothesized major middle-Tertiary right-lateral fault in central and southern California.* California Division of Mines and Geology, Special Report 129, p. 41-50 .

Spittler, T. E., 1974, Tertiary basaltic volcanism of the Orocopia Mountains, California, Geological Society of America, Abstracts with Programs, v. 6, p. 260.

Spittler, T. E. and M. A. Arthur, 1982, The Lower Miocene Diligencia Formation of the Orocopia Mountains, Southern California: Stratigraphy, Petrology, Sedimentology, and Structure, *In:* Ingersoll, R. V. and M. O. Woodburne, eds., *Cenozoic Nonmarine Deposits of California and Arizona*, Pacific Section, Society of Economic Paleontologists and Mineralogists, Bakersfield, CA, p. 83-99.

Swirydczuk, K., B. H. Wilkinson and G. R. Smith, 1979, The Pliocene Glenns Ferry oolite: Lake-margin carbonate deposition in the southwestern Snake River Plain: Journal of Sedimentary Petrology, v. 49, p. 995-1004.

Sylvester, A. G. and R. R. Smith, 1975, Structure Section Across the San Andreas Fault Zone, Mecca Hills, *In:* Crowell, J. C., ed., *San Andreas Fault in Southern California: A guide to San Andreas Fault from Mexico to Carrizo Plain*, California Division of Mines and Geology, Special Report 118, Sacremento, Ca, p. 111-118.

Terres, R. R., 1984, Paleomagnetism and tectonics of the central and eastern Transverse Ranges, southern California [Ph. D. Dissertation]: University of California, Santa Barbara, 323 pp.

Tunbridge, I. P., 1981, Sandy high-energy flood sedimentation- Some criteria for recognition, with an example from the Devonian of S.W. England: Sedimentary Geology, v. 28, p. 79-95.

Wernicke, B., 1985, Uniform-sense normal simple shear of the continental lithosphere: Canadian Journal of Earth Sciences, v. 22, p. 108-125.

Wernicke, B. and B. C. Burchfiel, 1982, Modes of extensional tectonics: Journal of Structural Geology, v. 4, (2), p. 105-115.

Wilson, J., E. L. Geist, R. M. Tosdal, D. A. Okaya and E. G. Frost, 1987, Crustal structure of the Chuckwalla Valley region, SE California from industry seismic profiles, Eos, Transactions of the American Geophysical Union, v. 68 (44), p. 1360.

Wolfe, J. A., 1986, Tertiary Plant Megafossils and Paleoclimeates of the Northern Hemisphere, *In:* Broadhead, T. W., ed., *Land Plants: Notes from a short course*, The Paleontological Society, San Antonio, Tx, p. 182-196.

Woodburne, M. O., 1974a, Chronology and Stratigraphy of Cenozoic non-marine deposits, Transverse Ranges and adjacent areas, southern California: Geological Society of America Bulletin, v. 85, p.

Woodburne, M. O., 1974b, Constraints for late Cenozoic offset on the San Andreas Fault system, southern California: Sedimentary basins of the Transverse Ranges and adjacent areas: Geological Society of America Bulletin, v. 85, p.

Woodburne, M. O. and D. P. Whistler, 1973, An early Miocene Oreodont (Merychynae, Mammalia) from the Orocopia Mountains, southern California: Journal of Paleontology, v. 74, p. 909-912.

Vita

Cole Davisson was born in Escondido, California in 1967. At age seven , his family moved to Hemet, California and they have lived there ever since. He attended school in this lovely hamlet, and graduated from Hemet High School in 1985.

After a couple of years of tribulation, he enrolled at the University of California, Santa Barbara, in the College of Creative Studies. He had great difficulty settling into a major, but eventually earned a bachelors degree in biology, with an emphasis in geology.

When he finished the Santa Barbara field camp in August of 1990, he hopped on a Greyhound and didn't get off until Christiansburg, Virginia. He came to Virginia Tech to study mineralogy, but soon found himself gravitating downstairs. Eventually, he ended up in the structural geology lab, working on a Tertiary sedimentology project under the supervision of an expert on crystal-plastic deformation processes, and an Archean stratigrapher.